Vegetation and fire regimes in the Neotropics over the last 21,000 years

Thomas Kenji Akabane^{1,2}; Cristiano Mazur Chiessi³; Paulo Eduardo De Oliveira^{1,4}; Jennifer Watling⁵; Ana Carolina Carnaval⁶; Vincent Hanquiez²; Dailson José Bertassoli Jr.¹; Thaís Aparecida Silva¹,

Marília H Shimizu⁷, Anne-Laure Daniau²

20

25

30

35

40

- 1 Institute of Geosciences, University of São Paulo, Rua do Lago 562, 05508-080 São Paulo SP, Brazil
- 2 University of Bordeaux, CNRS, Bordeaux INP, EPOC, UMR 5805, F-33600 Pessac, France
- 3 School of Arts, Sciences and Humanities, University of São Paulo, Av. Arlindo Bettio 1000, 03828-000 São Paulo SP, Brazil
- 4 Keller Science Action Center, The Field Museum of Natural History, 1400 S. Lake Shore Drive, 60605, Chicago IL, USA
 - 5 Museum of Archaeology and Ethnography, University of São Paulo, São Paulo 05508-070, Brazil
 - 6 Biology Department, City College of New York, New York, USA
 - 7 General Coordination of Earth Science, National Institute for Space Research, São José dos Campos, Brazil
- 15 Correspondence to: Thomas Kenji Akabane (thomask.akabane@gmail.com)

Abstract. Vegetation and fire activity have dynamically changed in response to past variations in global and regional climate. Here we investigate these responses across the Neotropics based on the analysis of modern vegetation distribution and fire activity in relation to modern climate patterns, and a compilation of 255 vegetation records and 131 charcoal records encompassing the last 21,000 years before present (ka) in relation to past climate changes. Our analyses on the dynamics of past tree cover and fire activity focus on seven subregions: (1) northern Neotropics (NNeo); (2) tropical Andes (TrAn); (3) Amazonia; (4) northeastern Brazil (NEB); (5) central-eastern Brazil (CEB); (6) southeastern South America (SESA); and (7) extratropical Andes (ExTrAn). The regionalized assessment unveils spatial heterogeneity in the timing and controls of vegetation and fire dynamics. Temperature, atmospheric CO₂ concentrations, and precipitation exhibit distinct and alternating roles as primary drivers of tree cover and fire regime changes with additional impacts from human activity. During the Last Glacial Maximum (LGM, here covering 21-19 ka), arboreal growth in high elevation sites (TrAn) and in sub- and extra-tropical latitudes (SESA and ExTrAn) was mainly limited by low temperatures and atmospheric CO2 concentrations, while fuel-limited conditions restrained fire activity. In warmer tropical regions (NNeo, Amazonia, CEB), moisture availability was likely the main controlling factor of both vegetation and fire, with the effects of low CO₂ amplifying these constraints. Throughout the deglacial phase (19-11.7 ka), progressive warming and increasing atmospheric CO2 concentrations fostered a gradual biomass expansion, and together these changes led to intensified fire activity in the sub- and extra-tropical temperature-limited regions. Meanwhile, increased (decreased) precipitation associated with millennial-scale events favored increases (decreases) in tree cover in regions such as CEB and NEB (NNeo). Between 14-13 ka, most southern latitude subregions (Amazonia, CEB, SESA, ExTrAn) saw a rise in fire activity coeval with a second rapid warming, contrary to decreased fire activity in NNeo amid relatively wetter conditions. Throughout the Holocene, when temperature and atmospheric CO₂ fluctuations were lower, shifts in precipitation became the primary driver of vegetation and fire dynamics across all the Neotropics. Changes in the Intertropical Convergence Zone and gradual intensification of the South American Summer Monsoon throughout the Holocene favored a continuous increase in tree cover over Amazonia, CEB, and SESA, but led to a forest cover decrease in NNeo and NEB. From the early- to the mid-Holocene, the strengthening of the Southern Westerly Winds promoted vegetation expansion and fire regime weakening in ExTrAn. In the late Holocene, human impacts became more pronounced, with a clearer effect on regional tree cover and fire activity, particularly in NNeo and TrAn.

1 Introduction

45

50

55

60

65

70

75

The Neotropics is the most species-rich biogeographical domain and home of at least one third of global biodiversity (Raven et al., 2020). It extends from the southern parts of North America to southernmost South America and encompasses a wide range of environments, from the wettest rainforests to the driest deserts on Earth. The distinctly high diversity in the region is attributed to a combination of biotic processes, such as *in situ* adaptation (Simon et al., 2009), species interchange (Antonelli et al., 2018) and ecological interactions (Fine et al., 2004), together with abiotic processes including landscape evolution (Hoorn et al., 2010; Richardson et al., 2001) and climate fluctuations throughout the Cenozoic (Cracraft et al., 2020; Jaramillo et al., 2006; Rull, 2011; Sawakuchi et al., 2022). Largely influenced by changes in the tectonic regime, the long-term climate cooling throughout the Cenozoic induced a retraction of warm tropical forests and culminated in the onset of pronounced glacial-interglacial cycles in the Quaternary (Morley, 2011; Westerhold et al., 2020).

Quaternary glacial-interglacial cycles together with millennial-scale climate changes played a significant role in shaping species distribution over time across the Neotropics. For instance, the distinct hydroclimate (Baker and Fritz, 2015; Wang et al., 2017), 3–8 °C colder temperatures (Bush et al., 2001; Chiessi et al., 2015; Colinvaux et al., 1996; Wille et al., 2001), and the ca. 100 ppm lower atmospheric CO₂ concentrations (CO_{2atm}) (Bereiter et al., 2015; Petit et al., 1999) of the Last Glacial Maximum (LGM, typically between 23,000–19,000 yr ago (23 – 19 ka)) induced substantial and widespread changes in vegetation composition and structure. These changes predominantly, but not exclusively, led to a lower biomass state with a weaker fire regime (e.g., Behling, 2002a; Bush et al., 2009; Bush and Flenley, 2007; Haas et al., 2023; Ledru, 2002; Nanavati et al., 2019; Power et al., 2010b). However, the magnitude and timing of these changes in vegetation and fire were hetereogeneous, resulting in diverse regional patterns. This variability highlights the complexity of environmental dynamics since the LGM and the need for region-specific analyses to understand ecosystem responses to past climatic shifts.

Investigating the primary mechanisms controlling ecosystem dynamics is crucial for anticipating the impacts of ongoing climate changes. The projected large-scale changes in specific climate system components, unprecedented in the instrumental record, may only find parallels in the geological past (Wunderling et al., 2024). In this sense, sedimentary pollen and charcoal records offer the oportunity to obtain valuable insights into long-term responses and a deeper understanding of the linkages between climate changes and environmental shifts (Daniau et al., 2012; Flantua et al., 2016; Marlon et al., 2013; Nanavati et al., 2019; Power et al., 2010a).

Here we use 255 pollen records and 131 charcoal records to reconstruct tree cover and fire regime changes in the Neotropics spanning the last 21 ka. We also use compiled archeological radiocarbon data available in literature and databases to discuss vegetation and fire changes in relation to potential anthropogenic impacts (Fig. A1). We focus on subregions including the (1) northern Neotropics (NNeo); (2) tropical Andes (TrAn); (3) Amazonia; (4) central-eastern Brazil (CEB); (5) northeastern Brazil (NEB); (6) southeastern South America (SESA); and (7) extratropical Andes (ExTrAn) (Fig. 1 and 2). These subregions were chosen based on data availability and are delimited by their present-day climatic and vegetation features. Thus, our scope focuses on the underlying controls of long-term and broad-scale patterns. Furthermore, we analyze modern fire patterns using satellite data to compare with climate and vegetation parameters to contribute to our interpretations. These analyses allow us to assess distinct vegetation and fire dynamics from each subregion and the competing drivers influencing their responses.

2 Vegetation and climate settings

80

85

90

95

100

105

110

- (1) The <u>northern Neotropics (NNeo)</u>, mainly comprising Central America and northernmost South America, is mostly covered by moist tropical forests, pine-oak forests, dry forests, and shrublands (Fig. 1a). The region exhibits a seasonal climate, with lowland mean annual temperatures ranging from 25 to 28 °C (Fig. 1b). Precipitation patterns are strongly influenced by the latitudinal shifts of the Intertropical Convergence Zone (ITCZ) with a regional mean of 1600 mm yr⁻¹. During boreal summer, when the ITCZ shifts further north, most of the rainfall is transported into the Central American region by the Caribbean Low Level Jet (Cook and Vizy, 2010) (Fig. 1d). Large wildfires in the region are associated with humid periods succeeded by extreme dry periods, often linked with El Niño Southern Oscillation (ENSO) variability with La Niña-driven wet events followed by El Niño-driven droughts (Ponce-Calderón et al., 2021).
- (2) <u>Amazonia</u> is the most extensive tropical rainforest on Earth, marked by weak seasonality, mean monthly temperatures ranging between 25 and 27 °C, and mean annual precipitation of 2300 mm yr¹ (Fisch et al., 1998; Marengo, 1992). Precipitation seasonality increases south- and eastwards, while parts of northwestern Amazonia remain wet throughout the year (Fisch et al., 1998; Marengo, 1992) (Fig. 1c,d). During austral summer, increased land-ocean thermal contrast enhances the atmospheric transport of humidity towards the continent promoting the South American Summer Monsoon (SASM), responsible for most of the precipitation over Amazonia (Garreaud et al., 2009; Vera et al., 2006) (Fig. 1c). Persistent moist conditions of the rainforest naturally inhibit wildfires. However, initial fire events whether triggered by severe droughts (e.g., related to El Niño), ongoing climate changes, and/or human impacts further increase forest flammability through canopy degradation and fuel accumulation. This favors subsequent fire events, thereby fostering a positive feedback loop (Brando et al., 2020; Bush et al., 2008; Cochrane et al., 1999; Nepstad et al., 1999).
- (3) The herein defined *Tropical Andes (TrAn)* comprises areas above 2200 m altitude, which include (i) upper montane forests from 2300 to 3300 m, (ii) the páramo, from ca. 3200, and (iii) the puna, from ca. 3700 m, to the snow line (Troll, 1968) (Fig. 1a). Precipitation patterns in the region are heterogeneous and partially linked to the SASM (Espinoza et al., 2020; Segura et al., 2019) (Fig. 1c). Andean montane forests feature the wettest parts of Amazonia recording more than 5000 mm yr⁻¹ in some areas (Espinoza et al., 2020) (Fig. 1c). The páramo and the puna, the alpine vegetation of the Andes, are biogeographically separated by the Huancabamba depression at ca. 6°S (Cuesta et al., 2017; Troll, 1968). Most of the páramo, located north of the Huancabamba depression, receives high precipitation between 1000 and 2000 mm yr⁻¹ (Cuatrecasas, 1968). The puna, located south of the Huancabamba depression, covers the Altiplano under precipitation from 200 to 500 mm yr⁻¹ (Vuille and Keimig, 2004) (Fig. 1c,d). Most of the annual precipitation in the region is related to moisture-laden easterly winds from Amazonia and associated with the onset of the Bolivian High, an upper-level highpressure cell linked to the SASM. The interannual precipitation variability is influenced by zonal winds modulated by sea surface temperatures (SST) across the tropical Pacific Ocean (Garreaud et al., 2003; Vuille, 1999). During weakened easterlies, such as during El Niño events, the incursion of dry-warm upper-level westerly winds inhibit precipitation in the Altiplano and weakens the Bolivian High. Contrarily, during La Niña events, the incursion of Amazon moisture conveyed by easterly winds is facilitated (Garreaud et al., 2003; Vuille, 1999). While natural fires in the forests of the TrAn are rare, wildfires in grasslands are frequent, generally of low-intensity, and predominantly driven by human activity (Bush et al., 2015; Gutierrez-Flores et al., 2024).
- (4) <u>Northeastern Brazil (NEB)</u> includes mostly the xeric vegetation of Caatinga (Fig. 1a). The region is characterized by mean annual temperatures of 24 to 28 °C and semiarid conditions with precipitation below 900 mm yr⁻¹, concentrated between February and May, while potential annual evapotranspiration exceeds 2200 mm yr⁻¹ (Pinheiro et al., 2016). Low precipitation in the region is driven by the Nordeste Low, a high-pressure cell dynamically linked to the Bolivian High

- (Lenters and Cook, 1997). In Caatinga, scarce fuel availability related to low biomass production limits regular fire events (Alvarado et al., 2020; Argibay et al., 2020).
 - (5) <u>Central-eastern Brazil (CEB)</u> is primarily associated with Cerrado vegetation, characterized by a mosaic of physiognomies, ranging from open grasslands and savannas to closed shrublands and woodlands, typically covered by a continuous herbaceous layer (Eiten, 1972). The climate of CEB is characterized by the austral summer establishment of the SASM, marked by the occurrence of the South Atlantic Convergence Zone (SACZ), followed by a dry season lasting four to six months, and has an annual precipitation of about 750 to 2000 mm yr⁻¹ (Eiten, 1972; Goodland, 1971; Vera et al., 2006) (Fig. 1c). In this ecosystem, wildfires are regular and play a key role in controlling vegetation physiognomy and biodiversity (Durigan and Ratter, 2016; Mistry, 1998; Moreira, 2000).

125

130

- (6) <u>Southeastern South America (SESA)</u> is mostly occupied by the Atlantic Forest, composed of both evergreen and semideciduous forests, as well as mixed forests in the southern and mountainous regions (Fig. 1a). SESA mean annual temperatures range from ca. 25 °C in the tropical forests to 12 °C in the southern mixed forests (Kamino et al., 2019; Ribeiro et al., 2011) (Fig. 1b). Coastal regions experience over 1800 mm yr⁻¹ of precipitation well-distributed throughout the year, while inland areas are relatively more seasonal, ranging from 1300 to 1600 mm yr⁻¹ (Kamino et al., 2019). Most annual precipitation in the regions influenced by the SACZ occurs during austral summer (Fig. 1c). Predominantly during austral autumn and winter, the South Atlantic anticyclone affects the region, leading to lower temperatures and reduced rainfall, whereas to the south of the SESA, cold fronts favor moderate precipitation levels (Kamino et al., 2019) (Fig. 1d). Wildfires are naturally rare in the Atlantic Forest due to high moisture and dense forest cover, however, large scale degradation, rising temperatures and extreme climatic events, such as those related to La Niña years, intensify wildfires frequency and severity (Jesus et al., 2022; da Silva Junior et al., 2020).
- (7) Extratropical Andes (ExTrAn), including Patagonia and Tierra del Fuego, primarily encompasses wet-temperate forests, alpine forests and grasslands. Mean annual temperature ranges from 3 to 16 °C between the latitudes 55 and 32°S (Fig. 1b). The zonal rainfall gradient is abruptly sharp, with the west part of the Andes cordillera receiving most of the precipitation, while drier conditions prevail in the eastern side (Coronato et al., 2005; Endlicher and Santana, 1988) (Fig. 1c,d). Precipitation is controlled by the Southern Westerly Winds (SWW), which shift southward during austral summer, while during austral winter they weaken and expand equatorward (Garreaud et al., 2009) (Fig. 1c,d). Fire activity in the region exhibits a gradient from fuel-limited conditions to the north of 32° S to moisture-limited conditions to the south of 40° S (Holz et al., 2012). Fire events are favored by intermediate productivity levels, with combined contribution of woody and herbaceous vegetation. Fires are primarily conditioned by dry and warm events in moisture-limited areas or anomalously positive rainfall over fuel-limited areas, usually associated with ENSO variability, changes in the Antarctic Oscillation, or in the Pacific Subtropical Anticyclone, which shifts the SWW poleward (Holz et al., 2012; Kitzberger et al., 2022; Kitzberger and Veblen, 1997).

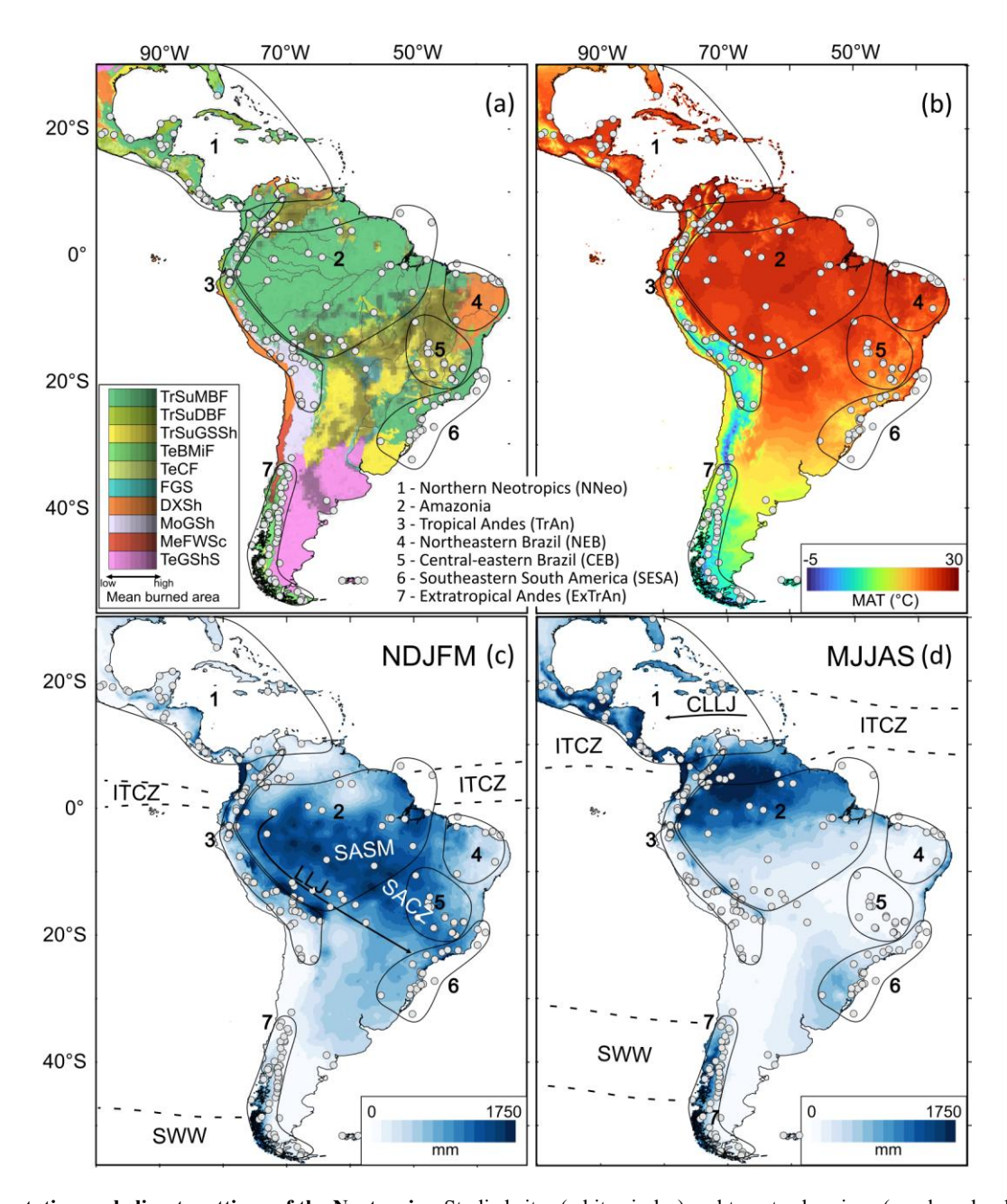


Fig. 1 – Vegetation and climate settings of the Neotropics. Studied sites (white circles) and target subregions (numbered polygons) are depicted. (a) Ecoregions, TrSuMBF – Tropical subtropical moist broadleaf forests; TrSuDBF – Tropical subtropical dry broadleaf forests; TrSuGSSh – Tropical subtropical grasslands, savannas, and shrublands; TeBMiF – Temperate broadleaf mixed forests; TeCF – Temperate coniferous forests; FGS – Flooded grasslands and savannas; DXSh – Desert and xeric shrublands; MoGSh – Montane grasslands and shrublands; MeFWSc – Mediterranean forests, woodlands, and scrubs; TeGShS – Temperate grasslands, shrublands, and savannas (Olson et al., 2001). Mean burned area of the last 12 years derived from Laurent et al. (2018). (b) Mean annual temperature (MAT) (Hijmans et al., 2005). (c,d) Precipitation during the extended austral (c) summer (November – March) and (d) winter (May – September) averaged from 1960 to 2021 using the data from Climatic Research Unit (Harris et al., 2020). CLLJ – Caribbean Low-level jets; ITCZ – Intertropical Convergence Zone; LLJ – Low-level jets; SACZ – South Atlantic Convergence Zone; SASM – South American Summer Monsoon; SWW – Southern Westerly Winds.

3 Material and methods

155

160

165

3.1 Compilation of records and data treatment

The study area spans the Neotropical realm between latitudes 28°N to 60°S and longitudes 33°W to 105°W (Fig. 2a). Pollen records were gathered from the Neotoma (210 entries) and Pangaea (6 entries) databases (Felden et al., 2023; Williams et al., 2018). Charcoal data were gathered from the Reading (94 entries) (Harrison et al., 2022), Neotoma (16

entries), DRYAD (4 entries) (McMichael et al., 2021), and Pangaea (2 entries) databases. Additionally, we digitalized and extracted 39 pollen and 15 charcoal records from publications without openly available data, directly from published diagrams by using WebPloterDigitalizer (WebPlotDigitizer version 5.2) (Fig. 2b) (for the full list of datasets and respective citations and sources, see Supplementary Table 1). For NEB, charcoal influx data is represented by three available curves from the region derived from De Oliveira et al. (1999), Bouimetarhan et al. (2018), and Ledru et al. (2006). A subset of these records was grouped into seven subregions (*Sect. 2*), delimited by similarities in dominant climate features and vegetation (Fig. 1 and 2a):

170

175

185

190

195

200

205

Northern Neotropics (NNeo) comprises 26 pollen and 25 charcoal records collected north of 7 °N, mostly from Central America, excluding high montane sites above 3000 m. Most frequent taxa include trees and shrubs such as *Pinus*, Moraceae/Urticaceae, *Quercus*, *Alnus*, *Acalypha*, *Bursera*, and *Piper* and herbs such as Poaceae, Cyperaceae, Asteraceae, and Amaranthaceae.

Amazonia includes mostly records from the eastern, southwestern, and northern borders of the Amazon River drainage basin (28 pollen, 31 charcoal). Most common woody taxa include Moraceae, Alchornea, Melastomataceae, Podocarpus, Myrtaceae, Mauritia, Cecropia, Euterpe, and Ilex, and herbs such as Poaceae, Asteraceae, and Cyperaceae.

Tropical Andes (TrAn) comprises 83 pollen and 24 charcoal records located between 9 °N and 24 °S, from Andean sites located above 2200 m (average altitude of the records: 3590 m). Main pollen taxa include herbs such as Poaceae, Asteraceae, Cyperaceae, and *Plantago*, while the woody component includes taxa such as Melastomataceae, *Weinmannia, Hedyosmum*, Moraceae/Urticaceae, *Alnus, Podocarpus*, and Myrica.

Northeastern Brazil (NEB) mostly encompasses the Caatinga, including marine records off the northern Brazilian margin, under major influence of NEB sources. The dearth of pollen (7) and charcoal (3) records prevent detailed vegetation and fire regime assessment. Some of the main taxa found in pollen records include herbs such as Poaceae, Cyperaceae, Asteraceae, Borreria, and Amaranthaceae, and woody taxa such as Cuphea, Alchornea, Arecaceae, Moraceae/Urticaceae, Dalbergia, Schefflera, Myrsine, Mimosa, and Platymiscium.

Central-eastern Brazil (CEB) is represented by 18 pollen and 8 charcoal records in the southeastern Cerrado. Characteristic pollen taxa include herbs such as Poaceae, Cyperaceae, Asteraceae, Apiaceae, and *Borreria*, and woody taxa such as Myrtaceae, *Cecropia*, Moraceae/Urticaceae, *Myroxylon*, *Mauritia*, and Melastomataceae.

Southeastern South America (SESA) encompasses 21 pollen and 12 charcoal records within the modern extent of the Atlantic Forest. Most common herbaceous taxa are Poaceae, Cyperaceae, Asteraceae, Eryngium, and Xyris while characteristic woody taxa include Myrtaceae, Moraceae/Urticaceae, Alchornea, Myrsine, Arecaceae, Melastomataceae, Ericaceae, Podocarpus, and Araucaria.

Extratropical Andes (ExTrAn) comprises 47 pollen records and 18 charcoal records located south of 32°S. Characteristic taxa from this subregion include herbs such as Poaceae, Cyperaceae, Asteraceae, Apiaceae, Misodendrum, and Brassicaceae and woody taxa such as Nothofagus, Austrocedrus, Cupressaceae, Ericaceae, Empetrum, Myrtaceae, and Podocarpus.

Datapoints outside the defined subregions (black dots in Fig. 2a) were excluded from subregional analyses. These include records that are either geographically isolated or located outside subregional definitions, e.g., high montane sites from NNeo > 3000 m; low altitudes from TrAn < 2200 m.

For Neotoma records, arboreal pollen (AP), which serves as an indicator of tree cover relative to herbaceous vegetation, was calculated as the percentage of woody taxa (trees, shrubs, and palms), considering taxa at the genus and family level divided by the total sum of trees and shrubs, palms, and herbs, excluding mangrove and aquatic taxa, fern spores, and

unidentified types. We used the Neotoma standardized classification of ecological groups (Supplementary Table 1). For manually extracted records, AP percentages were obtained from published pollen diagrams. Therefore, the criteria used to construct these AP curves may slightly differ from those applied in our calculations based on raw data. For instance, in CEB, *Mauritia* and Cyperaceae are often excluded from AP calculations, as these taxa are often over-represented due to strong local imprint from palm swamp vegetation (Barberi et al., 2000; Escobar-Torrez et al., 2023; Salgado-Labouriau et al., 1997). To maintain consistency within this specific region, we also excluded *Mauritia* and Cyperaceae from AP calculations from CEB records. Samples with pollen counts below 100 grains were removed. Records from sites highly influenced by coastal dynamics (> 15 % of mangrove taxa) were also removed from the AP composites. Although tree ferns can serve as important indicators of humid conditions in regions such as the Andes and Atlantic Forests, these were excluded from pollen sums due to inconsistent reporting across records, to ensure a standardized dataset suitable for regional-scale analyses.

For charcoal composites, records containing both micro- (< 100 µm) and macro- (> 100 µm) particles were included. Charcoal raw counts were converted into concentrations and then to influx using site-specific sedimentation rates to account for differences in sedimentation rates across sites (Marlon et al., 2016). Changes in charcoal records can be linked to past fire activity and used to infer shifts in fire regimes (Power et al., 2008; Daniau et al., 2010; Marlon et al., 2016). While our approach does not allow to resolve specific components of the fire regime (e.g., intensity, severity, frequency, seasonality, spatial extent of burned vegetation), it allows to identify collective changes in fire recorded as changes in charcoal influx within a given region over a long timescale. New age models were calculated for Neotoma charcoal entries as per Harrison et al. (2022). We used the 'Bacon' R package (Blaauw and Christen, 2011) and the IntCal20 (Reimer et al., 2020) and SHCal20 (Hogg et al., 2020) calibration curves for latitudes above 15°N and below 15°S, respectively, and a 50:50 mixed calibration curve for intermediate latitudes.

Transformation and standardization of AP and charcoal influx data followed Power et al. (2008) using the 'paleofire' R package (Blarquez et al., 2014). These steps are essential for appropriate comparisons between records that use different quantification techniques and report different charcoal particle sizes (Power et al., 2008). It also allows for comparisons among sites with different vegetation settings (e.g., swamp, peat, lake, and marine records) by emphasizing trends over absolute values. As such, values were transformed and standardized with a Box-Cox transformation ($\alpha = 0.01$) and 0-1 range rescaling and converted to z-scores using a common base period of 0.2–21 ka, so that all sites have a common mean and variance. Composite curves were constructed by fitting a locally weighted regression (LOWESS) curve to the pooled transformed and rescaled data, with confidence intervals (2.5th and 97.5th percentiles) generated through 1000 bootstrap replicates. A two-stage smoothing approach was applied using a pre-bin half width of 20 yr and a LOWESS smoothing of 1000 yr window half width to produce low resolution curves and a smoothing of 400 yr window half width for higher resolution curves (Daniau et al., 2012; Marlon et al., 2008). In general, caution is warranted when interpreting trends during periods with wide confidence intervals or when the composite curve approaches the upper or lower bounds of the confidence interval, or exhibits outlier shifts. These cases usually relate to periods with few records and indicate greater uncertainty and sensitivity to individual records, thus reflecting local variability of specific sites.

Recent studies have highlighted limitations of z-score scaling, including the distortion of charcoal peaks and the lack of consistency in representing fire absence across sites, particularly in tropical ecosystems where the documentation of both presence and absence is important (McMichael et al., 2021; Gosling et al., 2021). To assess the impact of methodological choices on the resulting curves, we also explored the alternative approach based on Proportional Relative Scaling (PRS) as per McMichael et al. (2021) (Supplementary Material). We produced curves using PRS and PRS applying a base period

(0.2 – 21 ka). We compare these two relative scaling-based curves with our z-score curves. Importantly, by applying the same base period to both PRS and z-score calculations, we ensured consistency across datasets for comparative purposes, although this approach was not assessed in McMichael et al. (2021).

Additionally, we produced maps displaying site-specific AP percentages and z-scores for both AP and charcoal influx for all data points to illustrate spatial patterns across time slices of the last 21 ka. Each site-specific data point represents a mean z-score calculated relative to its own long-term mean (base period: 21 to 0.2 kyr BP). As a result, the colors of the dots within a single map reflect deviations from local baseline conditions and should not be directly compared across sites to infer geographic gradients or absolute levels of fire activity or tree cover. However, clusters with similar z-score trends, such as consistently positive values in a region, may indicate homogeneous responses and coherent regional patterns, for example a general expansion in tree cover or intensification of the fire regime. For mapping purposes, the z-scores were divided into five equidistant categories: > +0.8 (strong positive anomalies), +0.8 to +0.4 (positive anomalies), +0.4 to -0.4 (weak positive or negative anomalies), -0.4 to -0.8 (negative anomalies), and < -0.8 (strong negative anomalies).

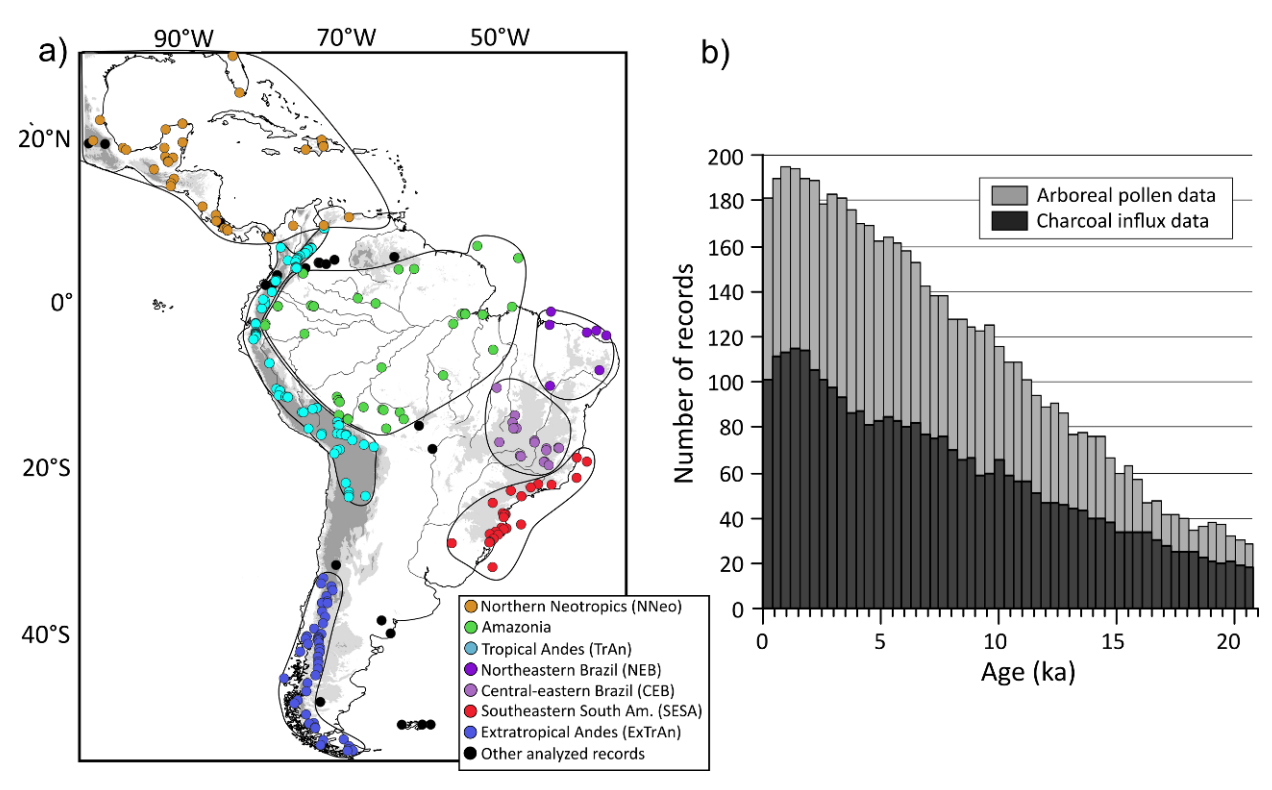


Fig. 2 – Spatial and temporal distribution of analyzed records. (a) Distribution of pollen and charcoal records compiled from Neotoma, Pangaea, and Reading databases, and manually extracted from publications (Felden et al., 2023; Harrison et al., 2022; Williams et al., 2018). Details on the reference, site location, and maximum spanning age from each site are available in Supplementary Table 1. Black circles indicate sedimentary records that were not included in the subregional analysis. Elevations greater than 500 m are represented in light gray, while areas above 1500 m altitude are shown in dark gray. Major rivers are displayed as black lines. (b) Number of pollen and charcoal records available for each 400-year time bin over the last 21 ka, providing an overview of temporal data coverage.

3.2 Radiocarbon ages from archeological sites

250

255

260

265

270

We generated summed probability density (SPD) curves as a proxy for human occupation trends (Contreras and Meadows, 2014; Williams, 2012), based on compiled ¹⁴C ages from archaeological sites available from literature (Araujo et al., 2025; Goldberg et al., 2016) and the Mesoamerican Radiocarbon database (MesoRad, 2020) (Fig. A1). Compiled data from Goldberg et al. (2016) are limited to ages older than 2 ka ¹⁴C ages. This approach assumes a proportional relationship

between human populations and the production of datable material, as well as the statistical representativeness of the actual dated samples in relation to the full spectrum of ¹⁴C samples from a region (Contreras and Meadows, 2014).

We produced SPD curves using 'rcarbon' R package, with 600-yr moving average window size to reduce the effects of the calibration process and 100-yr bins to account for potential biases associated to strong inter-site variability in sample size (Crema and Bevan, 2021). We used calibration curve SHCal20 (Hogg et al., 2020) for Southern Hemisphere ¹⁴C ages (Amazonia, NEB, CEB, SESA, TrAn) and IntCal20 (Reimer et al., 2020) for Northern Hemisphere ¹⁴C ages (NNeo). SPD curves are shown from the oldest non-zero values.

For NNeo, we use 14 C ages available from MesoRad (2020) (N = 1692) and at latitudes northern of 7°N from Goldberg et al. (2016) (N = 96). For Andean regions, such as TrAn (N = 873) and ExTrAn (N = 621), we use data compiled by Goldberg et al. (2016). For Amazonia (N = 751), NEB (N = 542), CEB (N = 593), and SESA (N =1589), we use data compiled by Araujo et al. (2025).

3.3 Modern fire patterns extraction and analysis

To assess the current relationship between climate, fire activity, and vegetation parameters, we extracted data from the global fire patch functional traits database (FRY) (Laurent et al., 2018). The FRY map resolution was rescaled from $0.002246^{\circ} \times 0.002246^{\circ}$ to grids of $0.45^{\circ} \times 0.45^{\circ}$ (2500 km² at the equator) using 20 yr of satellite monitoring data (2001 to 2020). For each rescaled grid, we obtained the mean fire radiative power, as a measure of fire intensity, and total burned area. Fire radiative power was then compared with WorldClim climate variables (Fick and Hijmans, 2017) (originally 10 minutes spatial resolution, $0.1667^{\circ} \times 0.1667^{\circ}$)—including mean annual temperature (MAT), maximum temperature of the warmest month, annual precipitation, precipitation of the driest quarter, and precipitation seasonality—and major vegetation types defined by ecoregions (Olson et al., 2001) (Fig. 3). For consistency, the climate models and ecoregion distribution were rescaled to match the FRY fire map.

4 Results

280

285

290

295

300

305

310

4.1 Modern fire, climate and vegetation relationship

Modern vegetation and fire patterns correlate with climate (Fig. 3). Tropical savannas are predominantly distributed in seasonal climates with annual precipitation ranging from 1000 to 2000 mm yr⁻¹ and mean annual temperature between 20 and 27 °C (Fig. 3a). Towards wetter climates, the conditions for the existence of savannas overlap with those of tropical moist forests, while towards drier climates, they overlap with those of xeric vegetation (Fig. 3a,b).

Regarding fire activity, tropical moist forests and xeric vegetation exhibit weaker fire activity in relation to savannas (Fig. 3c,d). Fire activity also weakens towards cooler subtropical and temperate savannas and montane grasslands. Fire radiative power, which is linearly correlated with the total burned area (Fig. 3e), is more intense in tropical savannas, specifically at intermediate annual rainfall levels (875–2000 mm yr⁻¹, peaking at ca. 1520 mm yr⁻¹, Fig. 3c) and precipitation under 100 mm during the driest month (Fig. 3d). Fire intensity rises with mean annual temperatures above 21 °C, reaching maximum values as temperatures rise (Fig. 3c). Regions with maximum temperatures of the warmest month above 29 °C concentrate most of the fire activity (Fig. 3d). The fire season in tropical America occurs during spring (i.e., March to May in the northern tropics and August to October in the southern tropics) (Fig. 3f), while along the southwestern flank of the Andes the fire season occurs during austral autumn.

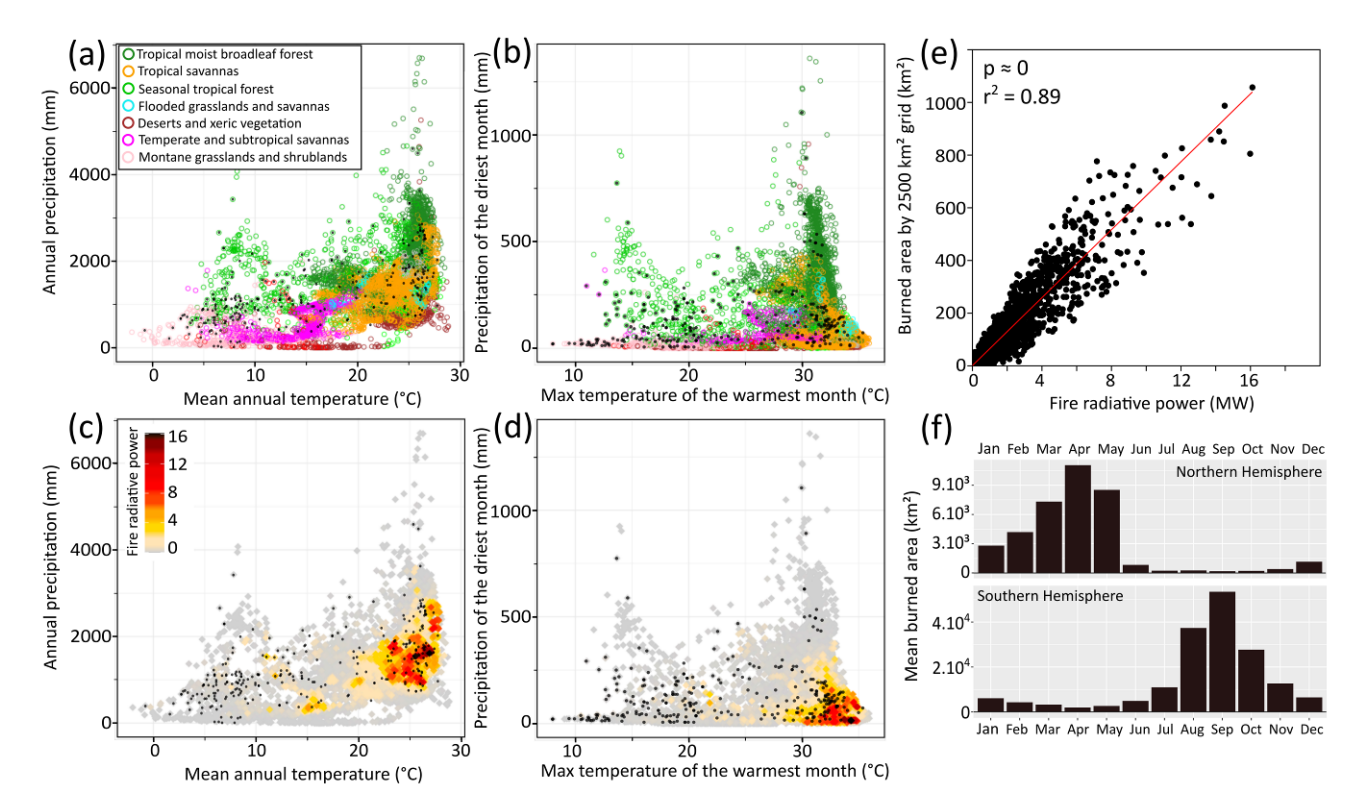


Fig. 3 – Climate, vegetation, and fire patterns across the Neotropics. (a-b) Distribution of ecoregions (Olson et al., 2001) and (c-e) fire radiative power (2001–2020) (Laurent et al., 2018) across the climate space. (a,c) Mean annual temperature × annual precipitation; (b,d) maximum temperature of the warmest month × precipitation of the driest month. Black dots denote records compiled in this study. (e) Relationship between total burned area and mean fire radiative power, averaged per 2500 km² grid cell. (f) Monthly relative burned area for the Northern and Southern Hemisphere regions of the Neotropics from MODIS (Fire Information for Resource Management System – FIRMS: https://firms.modaps.eosdis.nasa.gov/).

4.2 Pollen and charcoal records

315

320

325

330

4.2.1 Representativeness of the dataset

The existing records are distributed across the main subregions of the Neotropics, ranging from the moist tropical forests to the semiarid xeric vegetation (Fig. 1 and 2). While the Andes are particularly well sampled (Fig. 2a), areas such as central Amazonia, arid and semiarid regions (e.g., northeastern Brazil), and central regions of the Neotropics located between 20 and 40°S (Fig. 2a) are underrepresented.

In terms of chronological representation, site density increases towards the Holocene (Fig. 2b). Across the Neotropics, considering time bins of 400-yr intervals, the LGM (21–19 ka) is supported by an average of 30 pollen and 20 charcoal records, followed by the deglacial period (19–11.7 ka; 62 and 35, respectively), and the Holocene (< 11.7 ka; 152 and 82; Fig. 2b). Therefore, the Pleistocene and particularly millennial-scale events such as Heinrich stadial 1 (HS1, 18–14.8 ka), Antarctic Cold Reversal/Bølling–Allerød (ACR/BA) (14.8–12.9 ka), and the Younger Dryas (YD) (12.9–11.7 ka) are represented by fewer samples and consequently lower spatial representativity.

4.2.2 Arboreal pollen and charcoal influx compilation trends

340

345

355

360

Arboreal pollen and charcoal influx z-scores are positively correlated in TrAn (r = 0.41), SESA (r = 0.63), and ExTrAn (r = 0.78), and negatively correlated in NNeo (r = -0.56) (p < 0.001) and CEB (r = -0.34), while no clear correlation is observed for Amazonia (r = 0.18) (Fig. A2).

Despite being represented by a relatively small number of records, during the LGM (21 – 19 ka), positive AP z-scores are recorded in the Northern Hemisphere subregion NNeo (Fig. 4a), in opposition to mostly negative AP z-scores in Southern Hemisphere subregions (Fig. 4b-g). Meanwhile, charcoal influx z-scores are predominantly negative for all subregions (Fig. 4k).

By the onset of the deglacial period (19 – 11.7 ka), AP increases in TrAn, NEB, SESA, and ExTrAn (Fig. 4c,d,f,g), contrasting with AP decrease in NNeo (Fig. 4a). No clear long-term trend is detected for Amazonia and CEB. Charcoal influx z-scores in the Southern Hemisphere exhibit negative values during the deglaciation (Fig. 4i-m), followed by a stepwise increase towards interglacial levels at 14 to 13 ka. On the other hand, the Northern Hemisphere (NNeo) presents a decrease in charcoal influx z-scores at 13 ka, towards minimum EH values (Fig. 4h).

The Holocene period shows distinct regional patterns in AP z-scores and charcoal influx:

In the early Holocene (EH; 11.7 – 8.2 ka), AP z-scores reach high values for NNeo and TrAn (Fig. 4a,c), low values for NEB, CEB, and Amazonia (Fig. 4b,e), and maintain a continuous increase in ExTrAn and SESA (Fig. 4f,g). This period also records higher charcoal influx z-scores in Amazonia, CEB, SESA, and ExTrAn, and lower values in the NNeo.

In the mid Holocene (MH; 8.2 – 4.2 ka) AP z-scores values increase in Amazonia, NEB, CEB, SESA, and ExTrAn, opposed to decreasing values in NNeo. The charcoal influx reaches maximum values in the TrAn and increases in the NNeo, coinciding with decreasing AP trends. On the other hand, charcoal influx decreases slightly in the CEB and ExTrAn and remains relatively constant in Amazonia and SESA.

During the late Holocene (LH; 4.2 - 0 ka), NNeo, TrAn, and NEB show a drop in AP z-scores reaching the lowest Holocene levels. In NNeo, these shifts coincide with some increase in charcoal influx. Conversely, during the same period, AP z-scores attain maximum values in Amazonia, CEB, SESA, and ExTrAn, while charcoal influx decreases in CEB and increases in ExTrAn.

The comparison between z-scores and the proportional relative scaling method from McMichael et al (2021) shows that despite changes in the amplitude of variability, all regions hold mostly coherent patterns of changes and a similar temporal structure. In addition, z-scores appear more stable and better suited to capturing long-term trends in fire activity (see Supplementary Material).

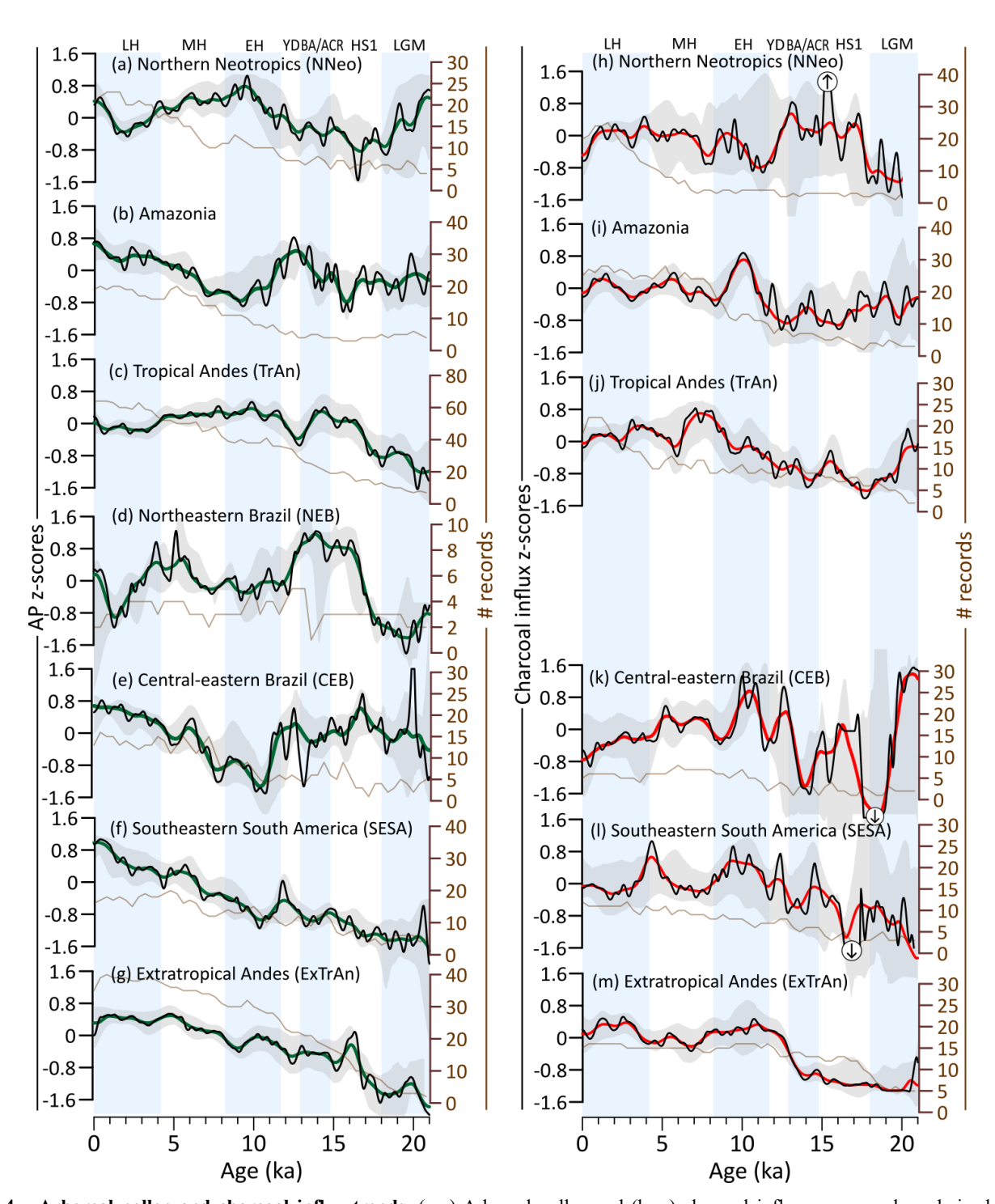


Fig. 4 – **Arboreal pollen and charcoal influx trends.** (a-g) Arboreal pollen and (h-m) charcoal influx z-score values derived from compilations for studied subregions. Green and red curves: 1000-yr window smoothed, black curves: 400-yr window smoothed. Brown curves show the number of records by 400-yr bins. Gray areas represent 2.5th and 97.5th confidence intervals. Note: Enough charcoal records from Northeastern Brazil were not available to generate a composite curve. Large charcoal anomalies that extend beyond +2 or -2 are indicated by circled arrows, which also depict low confidence periods.

5 Discussion

365

370

5.1 Modern climate-fire-vegetation relationships

The most intense fire activity occurs in the warm regions that combine intermediate annual precipitation levels (875–2000 mm yr⁻¹) and a marked dry season (less than 100 mm in the driest month, Fig. 3c-e). Sufficient moisture supports biomass

growth, while the dry season grants the necessary flammability for fire events (Fig. 3c-e). These fire-prone conditions are typical of tropical savannas and grasslands (Fig. 3a,b), such as in CEB, where a regular frequency of fire events is key in maintaining biodiversity and the physiognomy of vegetation (Bernardino et al., 2022; Mistry, 1998). In modern day CEB, however, fire regime is mostly limited by fuel moisture (moisture-limited condition, negative biomass-fire correlation) (Alvarado et al., 2020). In arid and semiarid environments, such as NEB, or high-altitude areas, such as higher areas of TrAn, fire activity is hindered due to biomass limitation (fuel-limited conditions, positive biomass-fire correlation) (Fig. 3a-e). On the other hand, under wet conditions of tropical rainforests, such as Amazonia or parts of NNeo, fire activity is limited due to constant fuel moisture (moisture-limited condition) (Fig. 3a,b). Natural and anthropogenic wildfires are more frequent at the dry-wet season transition, when biomass flammability is at its highest, which typically corresponds to the austral spring in Southern Hemisphere tropical regions (Fig. 3f) (Mistry, 1998; Ramos-Neto and Pivello, 2000). The modern fire regime has been heavily modified by human activity through the intensification of wildfires burning both fire-adapted and fire-sensitive vegetation (Argibay et al., 2020; Hantson et al., 2015; Pivello, 2011). Despite this limitation, insights can still be obtained on the feedbacks between fire, vegetation, and climate (Fig. 3a-e) as also suggested by global and local fire analyses, which show a combined climate and anthropogenic control on fire (Hantson et al., 2015; Kitzberger et al., 2022), reinforcing the interconnectedness of these factors.

5.2 Vegetation and fire regime changes over the last 21 ka

5.2.1 Northern Neotropics (NNeo)

During the LGM, high levels of tree cover and weak fire regimes (Fig. 5d,e) are consistent with estimates of 4–5°C drop in mean annual temperatures (Correa-Metrio et al., 2012) and wet conditions (Hodell et al., 2008; Deplazes et al., 2013; Fig. 5a,c). Throughout the deglaciation, a marked decrease in tree cover and intensification of the fire regime relate to predominant drier phases promoted by southward displacements of the ITCZ associated with millennial-scale events (HS1 and the YD) (Fig. 5b,c) (Deplazes et al., 2013; Haug et al., 2001). The wetter interval linked to BA/ACR (Deplazes et al., 2013; Fig. 5b) is not clearly detected in our analyses. Additionally, human occupation in the NNeo began during the late Pleistocene (Ardelean et al., 2020), although in smaller populations (Fig. 5d), and likely started contributing to environmental changes. These combined changes importantly affected megafaunal populations in NNeo, yet the implications of their decline and subsequent extinction for fire and vegetation dynamics remain unclear (Dávila et al., 2019; Rozas-Davila et al., 2021). Nevertheless, late Pleistocene tree cover and fire dynamics suggest predominant hydroclimate control (Fig. 5b-f) and an overall negative correlation between tree cover and fire activity (Fig. A2a) suggests moisture-limited conditions for fire.

At the onset of the Holocene, during the EH, a marked shift towards expansion of tree cover and minimum fire activity (Fig. 5 e,f; Fig. A2a) were induced by increasing wetter conditions (Haug et al., 2001; Hodell et al., 2008). During this period, human populations began engaging in agricultural activities, domesticating maize and squash by ca. 9 ka (Piperno et al., 2009), likely impacting local fire regimes. However, the gradual long-term tree cover decrease and fire activity increase synchronous with a progressive transition to drier conditions (Haug et al., 2001), still suggest a main climatic driver from the EH until ca. 4 ka (Fig. 5b,e,f). From ca. 4 ka onwards, the expanding anthropogenic pressure in Central America became a clear driver of vegetation and fire changes (Fig. 5d) (Harvey et al., 2019; Leyden, 2002). The LH drop in tree cover decouples from the more gradual climate-driven decrease observed since the onset of the Holocene (Fig. 5a,e; Fig. A2a). This latter shift in AP is coeval with the demographic expansion of Mesoamerican populations (Fig. 5d). Fire

activity also stays relatively high during this period (Fig. 5f). At ca. 1.2 ka, the increase in tree cover and decrease of fire activity was possibly related to the rapid decrease in populations likely associated with the collapse of the Maya civilization (Gill et al., 2007; Haug et al., 2003).

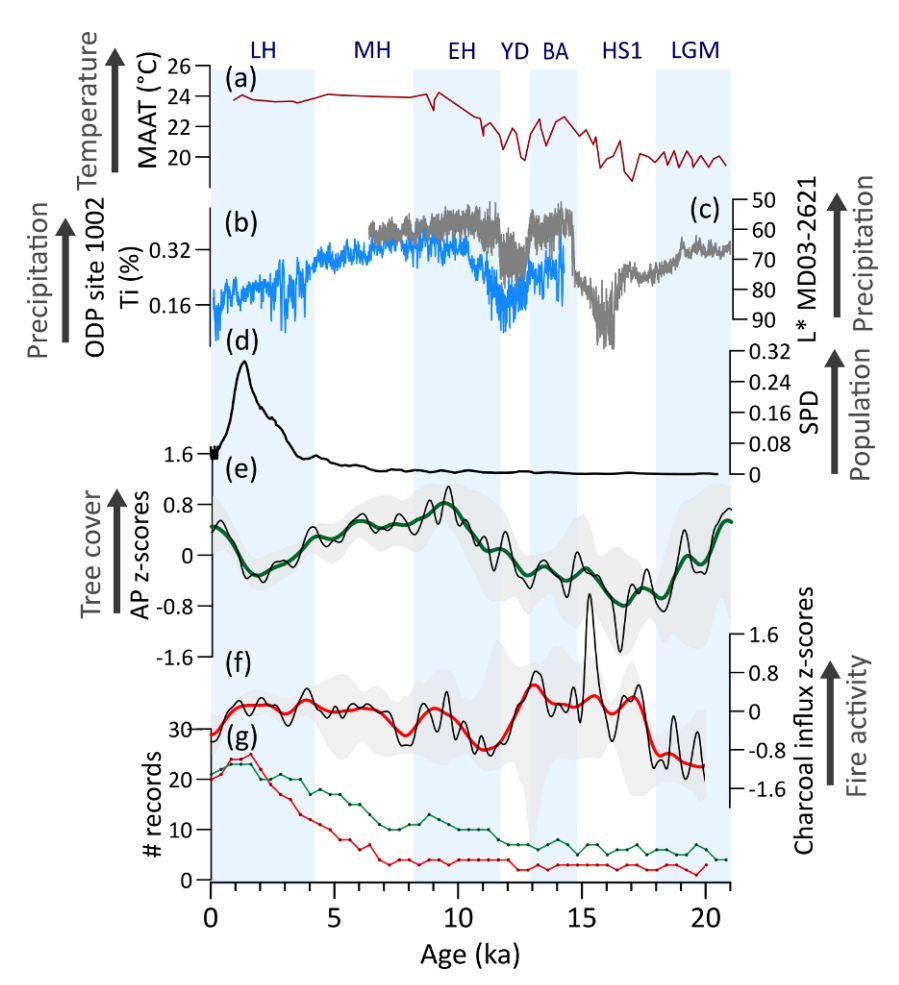


Fig. 5 – Northern Neotropics (NNeo) vegetation, fire, climate regimes, and human populations: (a) Pollen-based mean annual air temperature reconstruction from Petén-Itzá core PI-06 (Correa-Metrio et al., 2012). (b) Bulk sediment Ti content (Haug et al., 2001) and (c) bulk sediment reflectance (Deplazes et al., 2013) for Cariaco Basin. (d) Summed probability density (SPD) of ¹⁴C ages from archeological sites in Central America (MesoRad, 2020) and northern South America (Goldberg et al., 2016) (N = 1788). (e) Arboreal pollen (AP) and (f) charcoal influx z-scores composites using 1000-yr (green and red, respectively) and 400 yr (black) smoothing half-window. Gray areas represent 2.5th and 97.5th confidence intervals. (g) Number (#) of records with available pollen (green) and charcoal (red) data in a 400-yr time bin.

5.2.2 Amazonia

415

420

430

The gigantic extent of Amazonia and its equatorial positioning results in heterogeneous meridional and zonal environmental patterns for the region. Limited number of records in the LGM and deglacial period results in poor spatial and temporal constraints of tree cover and fire activity variability, thus preventing a generalization and detailed assessment of the observed patterns (Fig. 6f). Additionally, caution is needed when interpreting vegetation changes from fluvial and floodplain records, as edaphic factors, rather than climate, may control the observed patterns.

During the LGM, the region featured reduced tree cover, mainly at the ecotones and eastern areas, and weak fire activity (Fig. 6e,f), although its western and core regions remained mostly forested (Akabane et al., 2024; Colinvaux et al., 1996; Haberle and Maslin, 1999; Urrego et al., 2005). This pattern of low tree cover was likely a response to 4–6 °C colder

temperatures (Bush et al., 2001; Colinvaux et al., 1996; Stute et al., 1995), low CO_{2atm} (Fig. 6a) (Bereiter et al., 2015), and reduced rainfall in eastern Amazonia (Fig. 6b,c) (Häggi et al., 2017; Wang et al., 2017). Reduced fire activity, despite low tree cover, may also have been a consequence of colder conditions and reduced convective activity, which would result in fewer lightning ignitions, and absence of widespread human impacts.

435

440

445

460

During the deglacial period, our data indicate oscillating tree cover patterns during HS1 and highest deglacial AP values by 13–12 ka, coinciding with minimum fire activity (Fig. 6e,f), an intensified SASM (Cheng et al., 2013; Mosblech et al., 2012) and increased CO_{2atm} (Fig. 6a,b). These pronounced oscillations in AP and charcoal z-scores may arise from contrasting meridional changes in precipitation patterns associated with millennial-scale events. For instance, during HS1 and the YD, while drier conditions expanded over northern Amazonia (Akabane et al., 2024; Deplazes et al., 2013; Zular et al., 2019), southern areas experienced wetter conditions (Campos et al., 2019; Mosblech et al., 2012; Novello et al., 2017). The subsequent EH decline in AP was likely driven by a weakening of the SASM and the stepwise increase in fire activity (Fig. 6e,f), which was mainly concentrated to the eastern and southern areas (Gosling et al., 2021) and may have played an important role in reducing tree cover over ecotones. Moreover, the end of the Pleistocene marks the beginning of human occupation of the Amazon basin, which increased in the EH (Fig. 6d), when they were already engaging in resource management practices (Neves et al., 2021). The impacts of megafaunal extinction also initiated long-term changes in both nutrient distribution and species turnover (Doughty et al., 2013, 2016a). However, its correlation with overall tree cover and fire regime changes remains elusive for the region.

During the MH, a stepwise increase in tree cover is recorded at 7 ka, mostly reflecting forest expansion in northern Amazonia (Behling and Hooghiemstra, 2000) and coinciding with monsoon strengthening (Fig. 6b,e). Meanwhile, some increase in fire activity, amid forest expansion and progressively wetter conditions, may relate to expanding human populations in Amazonia (Cordeiro et al., 2014; Gosling et al., 2021; Riris and Arroyo-Kalin, 2019). The absence of a clear decrease in tree cover as consequence of anthropogenic activity is likely due to agroforestry practices that allowed for long fallow periods and forest recovery (Iriarte et al., 2020).

In the LH, gradual tree cover expansion is mainly driven by the southward forest expansion that formed the modern extent of the rainforest (Fontes et al., 2017; Mayle et al., 2000) associated with a further intensification of monsoon strength (Baker and Fritz, 2015) and moisture increase. Some increase in fire activity after ca. 3 ka has been potentially favored by dryness associated to intensifying ENSO activity (Kanner et al., 2013; Mark et al., 2022) in combination to expanding human populations (Fig. 6d). The decline in fire activity over the last 0.5 ka coincides with the indigenous demographic collapse following the European contact (Fig. 6d,f).

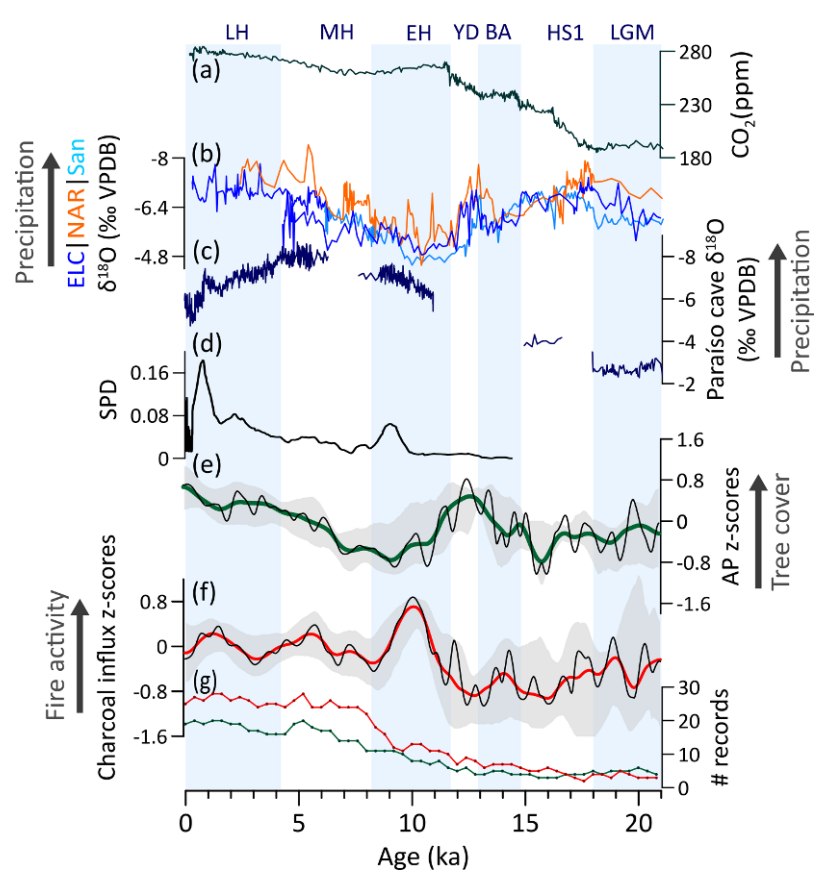


Fig. 6 – **Amazonia vegetation, fire, climate regimes, and human populations: (a)** Atmospheric concentration of CO₂ (Bereiter et al., 2015). Speleothem δ¹⁸O from **(b)** El-Condor (ELC), Cueva del Diamante (NAR), and Santiago (San) caves in western Amazonia (Cheng et al., 2013; Mosblech et al., 2012) and from **(c)** Paraíso cave in eastern Amazonia (Wang et al., 2017). **(d)** Summed probability density (SPD) of ¹⁴C ages from archeological sites (N = 732) (Araujo et al., 2025). **(e)** Arboreal pollen (AP) and **(f)** charcoal influx z-scores composites using 1000-yr (green and red, respectively) and 400 yr (black) smoothing half-window. Gray areas represent 2.5th and 97.5th confidence intervals. **(g)** Number (#) of records with available pollen (green) and charcoal (red) data in a 400-yr time bin.

5.2.3 Tropical Andes (TrAn)

465

470

475

480

485

Climate changes in the Andes were heterogeneous and asynchronous (Bush and Flenley, 2007). During the LGM, predominating open vegetation (Fig. 7e) was likely controlled by 5–8 °C cooler-than-modern temperatures exerting the main limiting factor for tree cover development, even though moist conditions prevailed (Baker et al., 2001; Bush et al., 2004; Cheng et al., 2013; Paduano et al., 2003; Valencia et al., 2010) (Fig. 7a,b). Subsequently, TrAn saw an increase in arboreal taxa from 18 to 14.8 ka, when the region became warmer and significantly wetter (Fig. 7a) (Martin et al., 2018; Palacios et al., 2020). Despite uncertainties related to the limited number of records, a slight fire increase in the second part of HS1 may have resulted from higher biomass availability (Fig. 7d). From 14 to 12.9 ka, pervasive decrease in tree cover throughout the BA/ACR until the onset of the YD likely relate to drier conditions in the southern TrAn and overall glacier expansion (Jomelli et al., 2014), which is then followed by a tree cover recovery throughout the YD potentially associated to further warming and the return of wetter conditions (Fig. 7a,d). Positive correlation of increasing fire activity throughout the LGM and deglacial period along with increasing trends of tree cover (Fig. A2c) point to fuel-limited conditions for fire, although prevailing wet conditions during the late Pleistocene may have also played a key role in restraining fire (Fig. 7a,b).

During the EH, tree cover achieved its highest elevation during the Holocene (Fig. 7a). This tree cover increase was likely maintained by warmer temperatures and rising of the tree line, despite relatively drier conditions in response to a weaker

SASM, as suggested by δ^{18} O data from ice cores and speleothems (Cheng et al., 2013; Thompson et al., 1998; Vuille et al., 2003) (Fig. 7a). As in NNeo and Amazonia, evidence for human agricultural activities in TrAn began during this period (Pagán-Jiménez et al., 2016). Additionally, an overall decline of megafauna in tropical Andes resulted in sensitive ecological consequences associated with vegetation turnover, e.g., the encroachment of both palatable and woody taxa, as well as fuel build-up (Bush et al., 2022; Pym et al., 2023). Several interacting factors, such as warming, hydroclimate changes, initial expansion of human populations, and megafaunal decline, collectively contributed to intensifying the fire regime in the region (Bush et al., 2022; Pym et al., 2023) (Fig. 7f). Consequently, increased fire activity hampered further development of a continuous tree cover above the tree line resulting in a sharper vegetation boundary (Rehm and Feeley, 2015). This suggests a complex interplay of abiotic and biotic drivers shaping the observed pattern.

490

495

500

505

510

515

520

The MH is characterized by a stepwise intensification of the fire regime, with tree cover only showing a slight decreasing trend, as indicated by our regional-integrating AP composite (Fig. 7d,e). However, subdividing TrAn at 8 °S in northern and southern sectors reveals distinct trends (Fig. A3): while fire activity increased across both regions, tree cover remained stable in the north but declines in the south. These trends are consistent with heterogeneous hydroclimatic patterns along Andes, with drier conditions recorded by lowered lake levels, mainly in the Altiplano (Baker et al., 2001; Bush and Flenley, 2007; Hillyer et al., 2009) and persistent wet conditions recorded in central sectors of the TrAn (Bustamante and Panizo, 2016; Cheng et al., 2013; Polissar et al., 2013) (Fig. 7a). Modern climate patterns indicate that anomalies in equatorial Pacific SST can produce different regional impacts in precipitation by affecting moisture-laden easterlies and the Bolivian High (Garreaud et al., 2003; Poveda et al., 2020; Vuille, 1999). For instance, reduced ENSO variability has been suggested to decrease moisture balance in parts of the Andes, particularly in the southern TrAn, parts of the northern TrAn and NNeo (Fig. A3; Fig. 7c) (Polissar et al., 2013). Accordingly, a potential correspondence between the zonal Pacific SST gradient anomaly and tree cover trends during the EH and MH may exist for southern TrAn but not for northern TrAn (Fig. A3). Furthermore, while $\delta^{18}O$ in ice and speleothem cores and δD from lake sediments primarily reflect rainy season precipitation (Cheng et al., 2013; Fornace et al., 2014; Vuille et al., 2003), fluctuations in lake levels are influenced by annual precipitation (Theissen et al., 2008). This may alternatively suggest that despite a gradual increase in summer precipitation throughout the Holocene, the MH featured a decrease in annual precipitation over the Altiplano. Nevertheless, the maintenance of tree cover was also favored by the persistence of moist microclimates (Ledru et al., 2013; Nascimento et al., 2019). These conditions, as well as anthropogenic activities, would have favored a regional intensification of the fire regime and decline in tree cover. By ca. 6 ka, agropastoral systems based on maize agriculture and llama herding became widespread (Nascimento et al., 2020).

The LH marks a major decrease in tree cover and high fire activity in the whole TrAn (Fig. 7c), probably related to the expansion of human impacts in the region and increasing sedentism (Goldberg et al., 2016; Valencia et al., 2010). Anthropogenic activity likely maintained fire activity at similar rates to the previous MH dry phase (Fig. 7f) despite moisture increase, maintaining a lowered and sharper tree line (Schiferl et al., 2023). During the last 0.5 ka, tree cover expansion and decreased fire activity may point to the abandonment of sites as consequence of the European contact and demographic collapse in the region (Koch et al., 2019).

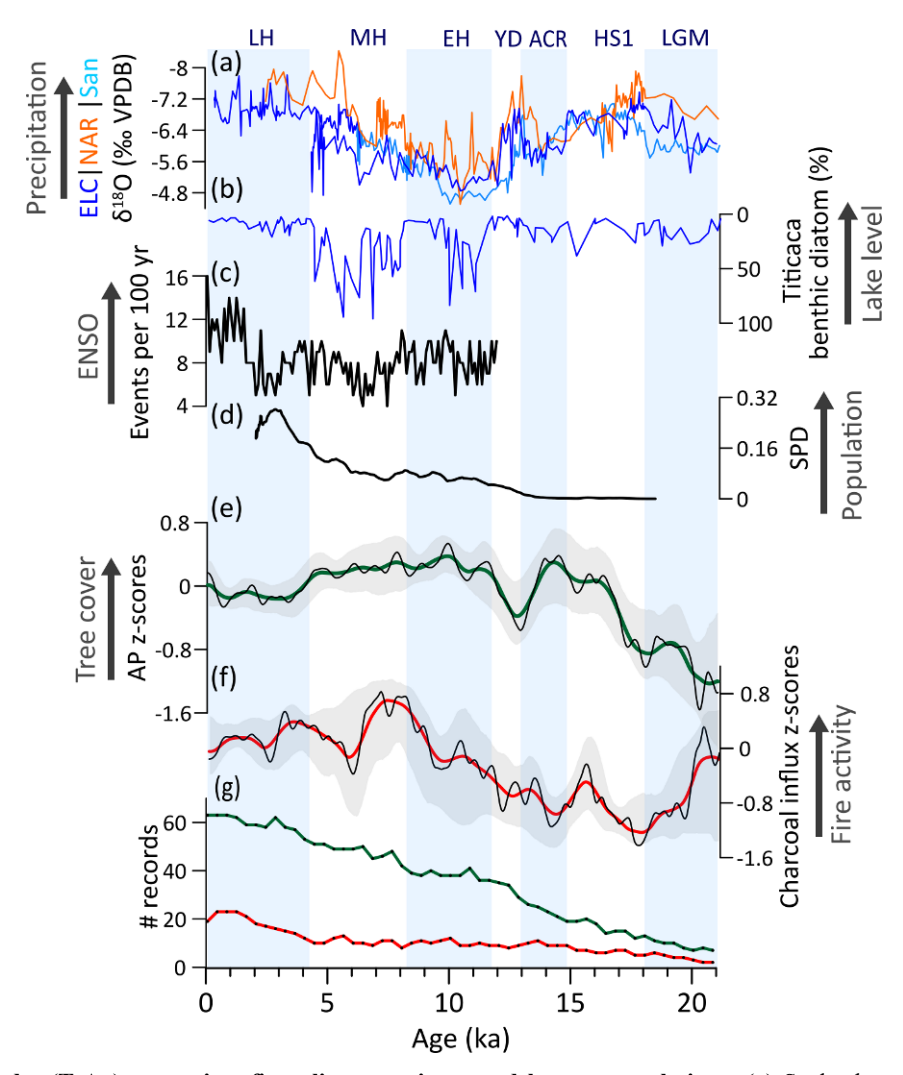


Fig. 7 – Tropical Andes (TrAn) vegetation, fire, climate regimes, and human populations: (a) Speleothem δ¹⁸O from El-Condor (ELC), Cueva del Diamante (NAR), and Santiago (San) caves (Cheng et al., 2013; Mosblech et al., 2012). (b) Freshwater benthic diatom (%) from Titicaca Lake (Baker et al., 2001). (c) Summed density probability of ¹⁴C ages from archeological sites in TrAn (Goldberg et al., 2016) (N = 949). (d) Arboreal pollen (AP) and (e) charcoal influx z-scores composites using 1000-yr (green and red, respectively) and 400 yr (black) smoothing half-window. Gray areas represent 2.5th and 97.5th confidence intervals. (f) Number (#) of records with available pollen (green) and charcoal (red) data in a 400-yr time bin.

5.2.4 Northeastern Brazil (NEB)

525

530

535

540

In NEB, the scarcity of records decreases the precision and accuracy of the observed trends (Fig. 8f) and prevents producing a composite curve using charcoal data. Therefore, we only discuss major features of tree cover and fire dynamics.

During the LGM, the region experienced low tree cover driven by prevailing dry conditions (Cruz et al., 2009; Dupont et al., 2001; Mulitza et al., 2017). The deglaciation period is marked by tree cover expansion, associated with phases of southward displaced ITCZ during HS1 and YD (Fig. 8a,b,d) (Bouimetarhan et al., 2018; Cruz et al., 2009; Dupont et al., 2001; Mendes et al., 2019; Venancio et al., 2020). These periods featured the onset of forest corridors connecting Amazon and Atlantic forests and decreased fire activity during YD (Bouimetarhan et al., 2018; Dupont et al., 2009; Ledru and de Araújo, 2023; De Oliveira et al., 1999), which is depicted as the interval with highest AP z-scores over the last 21 ka (Fig. 8d).

During the EH, decrease in tree cover is likely a consequence to both climate changes and increasing human impacts. This period features drier conditions relative to YD in northern NEB due to the northward displacement of the ITCZ (Fig. 8a) (Mendes et al., 2019; Prado et al., 2013a; Venancio et al., 2020) and the expansion of human populations in the region (Araujo et al., 2025) (Fig. 8c). In the subsequent MH period, increasing trends in tree cover (Fig. 8d) may reflect relatively wet conditions due to a weak Nordeste Low (Cruz et al., 2009; Prado et al., 2013b) (Fig. 8b) and southward shifted seasonal migration range of the ITCZ (Chiessi et al., 2021), in addition to decreased human populations in inland parts of NEB (Araujo et al., 2025) (Fig. 8c). The LH was marked by a decrease in tree cover and intensification of the fire regime, likely in response to the establishment of the modern semiarid conditions over most NEB (Chiessi et al., 2021; Cruz et al., 2009; Utida et al., 2020) and rapid increase in human populations (Fig. 8c) (Araujo et al., 2025).

The relationship between tree cover and fire in the NEB remains elusive due to the limited number of records (Fig. 8e). Charcoal records suggest a negative correlation between tree cover and fire (Fig. 8f). This observation, however, is apparently counterintuitive, given that Caatinga currently exhibits the opposite pattern (fuel-limited conditions), where the lack of fuel inhibits fire activity (Argibay et al., 2020) (Fig. 4a,c). We propose two potential explanations for this apparent discrepancy. First, the fire records are located at the margins of the semiarid region, thus capturing influences from adjacent tropical savannas and forests, rather than exclusively reflecting xeric vegetation-fire dynamics. Second, increasing human occupation during the LH (Fig. 8c) may have intensified burning activities, even as natural fire frequencies declined. While NEB contains the earliest evidence of human occupation of the Americas (Boëda et al., 2014), only the LH saw a proliferation of more sedentary, possibly agricultural, ceramic-producing societies (Oliveira, 2002).

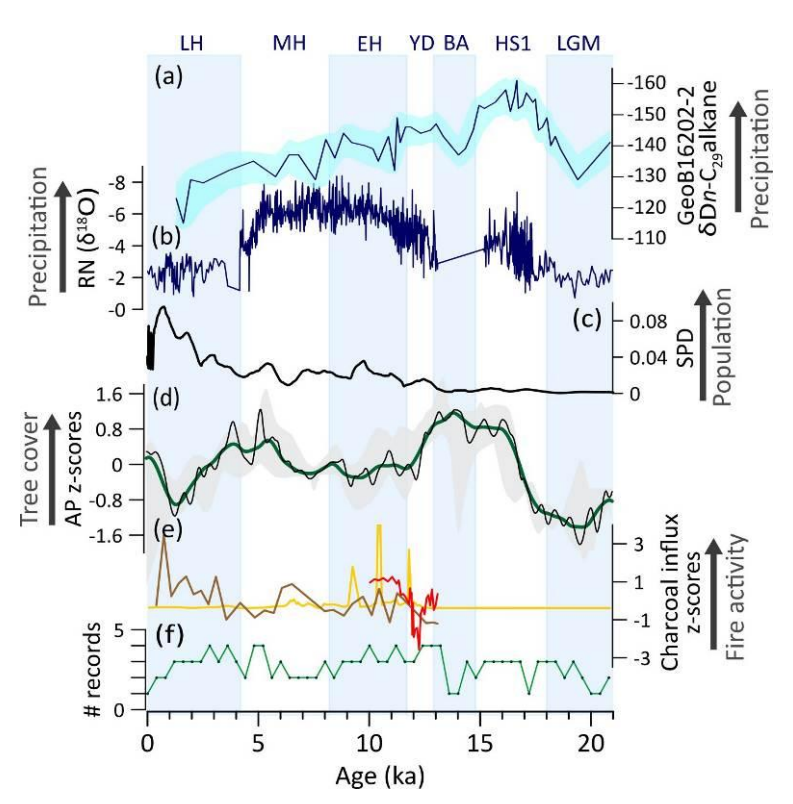


Fig. 8 – Northeastern Brazil (NEB) vegetation, fire, climate regimes, and human occupation: (a) δD n- C_{29} alkane from GeoB16202-2 (Mulitza et al., 2017). (b) Speleothem $\delta^{18}O$ from Rio Grande do Norte cave (RN) (Cruz et al., 2009). (c) Summed density probability of ^{14}C ages from archeological sites in NEB (N = 542) (Araujo et al., 2025). (d) Arboreal pollen (AP) z-scores composites using 1000-yr (green) and 400 yr (black) smoothing half-window. Gray areas represent 2.5th and 97.5th confidence intervals. (e) charcoal influx z-scores from single sites (yellow: Ledru et al., 2006; brown: De Oliveira et al., 1999; red: Bouimetarhan et al., 2018). (f) Number (#) of records with available pollen data in a 400-yr time bin.

5.2.5 Central-eastern Brazil (CEB)

580

585

590

During the LGM, tree cover and fire activity exhibit high trends; however, the scarcity of records hampers a regional generalization and underscores the need for additional data from this period (Fig. 9f). During the deglacial period, high tree cover and low fire activity trends were favored by periods of intensified rainfall in the region, i.e., HS1 and the YD (Fig. 9a,b,d,e) (Campos et al., 2019; Martins et al., 2023; Meier et al., 2022; Stríkis et al., 2015, 2018), which allowed the widespread migration of cold- and moist-adapted tree taxa through central Brazil (Pinaya et al., 2019). An increase in fire activity centered in ca. 16.5 ka may result from a short dry incursion during HS1 (Stríkis et al., 2015), which has yet to be confirmed, as the scarcity of data prevents detailed assessment of the observed pattern (Fig. 9e).

Our compilation suggests a prevailing decrease in tree cover and intensification in fire activity from the YD to the EH (Fig. 9d,e). These trends were likely a response to a weaker SASM/SACZ led by low austral summer insolation, which yielded drier conditions in the region (Cruz et al., 2005; Prado et al., 2013a; Wong et al., 2023). The stepwise increase in fire activity, peaking at ca. 10.5 ka, further contributed to the tree cover rapid decrease (Fig. 9d,e). Additionally, human activity probably also contributed to tree cover and fire trends during this period, as archaeological records show well-established occupations from ca. 13 ka onwards and expanding population in the EH (Fig. 9c) (Araujo et al., 2025; Strauss et al., 2020). Furthermore, the megafauna functional extinction during this period likely initiated long-term changes in vegetation composition (Raczka et al., 2018) and potential increase of fuel loads (as in Gill, 2014). This effect, however, seems to have been secondary, as a decrease in tree cover is opposite to the expected response by megafaunal extinction alone (Doughty et al., 2016b; Macias et al., 2014).

Throughout the MH and the LH, the progressive increase in rainfall driven by a progressive strengthening of the SACZ (Cruz et al., 2005; Meier et al., 2022) (Fig. 9b) favored the expansion of tree cover and the attenuation of fire activity (Fig. 9d,e). In the LH, despite a second wave of human impacts in the region after an occupation hiatus in the MH (Araujo et al., 2005, 2025), tree cover exhibits a continuous increase and fire activity a decreasing trend (Fig. 9c,d,e).

In CEB, long-term tree cover changes are negatively correlated with fire activity (Fig. 9d,e, Fig. A2d). This pattern points to a feedback mechanism in which herbaceous vegetation facilitates fire activity, while fire, in turn, contributes to the dominance of herbs by limiting tree encroachment. Conversely, moisture-driven development of woody formations leads to the suppression of fire, which further contributes to tree cover expansion (Fig. 9d,e).

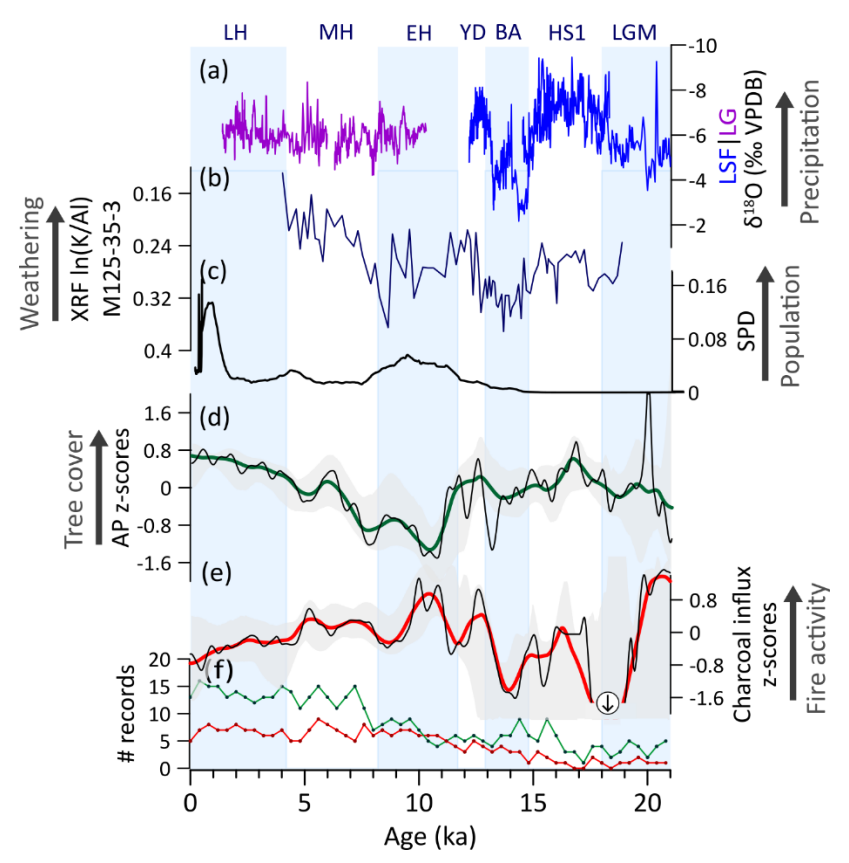


Fig. 9 – Central-eastern Brazil (CEB) vegetation, fire, climate regimes, and human occupation: (a) Speleothem δ^{18} O from Lapa sem Fim (LSF) and Lapa Grande (LG) caves (Stríkis et al., 2011, 2018). Downcore $\ln(K/Al)$ from marine sediment core M125-35-3, which reflects changes in the clay mineral composition and increases with chemical weathering intensity and hence, moisture availability (Meier et al., 2022). (b) Summed density probability of 14 C ages from archeological sites in CEB (N = 481). (c) Arboreal pollen (AP) and (d) charcoal influx z-scores composites using 1000-yr (green and red, respectively) and 400 yr (black) smoothing half-window. Charcoal z-score negative anomaly reaching -2.2 is indicated by a circled arrow. Gray areas represent 2.5th and 97.5th confidence intervals. (e) Number (#) of records with available pollen (green) and charcoal (red) data in a 400-yr time bin.

5.2.6 Southeastern South America (SESA)

During the LGM, the low arboreal pollen z-scores reflect the dominating open physiognomies (Fig. 10c) (Behling, 2002b; Gu et al., 2018), despite moist conditions sustained by a strong SASM/SACZ influence (Cruz et al., 2005). This predominating open vegetation was likely controlled by 3–7 °C lower temperatures (Behling, 2002a; Chiessi et al., 2015) and reduced CO_{2atm} levels (Fig. 10a,b) (Bereiter et al., 2015). Moreover, stronger Antarctic cold fronts may have shifted the woody savanna and forest boundaries further north, favoring the prevalence of open grasslands. The presence of a diverse megafauna potentially contributed by restricting both woody encroachment and fuel accumulation (Furquim et al., 2024; Macias et al., 2014; Prates and Perez, 2021; da Rosa et al., 2023). The combination of low woody biomass, higher impact of herbivory, cold and moist conditions restricted fire activity during this period (Fig. 10f). The long-term and gradual trend of tree cover expansion and fire intensification from the LGM to the EH suggests that scarcity of fuel was a limiting factor for fire activity during the Pleistocene (positive tree cover-fire correlation) (Fig. 10e,f, Fig. A2e). Alternatively, or concurrently, both trends may have been driven by progressive deglacial warming. Notably, our composite curves of tree cover and fire activity show no clear correlation with millennial-scale hydroclimate variability throughout most of the late Pleistocene, suggesting that moisture availability was not the primary driver, with temperature and CO_{2atm} exerting greater control. However, Campos et al. (2019) suggested that no generalized increase in precipitation occurred in SESA during

HS1 and the YD. Furthermore, while human occupation began at ca. 14-13 ka in the region, impacts were likely still limited (Araujo et al., 2025; Araujo and Correa, 2016; Suárez, 2017).

620

625

630

635

640

During the EH, a peak in fire activity (Fig. 10f) was facilitated by the availability of biomass coupled with warmer temperatures and relatively drier conditions (Fig. 10b,c,e,f). The intensified fire regime, on the other hand, probably contributed to the retraction of forest formations during this period (Fig. 10e,f). Throughout the Holocene, a continuous increase in arboreal biomass decoupled from CO_{2atm} and temperature trends suggests a forest expansion mainly driven by increasing precipitation and the gradual suppression of fire activity (Fig. 10c,e,f). The extinction of megafauna by the end of the EH potentially contributed, at least in part, to the expansion of woody taxa (Behling et al., 2023; Macias et al., 2014). From 6 to 3.5 ka, the continuous expansion of tree cover is slowed down, coinciding with a peak in fire activity and expanding human populations in the region (Fig. 10d-f). In the last 2 ka, despite an increase in human populations, tree cover and fire activity do not exhibit a clear response.

The Pleistocene to Holocene transition likely represents a transition from temperature/ CO_{2atm} -limited to moisture-limited conditions, when an inflexion in the correlation of tree cover and fire is observed (Fig. A2e). Over the 21-kyr analyzed period, tree cover and fire activity show a positive correlation with both increasing in the long-term but with a negative correlation on detrended data (r = -0.48, p < 0.001, not shown) (Fig. 10c,d). This suggests different relationships at different timescales. In the long-term, either the strengthening of the fire regime was driven by increase in fuel availability from woody biomass, or both tree cover and fire responded to the same external forcing (i.e., deglacial warming). In the short-term, fire events likely acted as a limiting factor for tree cover development.

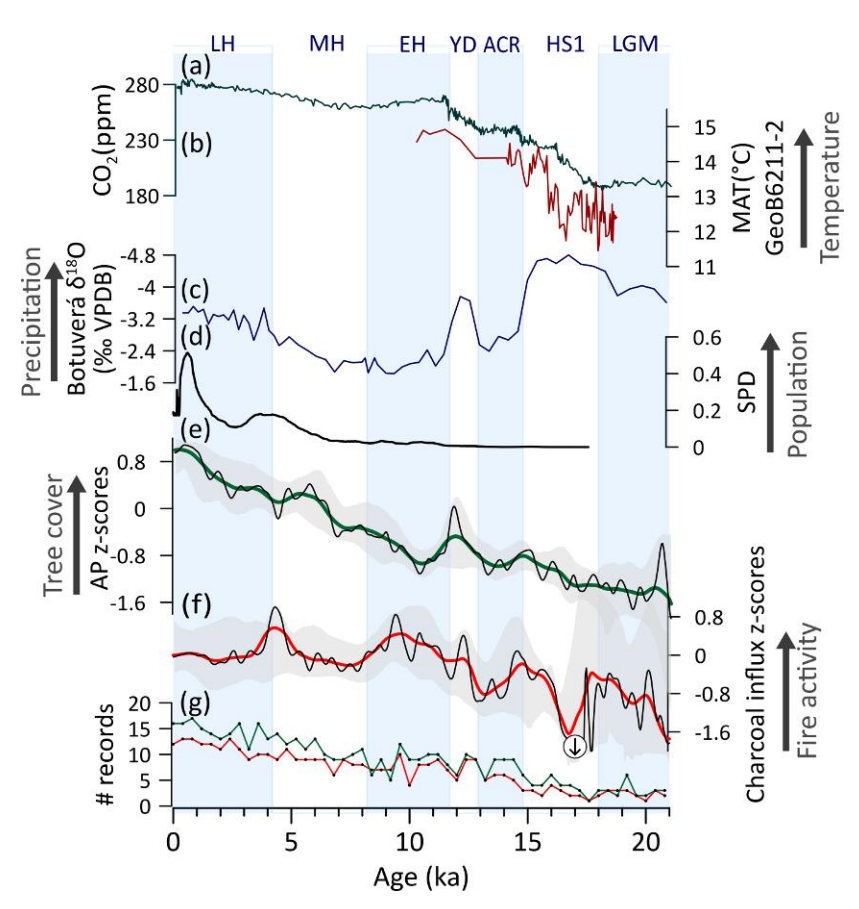


Fig. 10 – Southeastern South America (SESA) vegetation, fire, climate regimes, and human occupation: (a) Atmospheric concentration of CO₂ (Bereiter et al., 2015). (b) Estimated mean annual temperature (Chiessi et al., 2015). (c) Speleothem δ^{18} O from Botuverá cave (Wang et al., 2007). (d) Summed density probability of 14 C ages from archeological sites in SESA (N = 1701) (Araujo et al. 2025). (e) Arboreal pollen (AP) and (f) charcoal influx z-scores composites using 1000-yr (green and red, respectively) and 400 yr

(black) smoothing half-window. Gray areas represent 2.5th and 97.5th confidence intervals. **(g)** Number (#) of records with available pollen (green) and charcoal (red) data in a 400-yr time bin. Large charcoal negative anomaly extending beyond -2 is indicated by a circled arrow.

5.2.7 Extratropical Andes (ExTrAn)

645

650

655

660

665

670

675

680

During the LGM, ExTrAn was characterized by open physiognomies and a weak fire regime (Fig. 11e,f). This was likely consequence of significantly cold conditions (Fig. 11a,b) (Massaferro et al., 2009), while both wet and dry conditions have also been suggested along ExTrAn (Montade et al., 2013; Moreno et al., 2018). After ca. 18 ka, tree cover increases along with warming temperatures (Kaiser et al., 2005) and rising CO_{2atm} (Fig. 11a,b), with an accelerated tree cover increase during HS1 coinciding with a warming phase and retreating glaciers in the region (Fig. 11b,e,f) (Barker et al., 2009; Kaiser et al., 2005; Moreno et al., 2015; Palacios et al., 2020). This warming period also coincides with evidences of human presence in the region (Dillehay et al., 2015). Fire activity features a stepwise increase from 13.8 to 12 ka, corresponding to the second deglacial warming phase (Fig. 11a,b,e), under decreasing, albeit still high, precipitation levels (Montade et al., 2019) and drier summers (Moreno, 2020). This threshold in the fire regime was likely induced by warming temperatures and availability of biomass. The positive correlation between woody biomass and fire activity supports a fuel-limited fire regime in the region, and/or suggests that observed increases in tree cover and fire activity were both driven by deglacial warming (Fig. A2f). Nevertheless, peak fire activity in the region is currently achieved at intermediate levels of both woody and herbaceous biomass (Holz et al., 2012), supporting the role of increasing woody vegetation in creating optimal conditions for fire. This is also suggested by the relevant contribution of wood charcoal in lakes from the region (Whitlock et al., 2006). Human populations only started to expand after the ACR and likely also contributed to the intensification of the fire regime (Fig. 11d) (Perez et al., 2016; Salemme and Miotti, 2008). At ca. 13-12 ka, Nothofagus emerges as the predominant taxon and marks the widespread expansion of temperate forests. This expansion exhibited latitudinal variability, with a gradual trend in southern areas and a steeper increase after 15 ka in northern regions (Nanavati et al., 2019). As a result of combined human pressure and environmental changes, the extinction of megaherbivores could have contributed to arboreal growth and fuel accumulation; however, the extent of this impact is still unclear (Abarzúa et al., 2020; Villavicencio et al., 2016).

During the EH, peak fire activity potentially contributed to the deacceleration of tree cover expansion (Fig. 11d,e), which were both favored by a decrease in moisture due to the weakened and poleward shifted Southern Westerly Winds (SWW) (Lamy et al., 2010; Moreno et al., 2021; Nehme et al., 2023) (Fig. 11c) coupled with relatively warmer conditions. The EH climate amelioration also allowed human populations to spread and colonize other localities in the region (Miotti and Salemme, 2003; Perez et al., 2016; Salemme and Miotti, 2008), expanding its contribution to increased fire activity. In the MH, the expansion of forests and decrease in fire activity (Fig. 11e,f) was potentially driven by increased moisture due to a strengthening and equatorward shift of the northern boundary of the SWW (Fig. 1c,d) (Razik et al., 2013; Villa-Martínez et al., 2003) and reduced ENSO (Mark et al., 2022; Rein et al., 2005). Unlike other regions of South America (e.g., TrAn, CEB, NEB), the MH marks a rapid growth in human populations in ExTrAn, which continued through the LH and may have benefited from expanding forests (Fig. 11e) and consequent increase in availability of resources. By 5.5 ka, the region experiences the highest tree cover, whereas fire activity attains peak values after 3.5 ka, concurrent with a major expansion of human populations (Perez et al., 2016) and intensification of ENSO variability (Mark et al., 2022; Rein et al., 2005; Whitlock et al., 2006).

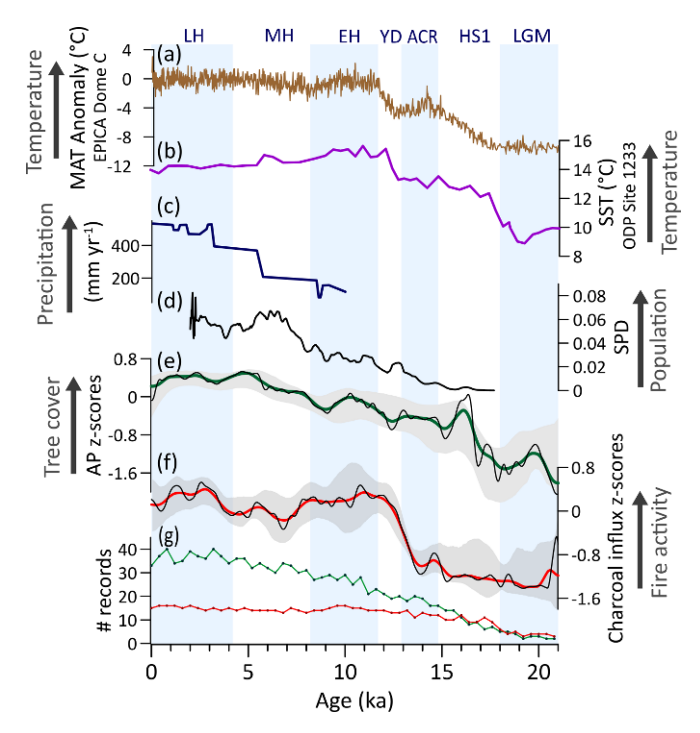


Fig. 11 – Extratropical Andes (ExTrAn) vegetation, fire, climate regimes, and human occupation: (a) Surface mean annual temperature anomaly reconstructed from EPICA Dome C, Antarctica (Jouzel et al., 2007). (b) Sea surface temperature reconstruction for the eastern South Pacific (Kaiser et al., 2005). (c) Rainfall estimates from Lake Aculeo (34°S; northern portion of the Southern Westerly Winds) based on multiproxy lake-level reconstructions (Jenny et al., 2003). (d) Summed density probability of ¹⁴C ages from archeological sites in ExTrAn (N = 621) (Goldberg et al., 2016). (e) Arboreal pollen (AP) and (f) charcoal influx z-scores composites using 1000-yr (green and red, respectively) and 400 yr (black) smoothing half-window. Gray areas represent 2.5th and 97.5th confidence intervals. (g) Number (#) of records with available pollen (green) and charcoal (red) data in a 400-yr time bin.

5.3 Controls on neotropical vegetation and fire regime

5.3.1 Late Pleistocene (21 – 11.7 ka)

685

690

695

700

705

The different changes in vegetation and fire activity observed across the Neotropics highlights the influence of competing and context-dependent drivers that operate on different spatial and temporal scales. In general, low levels of CO_{2atm}, such as during the LGM, reduce photosynthetic efficiency, mainly in C3 plants, limiting tree biomass potential growth and favoring C4 grasses (Boom et al., 2002; Foley, 1999; Maksic et al., 2022). A stronger impact of low CO_{2atm} is expected on vegetation in warm tropical regions (e.g., NNeo, Amazonia, CEB, NEB) compared to cold regions (e.g., ExTrAn, SESA, TrAn) (Sage and Coleman, 2001). Reduced CO_{2atm} is also suggested by modelling data to weaken the fire regime by altering availability and properties of biomass (Haas et al., 2023), while it can also increase the severity of fires by slowing post-burn tree recovery (Bond et al., 2003).

In sub- and extra-tropical latitudes (ExTrAn, SESA) and high-altitude sites (TrAn), temperatures 3–8°C lower than present likely constrained biomass growth during LGM, even in locally moist areas (Fig. 12a) (Cruz et al., 2005; Massaferro et al., 2009; Moreno et al., 2018). While cooler temperatures can improve water-use efficiency, frost events can produce long-term plant mortality and shape forest-savanna boundaries (Hoffmann et al., 2019; Inouye, 2000). Weak fire regime over these regions likely resulted from limited biomass in addition to lower temperatures and high moisture levels (Fig. 12g).

In warmer tropical regions (NNeo, Amazonia, CEB, NEB) precipitation seems to have played a pivotal role in the control of vegetation and fire dynamics. In NNeo, high tree cover and low fire activity were sustained by moist conditions (Fig. 12a,d). Strengthened SASM and an east-west precipitation dipole (wet west Amazonia and dry central-east Amazonia and NEB) (Cheng et al., 2013; Cruz et al., 2009; Kukla et al., 2023; Wang et al., 2017), led to decreased tree cover in

Amazonian ecotones and in NEB (Fig. 12a,d). In CEB, tree cover and fire patterns were heterogeneous (Fig. 12d) and influenced by both climatic and edaphic conditions. Nevertheless, colder and wetter conditions favored the increase in tree cover and migration of woody taxa across central Brazil (Pinaya et al., 2024). Fire activity remained mostly weak in tropical regions (Fig. 12g), likely constrained by low biomass availability due to reduced CO_{2atm} and dryness in NEB (fuel-limited conditions) or by persistent moisture in NNeo and western Amazonia (moist-limited conditions).

The deglaciation is marked by progressive warming (Shakun et al., 2012) and rising CO_{2atm} levels (Bereiter et al., 2015), along with substantial shifts in precipitation linked to millennial-scale events. In the Neotropics, HS1 (18-14.8 ka) and the YD (12.9-11.7 ka) were characterized by wetter conditions in south tropical latitudes (Campos et al., 2019; Meier et al., 2022; Mulitza et al., 2017) and drier conditions in north tropical latitudes (Deplazes et al., 2013; Zular et al., 2019), driven by southward ITCZ shifts. While our analyses can address the long-term trends shaped by these events, the low availability of high temporal resolution and continuous records with robust chronological control hinders a more detailed assessment of site-specific vegetation and fire anomalies over time.

Between 19 and 14.8 ka, Southern Hemisphere tropical regions (TrAn, NEB, SESA, ExTrAn) exhibit increasing tree cover and decreasing fire activity, mostly driven by rising temperatures and enhanced rainfall (Fig. 12e,h) (Campos et al., 2019; Shakun et al., 2012). In contrast, NNeo exhibits the opposite trends (Fig. 12e). In the second part of deglaciation, 14.8–11.7 ka, a generalized increase in tree cover and fire activity (Fig. 12f,i) coincides with further warming (Shakun et al., 2012) and CO_{2atm} rise (Bereiter et al., 2015). TrAn and the northern parts of ExTrAn indicate an increase in tree cover (Fig. 12f), likely related to the combination of warming and wet conditions (Baker and Fritz, 2015; Montade et al., 2019). Notably, vegetation and fire responses in NEB (wetter) and SESA (drier) may reflect the prevailing precipitation dipole pattern (Campos et al., 2022; Cruz et al., 2009; Wong et al., 2023), although lower temperatures could have still played a key role in limiting tree cover in SESA (Fig. 12c,f). The stepwise intensification in southern hemisphere fire during this period, ca. 14–13 ka, agrees with a worldwide shift in fire regime intensification (Daniau et al., 2012), indicating that warmer conditions, contingent to fuel availability, were critical for this shift.

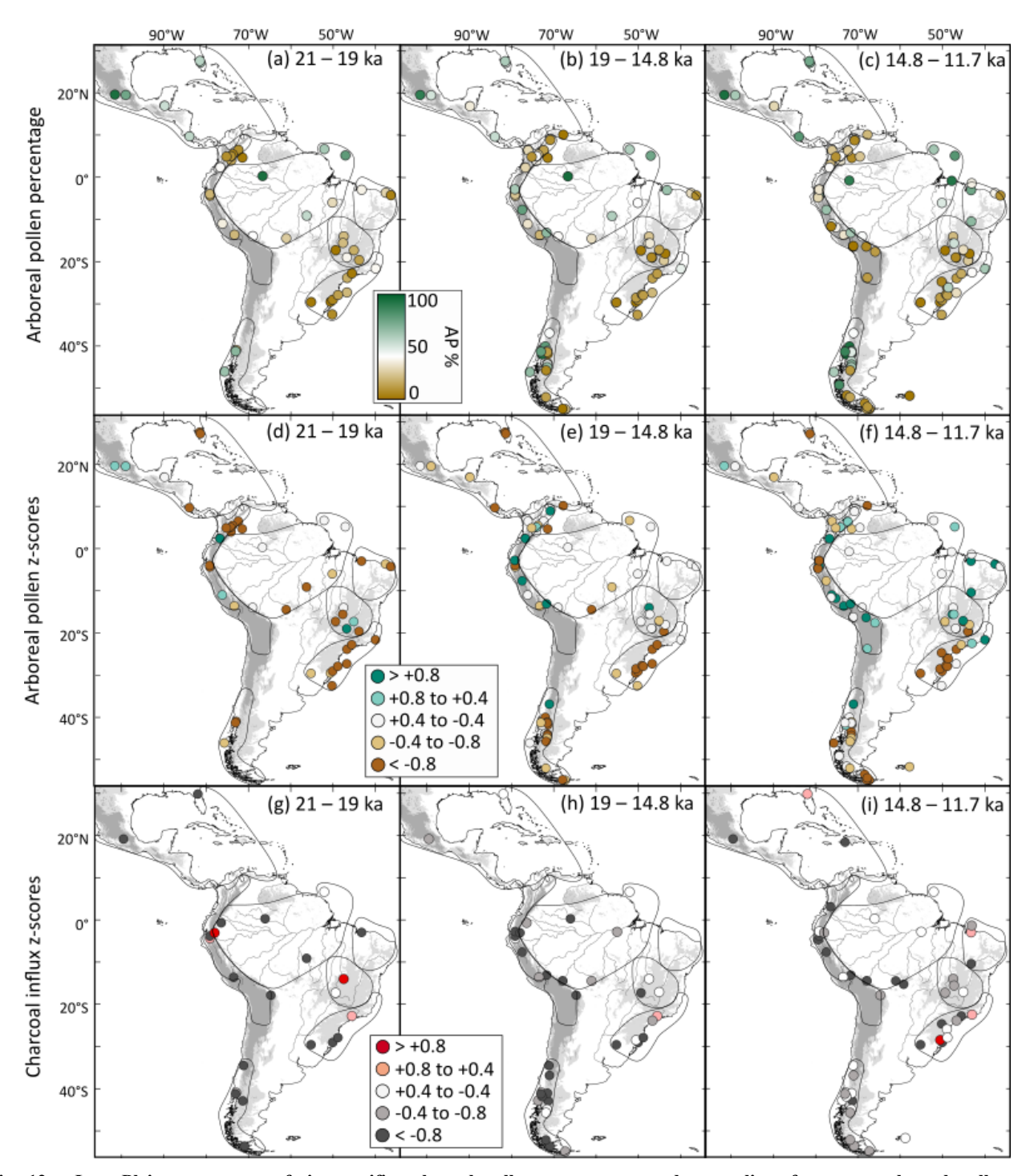


Fig. 12 – Late Pleistocene maps of site-specific arboreal pollen percentages and anomalies of average arboreal pollen and charcoal influx z-score values by time period: (a-c) arboreal pollen percentages, (d-f) arboreal pollen (AP) and (g-h) charcoal influx. Three time slices are considered: (a, d, g) Last Glacial Maximum (21 – 19 ka); (b, e, h) first part of the deglacial period encompassing the first stepwise warming (19 – 14.8 ka); (c, f, i) and second part of the deglacial period, encompassing the second stepwise warming (14.8 – 11.7 ka). Sites with positive or negative z-score anomalies indicate a record with predominantly higher or lower tree cover/fire activity than the average over the last 21 kyr. Elevations greater than 500 m are represented in light gray, while areas above 1500 m altitude are shown in dark gray. Major rivers are displayed as black lines.

5.3.2 Holocene (11.7 – 0 ka)

735

740

The greater availability of continuous records spanning the Holocene allows for a more detailed spatial assessment of vegetation and fire dynamics (Fig. 13). The similarities of tree cover and fire activity changes with precipitation shifts

suggest that moisture availability became a more important driver of Holocene vegetation and fire dynamics in the whole Neotropics.

Compared to the YD, the EH is characterized by negative tree cover trends in Amazonia, NEB, and CEB, slow tree cover increase in SESA and ExTrAn, where fire activity also increased, and opposite trends in NNeo (Fig. 13a,d,g). These changes are coherent with hydroclimate patterns related to a northward-displaced ITCZ and weaker SASM/SACZ resulting in drier conditions in most southern tropical regions (Cheng et al., 2013; Cruz et al., 2005), relatively drier but still humid northeastern Brazil (Cruz et al., 2009; Venancio et al., 2020), and wetter conditions in northern Neotropical latitudes (Haug et al., 2001). This period also featured a weaker, southward-displaced SWW, but relatively strengthened in its core (ca. 53°S) (Lamy et al., 2010), contributing to drier conditions in most of ExTrAn. Additionally, evidence of increasing human populations in Central and South America (Araujo et al., 2025; Goldberg et al., 2016; MesoRad, 2020) and plant domestication in NNeo, TrAn and Amazonia (Piperno, 2011) suggests that, although still limited, they played an active role as ecosystem engineers, influencing fire regimes and landscape dynamics.

In the MH, tree cover expanded over northern Amazonia, NEB, CEB, SESA, and ExTrAn (Fig. 13b,e). This pattern coincides with gradual precipitation changes driven by a southward expanded migration range of the ITCZ (Chiessi et al., 2021; Haug et al., 2001), a gradual intensification of the SASM/SACZ (Cheng et al., 2013; Prado et al., 2013a; Wong et al., 2023), and a weakening of the Nordeste Low (Cruz et al., 2009). The increase in fire activity over SESA and southwestern and western Amazonia during this period may have also resulted from increasing human activity over these regions (Araujo et al., 2025; Brugger et al., 2016; Lombardo et al., 2020), while in most of the southern Neotropics this period is marked by an occupation hiatus (Araujo et al., 2005, 2025). Although humans have been present in the Neotropics since the late Pleistocene (Goebel et al., 2008), their large-scale influence on tree cover and fire regimes became more pronounced by the end of MH, as consequence of a marked demographic expansion (Gill et al., 2007; Goldberg et al., 2016; Maezumi et al., 2018). This period also featured an intensification of the SWW and a northward migration of its northern boundary (Lamy et al., 2010; Razik et al., 2013) and a reduced strength/frequency of ENSO variability compared to the EH (Koutavas and Joanides, 2012; Polissar et al., 2013). This may have contributed to the ExTrAn moisture and arboreal vegetation increase and fire decrease, while in the Altiplano, centered around 12 °S, tree cover reduced and fire intensified amid dry conditions (Fig. 13e,h; Fig. A3).

During the LH, tree cover expanded in southern Amazonia, SESA, and part of CEB (Fig. 13c,f). This pattern was facilitated by increased moisture in these regions due to the strengthening of the SASM/SACZ (Cheng et al., 2013; Cruz et al., 2005). While our study did not assess for vegetation compositional changes that might highlight human impacts in these regions (Flantua and Hooghiemstra, 2023), intensified fire activity, despite increased moisture, may point to human influence. In contrast, tree cover declined in NNeo and NEB, where fire activity intensified. These declines were likely a result of both intensified human activity and climatic shifts toward drier conditions. The LH period marks the onset of semi-arid conditions in NEB (Cruz et al., 2009; Chiessi et al., 2021) and precipitation reduction in NNeo (Haug et al., 2001). Meanwhile, in TrAn, tree cover also declined despite moist conditions related to a strengthened SASM. Notably, NNeo and TrAn became densely populated during the LH, and the environmental impacts of human activities specially in these areas likely outweighed those driven by climate alone. In ExTrAn, tree cover remained relatively stable and fire activity increased, despite the rising moisture (Fletcher and Moreno, 2012; Lamy et al., 2010), also suggesting the influence of human activities in this region. In the Neotropics, numerous pollen records indicate human activity, particularly in the last 2 ka (Flantua et al., 2016; Flantua and Hooghiemstra, 2023), in line with our observations.

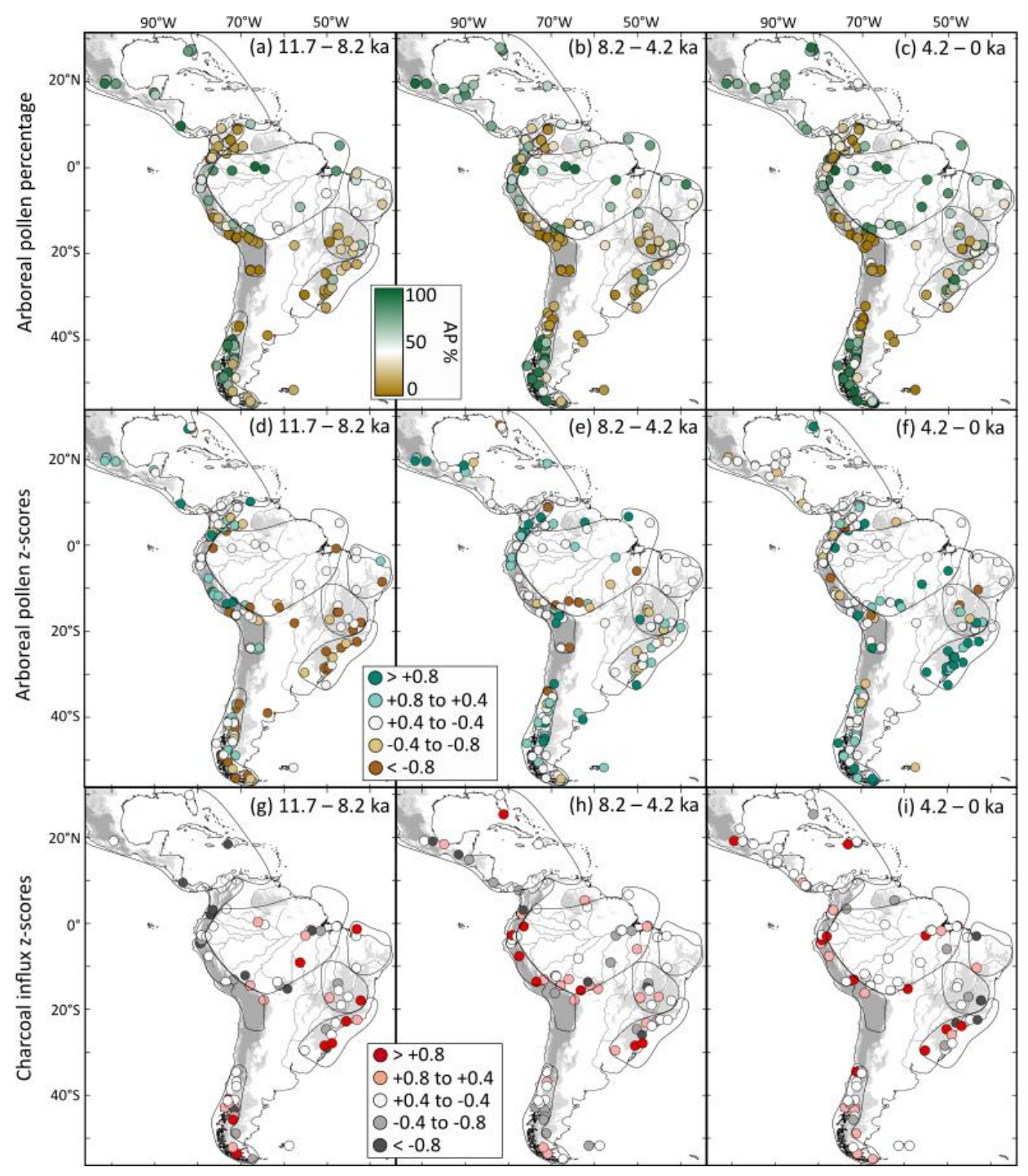


Fig. 13 – Holocene maps of site-specific arboreal pollen percentages and anomalies of average arboreal pollen and charcoal influx z-score values by time period: (a-c) arboreal pollen percentages, (d-f) arboreal pollen (AP) and (g-h) charcoal influx. Three time slices are considered: (a, d, g) early Holocene (11.7 - 8.2 ka); (b, e, h) mid Holocene (8.2 - 4.2 ka); and (c, f, i) late Holocene (4.2 - 0.0 ka). Sites with positive or negative z-score anomalies indicate a record with predominantly higher or lower tree cover/fire activity than the average over the last 21 kyr. Elevations greater than 500 m are represented in light gray, while areas above 1500 m altitude are shown in dark gray. Major rivers are displayed as black lines.

6 Conclusions

785

790

Our assessment of modern climate-vegetation-fire dynamics, combined with a compilation of pollen and charcoal records from the Neotropics contributes to elucidating key environmental controls on vegetation and fire changes in the region over the last 21,000 yr. Our findings reveal contrasting shifts in vegetation and fire activity across the Neotropics, highlighting the complex interplay of various competing drivers, such as temperature, CO_{2atm}, precipitation, vegetation-fire feedback, in addition to human impacts. We also indicate that the relative importance of different parameters affecting climate–vegetation–fire interactions vary across temporal and spatial scales.

800

805

810

815

820

In the southern latitudes (ExTrAn, SESA) and high Andes (TrAn), 3–8°C lower temperatures were the critical limiting factor for tree cover development during the glacial period. In contrast, in the warmer tropical regions (NNeo, Amazonia, CEB, NEB) precipitation played a pivotal role. We thereby suggest that shifts towards open arboreal cover during the glacial period should not be interpreted solely as indicators of dry conditions, particularly in regions where low temperatures and CO_{2atm} constrained biomass growth, i.e., extra- and sub-tropical and high-montane regions. Fire activity, in turn, exhibits a non-linear response, increasing with biomass availability in fuel-limited conditions (ExTrAn, SESA, TrAn), but decreasing with moisture availability under moisture-limited conditions (NNeo, CEB). On the other hand, intensification in fire activity can hamper woody biomass growth. The deglacial stepwise increase in fire activity in several subregions of the Neotropics also suggests that warming thresholds can trigger rapid intensification of fire regimes, provided sufficient biomass is available.

During the Holocene, when variations in temperature and CO_{2atm} were less pronounced, precipitation became a primary climatic determinant of tree cover and fire dynamics in the Neotropics. For instance, long-term Holocene increase in tree cover in Amazonia, CEB, and SESA were likely promoted by progressively increasing moisture, in opposition to NNeo and NEB. In addition to environmental controls, especially in the later parts of the Holocene, accelerated human demographic growth promoted widespread landscape transformation. The Holocene intensification of the fire regime probably resulted from a combination of warming and drying in some regions (NNeo, NEB) and direct human impacts (e.g., NNeo, TrAn), which further induced low tree cover states or delayed tree cover recovery. This finding raises concern for the future, as potential increases in extreme hot and dry events across parts of the Neotropics are likely to intensify fire regimes and tree cover loss in the region.

Our compilation underscores the scarcity of records spanning the last 21,000 years with both high temporal resolution and precise chronological control. Therefore, further downcore studies are required to better constrain the effects of short-lasting events on vegetation and fire dynamics. These efforts are crucial to better constrain the impacts of short-lived climatic events and human impacts on vegetation and fire dynamics, which may help to assess more rapid environmental responses as expected in the future.

7 Appendices

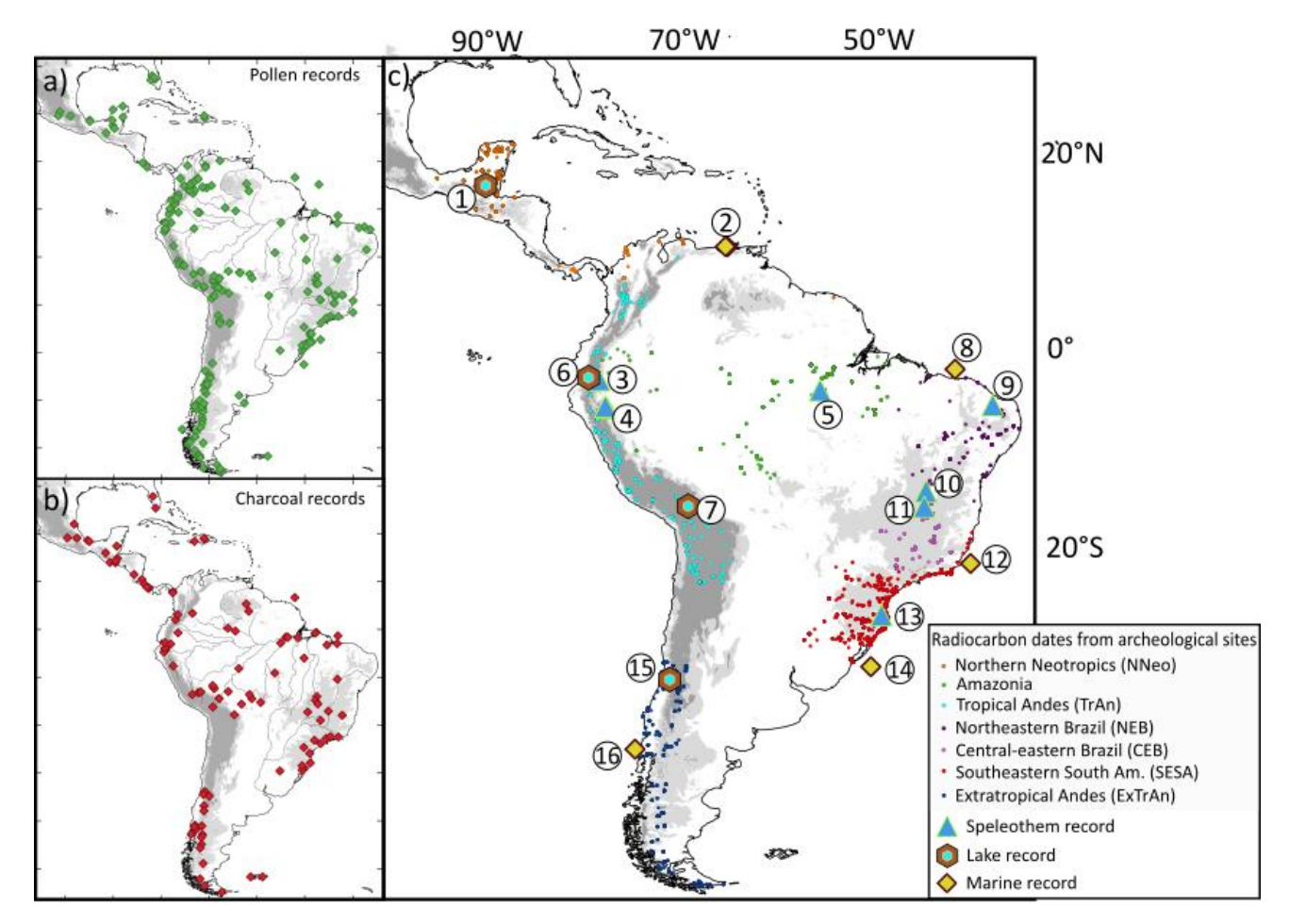


Fig. A1 – Location of supporting data used in this study. Sites with (a) pollen and (b) charcoal records used in the regional synthesis. (c) Sites from which data were extracted for this study and locations of radiocarbon-dated archaeological sites used to calculate summed probability distributions. 1 – Péten-Itza (PI-6) (Correa-Metrio et al., 2012); 2 – ODP site 1002 (Haug et al., 2001) and MD03-2621 (Deplazes et al., 2013); 3 – Santiago cave (Mosblech et al., 2012); 4 – Cueva del Diamante (NAR) and El Condor (ELC) caves (Cheng et al., 2013); 5 – Paraíso cave (Wang et al., 2017); 6 – Laguna Pallcacocha (Mark et al., 2022); 7 – Titicaca Lake (Baker et al., 2001); 8 – GeoB16202-2 (Mulitza et al., 2017); 9 – Rainha (RN) cave (Cruz et al., 2009); 10 – Lapa sem Fim (LSF) cave (Stríkis et al., 2018); 11 – Lapa Grande (LG) cave (Stríkis et al., 2011); 12 – M125-35-3 (Meier et al., 2022); 13 – Botuverá cave (Cruz et al., 2005); 14 – GeoB6211-2 (Chiessi et al., 2015); 15 – Lake Aculeo (Jenny et al., 2003); 16 – ODP site 1233 (Kaiser et al., 2005). Dots represent radiocarbon dates from archeological sites (Araujo et al., 2025; Goldberg et al., 2016; MesoRad, 2020). Elevations greater than 500 m are represented in light gray, while areas above 1500 m altitude are shown in dark gray.

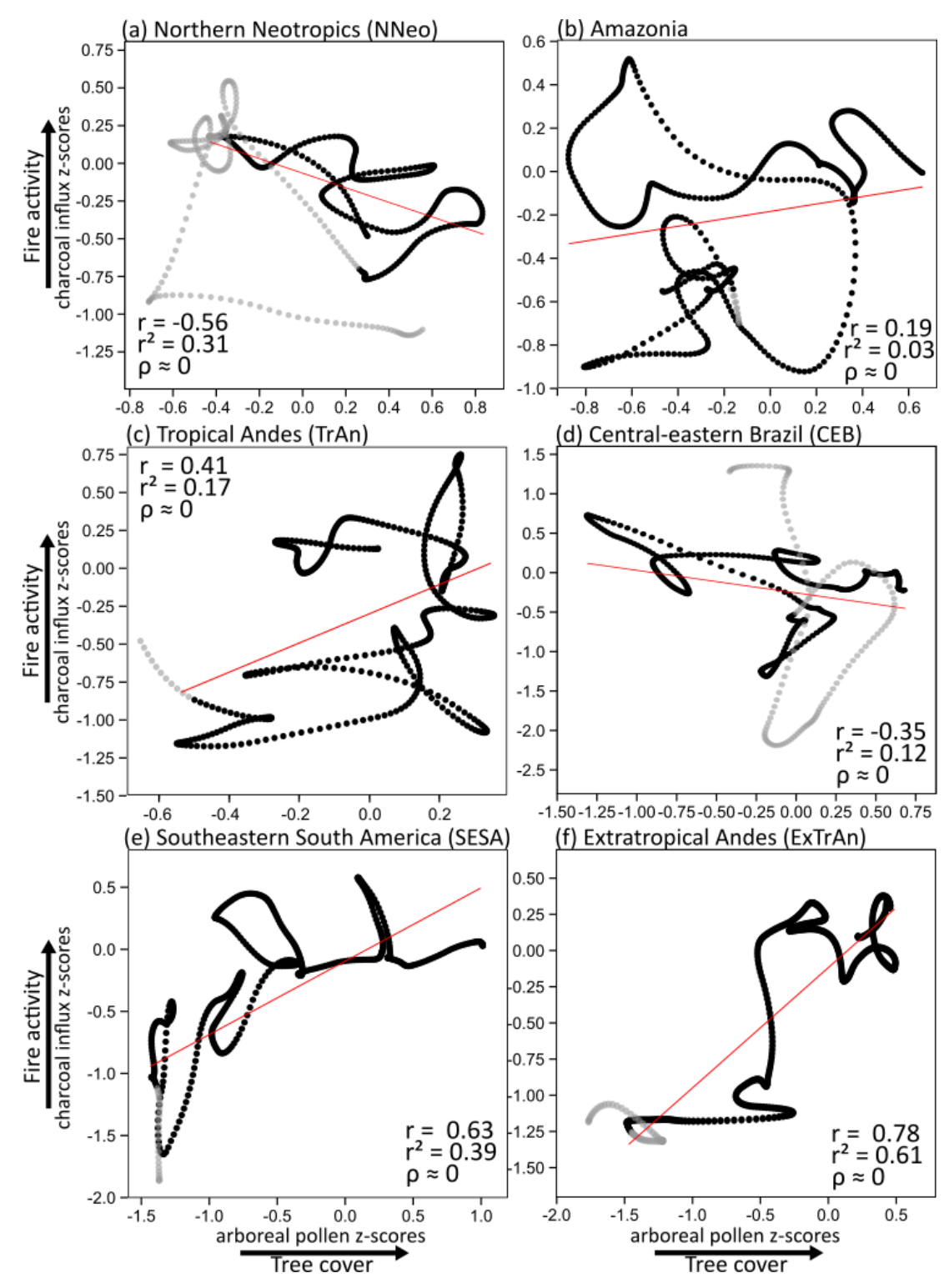
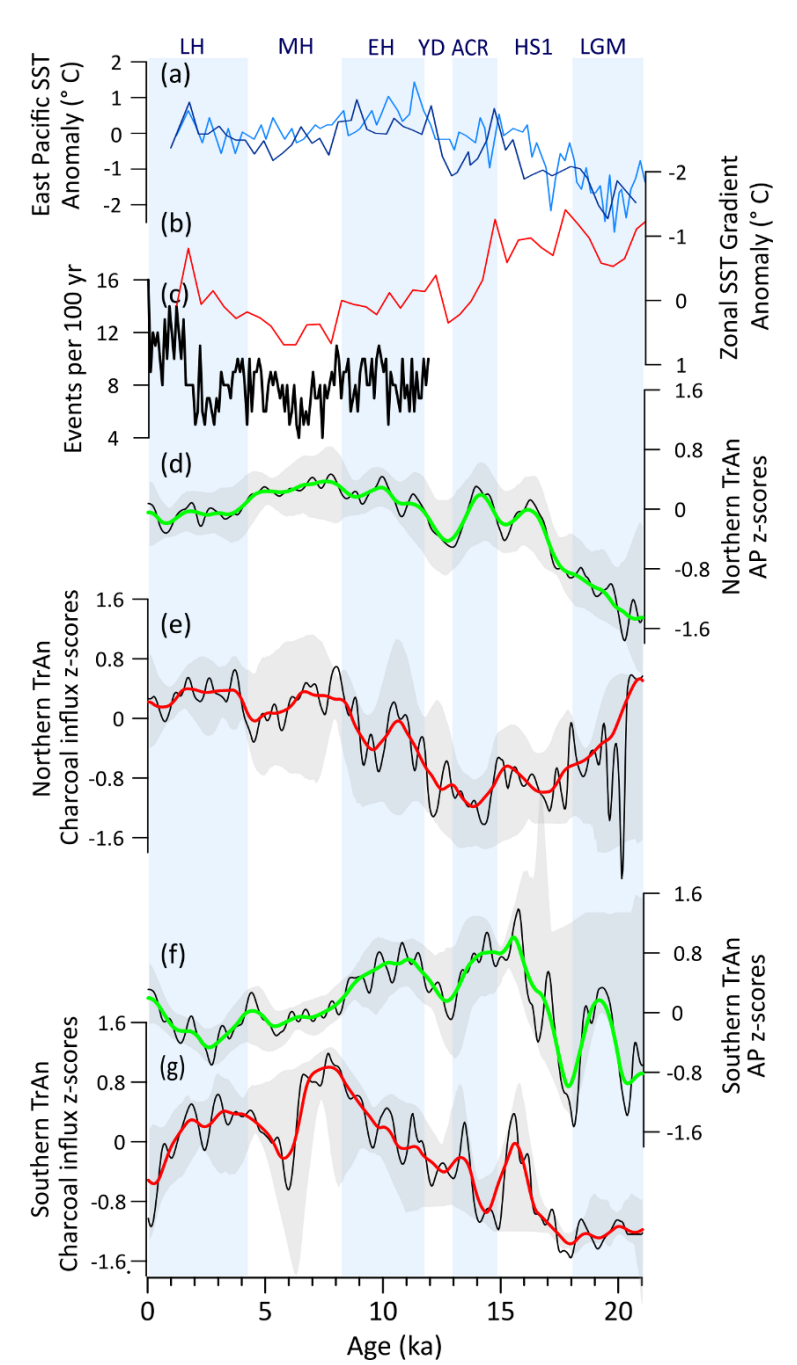


Fig. A2 – Correlation between arboreal pollen z-scores and charcoal influx z-scores by subregion. Correlations were calculated for periods in which at least four records were available for both AP and charcoal influx z-score composites (black dots), periods with lower availability of records are shown (gray dots) but not included in calculations. A strong and significant positive correlation between tree cover and fire activity (c, e, f) indicates fuel-limited conditions, where an increase in biomass availability enhances fire potential. Conversely, a strong significant negative correlation (b) suggests climate-limited conditions, where climate variables, such as moisture, predominantly regulate fire dynamics.



Age (ka)

Fig. A3 – Tropical Andes (TrAn) subdivided in northern and southern sectors at 8 °S: (a) East Pacific SST anomaly (Koutavas and Joanides, 2012; Lea et al., 2006). (b) Zonal SST gradient anomaly between east and west Pacific (Koutavas and Joanides, 2012). (c) El Niño events per 100 years estimated from XRF data from Lake Pallcacocha (Mark et al., 2022). (d) Arboreal pollen (AP) and (e) charcoal influx z-scores composites from all records from TrAn located north of 8 °S. (f) Arboreal pollen (AP) and (g) charcoal influx z-scores composites from all records from TrAn located south of 8 °S. AP and charcoal-influx z-scores were produced using 1000-yr (green and red, respectively) and 400 yr (black) smoothing half-window. Gray areas represent 2.5th and 97.5th confidence intervals.

8 Code availability

860

865

870

875

880

885

The analyses were primarily performed using code from already developed R packages "paleofire", "Neotoma" and "rearbon". However, the specific scripts used, based on these packages, can be found on GitHub at https://github.com/tkakabane/APcomp

9 Data availability

The authors declare that all data supporting the findings of our study are publicly available from the web or upon request to the authors. Pollen and charcoal data are available from Neotoma Paleoecology (http://www.neotomadb.org), Pangaea (https://www.pangaea.de/), and Reading databases. Present climate models are available from WorldClim (https://www.worldclim.org/), modern fire activity from the global fire patch functional traits database (FRY), and Wildlife terrestrial ecoregions be found the World can on Fund website (https://www.worldwildlife.org/publications/terrestrial-ecoregions-of-the-world).

10 Supplementary data

Supplementary data 1 – Site_info: Details of the sites included in the study: site coordinates, site name, altitude, maximum and minimum estimated ages, and publication reference. Composite curves: Results from the composites using 1000-yr and 400-yr smoothing half-width. Neotoma_ecogroup: Taxa classification into trees and shrubs (TRSH), palms (PALM), upland herbs (UPHE), and mangrove (MANG).

11 Author contribution

TKA and ALD designed the experiments and TKA carried them out. TKA, CMC, ALD, and PEO prepared the manuscript with contributions from all co-authors. VH extracted data for analyses of modern fire pattern characterization. CMC, ALD, PEO, JW, ACC, DJBJ, MHS, and TAS contributed to interpretations, discussions and critical revision of the manuscript.

12 Acknowledgments

TKA thanks the financial support from FAPESP (grants 2019/19948-0 and 2021/13129-8) and CAPES-COFECUB program (grant 88887.989386/2024-00). This study was financed, in part, by the São Paulo Research Foundation (FAPESP), Brazil, processes number 2018/15123-4 and 2019/24349-9. CMC acknowledges the financial support from CNPq (grant 312458/2020-7), and the CAPES-COFECUB program (grants 8881.712022/2022-1 and 49558SM). We thank UMR EPOC 5805 (France) for the support in conducting this research. We thank the insightful comments from the reviewers Nicholas O'Mara, Raquel Franco Cassino, and Paula A Rodríguez-Zorro, the community member Kees Nooren, and the editor Christian Franzke. Data were obtained from the Neotoma Paleoecology (https://www.neotomadb.org), and Reading databases. The work of data contributors, data stewards, and the community involved in these databases are gratefully acknowledged.

13 Competing interests

The authors declare that they have no conflict of interest.

14 References

890

895

905

915

920

- Abarzúa, A. M., Martel-Cea, A., and Lobos, V.: Vegetation–Climate–Megafauna Interactions During the Late Glacial in Pilauco Site, Northwestern Patagonia, 157–173, https://doi.org/10.1007/978-3-030-23918-3 9, 2020.
 - Akabane, T. K., Chiessi, C. M., Hirota, M., Bouimetarhan, I., Prange, M., Mulitza, S., Bertassoli Jr, D. J., Häggi, C., Staal, A., Lohmann, G., Boers, N., Daniau, A. L., Oliveira, R. S., Campos, M. C., Shi, X., and De Oliveira, P. E.: Weaker Atlantic overturning circulation increases the vulnerability of northern Amazon forests, Nat. Geosci., 17, 1284–1290, https://doi.org/10.1038/s41561-024-01578-z, 2024.
- Alvarado, S. T., Andela, N., Silva, T. S. F., and Archibald, S.: Thresholds of fire response to moisture and fuel load differ between tropical savannas and grasslands across continents, Glob. Ecol. Biogeogr., 29, 331–344, https://doi.org/10.1111/geb.13034, 2020.
 - Antonelli, A., Zizka, A., Carvalho, F. A., Scharn, R., Bacon, C. D., Silvestro, D., and Condamine, F. L.: Amazonia is the primary source of Neotropical biodiversity, Proc. Natl. Acad. Sci. U. S. A., 115, 6034–6039, https://doi.org/10.1073/pnas.1713819115, 2018.
 - Araujo, A. G. M. and Correa, L.: First notice of a Paleoindian site in central São Paulo State, Brazil: Bastos site, Dourado County, Palaeoindian Archaeol., 1, 04–17, 2016.
 - Araujo, A. G. M., Neves, W. A., Piló, L. B., and Atui, J. P. V.: Holocene dryness and human occupation in Brazil during the "Archaic Gap," Quat. Res., 64, 298–307, https://doi.org/10.1016/j.yqres.2005.08.002, 2005.
- Araujo, A. G. M., Correa, L. C., Perez, G. C., Di Gregorio, E. D., and Okumura, M.: Human-environment interaction during the Holocene in Eastern South America: Rapid climate changes and population dynamics, PLoS One, 20, 1–63, https://doi.org/10.1371/journal.pone.0315747, 2025.
 - Ardelean, C. F., Becerra-Valdivia, L., Pedersen, M. W., Schwenninger, J.-L., Oviatt, C. G., Macías-Quintero, J. I., Arroyo-Cabrales, J., Sikora, M., Ocampo-Díaz, Y. Z. E., Rubio-Cisneros, I. I., Watling, J. G., de Medeiros, V. B., De Oliveira, P. E., Barba-Pingarón, L., Ortiz-Butrón, A., Blancas-Vázquez, J., Rivera-González, I., Solís-Rosales, C., Rodríguez-Ceja, M., Gandy, D. A., Navarro-Gutierrez, Z., De La Rosa-Díaz, J. J., Huerta-Arellano, V., Marroquín-Fernández, M. B., Martínez-Riojas, L. M., López-Jiménez, A., Higham, T., and Willerslev, E.: Evidence of human occupation in Mexico around the Last Glacial Maximum, Nature, 584, 87–92, https://doi.org/10.1038/s41586-020-2509-0, 2020.
 - Argibay, D. S., Sparacino, J., and Espindola, G. M.: A long-term assessment of fire regimes in a Brazilian ecotone between seasonally dry tropical forests and savannah, Ecol. Indic., 113, https://doi.org/10.1016/j.ecolind.2020.106151, 2020.
 - Baker, P. A. and Fritz, S. C.: Nature and causes of Quaternary climate variation of tropical South America, Quat. Sci. Rev., 124, 31–47, https://doi.org/10.1016/j.quascirev.2015.06.011, 2015.
 - Baker, P. A., Seltzer, G. O., Fritz, S. C., Dunbar, R. B., Grove, M. J., Tapia, P. M., Cross, S. L., Rowe, H. D., and Broda, J. P.: The history of South American tropical precipitation for the past 25,000 years, Science, 291, 640–643, https://doi.org/10.1126/science.291.5504.640, 2001.
 - Barberi, M., Salgado-Labouriau, M. L., and Suguio, K.: Paleovegetation and paleoclimate of "Vereda de Aguas

- Emendadas", central Brazil, J. South Am. Earth Sci., 13, 241–254, https://doi.org/10.1016/S0895-9811(00)00022-5, 2000.
- Barker, S., Diz, P., Vautravers, M. J., Pike, J., Knorr, G., Hall, I. R., and Broecker, W. S.: Interhemispheric Atlantic seesaw response during the last deglaciation, Nature, 457, 1097–1102, https://doi.org/10.1038/nature07770, 2009.
 - Behling, H.: Late Quaternary vegetation and climate dynamics in southeastern Amazonia inferred from Lagoa da Confusão Tocantins State, northern Brazil, Amazoniana, 17, 27–39, 2002a.
 - Behling, H.: South and southeast Brazilian grasslands during Late Quaternary times: A synthesis, Palaeogeogr. Palaeoclimatol. Palaeoecol., 177, 19–27, https://doi.org/10.1016/S0031-0182(01)00349-2, 2002b.
- Behling, H. and Hooghiemstra, H.: Holocene Amazon rainforest-savanna dynamics and climatic implications: High-resolution pollen record from Laguna Loma Linda in eastern Colombia, J. Quat. Sci., 15, 687–695, https://doi.org/10.1002/1099-1417(200010)15:7<687::AID-JQS551>3.0.CO;2-6, 2000.

940

945

950

960

- Behling, H., Pillar, V. D., and Overbeck, G. E.: Dynamics of South Brazilian Grasslands During the Late Quaternary, in: South Brazilian Grasslands, Springer International Publishing, Cham, 83–99, https://doi.org/10.1007/978-3-031-42580-6 4, 2023.
- Bereiter, B., Eggleston, S., Schmitt, J., Nehrbass-Ahles, C., Stocker, T. F., Fischer, H., Kipfstuhl, S., and Chappellaz, J.: Revision of the EPICA Dome C CO2 record from 800 to 600-kyr before present, Geophys. Res. Lett., 42, 542–549, https://doi.org/10.1002/2014GL061957, 2015.
- Bernardino, P. N., Dantas, V. L., Hirota, M., Pausas, J. G., and Oliveira, R. S.: Savanna–Forest Coexistence Across a Fire Gradient, Ecosystems, 25, 279–290, https://doi.org/10.1007/s10021-021-00654-4, 2022.
- Blaauw, M. and Christen, J. A.: Flexible paleoclimate age-depth models using an autoregressive gamma process, Bayesian Anal., 6, 457–474, https://doi.org/10.1214/ba/1339616472, 2011.
- Blarquez, O., Vannière, B., Marlon, J. R., Daniau, A. L., Power, M. J., Brewer, S., and Bartlein, P. J.: Paleofire: An R package to analyse sedimentary charcoal records from the Global Charcoal Database to reconstruct past biomass burning, Comput. Geosci., 72, 255–261, https://doi.org/10.1016/j.cageo.2014.07.020, 2014.
- Boëda, E., Clemente-Conte, I., Fontugne, M., Lahaye, C., Pino, M., Felice, G. D., Guidon, N., Hoeltz, S., Lourdeau, A., Pagli, M., Pessis, A. M., Viana, S., Da Costa, A., and Douville, E.: A new late Pleistocene archaeological sequence in South America: The Vale da Pedra Furada (Piauí, Brazil), Antiquity, 88, 927–941, https://doi.org/10.1017/S0003598X00050845, 2014.
- Boom, A., Marchant, R., Hooghiemstra, H., and Sinninghe Damsté, J. S.: CO2- and temperature-controlled altitudinal shifts of C4- and C3-dominated grasslands allow reconstruction of palaeoatmospheric pCO2, Palaeogeogr. Palaeoclimatol. Palaeoecol., 177, 151–168, https://doi.org/10.1016/S0031-0182(01)00357-1, 2002.
 - Bond, W. J., Midgley, G. F., and Woodward, F. I.: The importance of low atmospheric CO2 and fire in promoting the spread of grasslands and savannas, Glob. Chang. Biol., 9, 973–982, https://doi.org/10.1046/j.1365-2486.2003.00577.x, 2003.
 - Bouimetarhan, I., Chiessi, C. M., González-Arango, C., Dupont, L., Voigt, I., Prange, M., and Zonneveld, K.: Intermittent development of forest corridors in northeastern Brazil during the last deglaciation: Climatic and ecologic evidence, Quat. Sci. Rev., 192, 86–96, https://doi.org/10.1016/j.quascirev.2018.05.026, 2018.
 - Brando, P., Macedo, M., Silvério, D., Rattis, L., Paolucci, L., Alencar, A., Coe, M., and Amorim, C.: Amazon wildfires: Scenes from a foreseeable disaster, Flora, 268, 151609, https://doi.org/10.1016/j.flora.2020.151609, 2020.
 - Brugger, S. O., Gobet, E., van Leeuwen, J. F. N., Ledru, M. P., Colombaroli, D., van der Knaap, W. O., Lombardo, U.,

- Escobar-Torrez, K., Finsinger, W., Rodrigues, L., Giesche, A., Zarate, M., Veit, H., and Tinner, W.: Long-term manenvironment interactions in the Bolivian Amazon: 8000 years of vegetation dynamics, Quat. Sci. Rev., 132, 114–128, https://doi.org/10.1016/j.quascirev.2015.11.001, 2016.
- Bush, M. B. and Flenley, J. R.: Tropical Rainforest Responses to Climatic Change, Trop. Rainfor. Responses to Clim. Chang., https://doi.org/10.1007/978-3-540-48842-2, 2007.
 - Bush, M. B., Stute, M., Iedru, M., Behling, H., and Colinvaux, P. a: Paleotemperature Estimates for the Lowland Americas, Am., 2001.
 - Bush, M. B., Silman, M. R., and Urrego, D. H.: 48,000 Years of Climate and Forest Change in a Biodiversity Hot Spot, Science, 303, 827–829, https://doi.org/10.1126/science.1090795, 2004.

975

985

990

995

- Bush, M. B., Silman, M. R., McMichael, C., and Saatchi, S.: Fire, climate change and biodiversity in Amazonia: A Late-Holocene perspective, Philos. Trans. R. Soc. B Biol. Sci., 363, 1795–1802, https://doi.org/10.1098/rstb.2007.0014, 2008.
- Bush, M. B., Correa-metrio, A. Y., Hodell, D. A., Brenner, M., Anselmetti, F. S., Ariztegui, D., Mueller, A. D., Curtis, J.
 H., Grzesik, D. A., Burton, C., and Gilli, A.: Re-evaluation of Climate Change in Lowland Central America During the Last Glacial Maximum Using New Sediment Cores from Lake Petén Itzá, Guatemala, 113–128, https://doi.org/10.1007/978-90-481-2672-9 5, 2009.
 - Bush, M. B., Alfonso-Reynolds, A. M., Urrego, D. H., Valencia, B. G., Correa-Metrio, Y. A., Zimmermann, M., and Silman, M. R.: Fire and climate: Contrasting pressures on tropical Andean timberline species, J. Biogeogr., 42, 938–950, https://doi.org/10.1111/jbi.12470, 2015.
 - Bush, M. B., Rozas-Davila, A., Raczka, M., Nascimento, M., Valencia, B., Sales, R. K., McMichael, C. N. H., and Gosling,
 W. D.: A palaeoecological perspective on the transformation of the tropical Andes by early human activity, Philos.
 Trans. R. Soc. B Biol. Sci., 377, https://doi.org/10.1098/rstb.2020.0497, 2022.
 - Bustamante, M. and Panizo, G.: Holocene changes in monsoon precipitation in the Andes of NE Peru based on d180 speleothem records, Quat. Sci. Rev., 146, 274–287, https://doi.org/10.1016/j.quascirev.2016.05.023, 2016.
 - Campos, M. C., Chiessi, C. M., Prange, M., Mulitza, S., Kuhnert, H., Paul, A., Venancio, I. M., Albuquerque, A. L. S., Cruz, F. W., and Bahr, A.: A new mechanism for millennial scale positive precipitation anomalies over tropical South America, Quat. Sci. Rev., 225, 105990, https://doi.org/10.1016/j.quascirev.2019.105990, 2019.
 - Campos, M. C., Chiessi, C. M., Novello, V. F., Crivellari, S., Campos, J. L. P. S., Albuquerque, A. L. S., Venancio, I. M., Santos, T. P., Melo, D. B., Cruz, F. W., Sawakuchi, A. O., and Mendes, V. R.: South American precipitation dipole forced by interhemispheric temperature gradient, Sci. Rep., 12, https://doi.org/10.1038/s41598-022-14495-1, 2022.
 - Cheng, H., Sinha, A., Cruz, F. W., Wang, X., Edwards, R. L., D'Horta, F. M., Ribas, C. C., Vuille, M., Stott, L. D., and Auler, A. S.: Climate change patterns in Amazonia and biodiversity, Nat. Commun., 4, 1411, https://doi.org/10.1038/ncomms2415, 2013.
- 1000 Chiessi, C. M., Mulitza, S., Mollenhauer, G., Silva, J. B., Groeneveld, J., and Prange, M.: Thermal evolution of the western South Atlantic and the adjacent continent during Termination 1, Clim. Past, 11, 915–929, https://doi.org/10.5194/cp-11-915-2015, 2015.
 - Chiessi, C. M., Mulitza, S., Taniguchi, N. K., Prange, M., Campos, M. C., Häggi, C., Schefuß, E., Pinho, T. M. L. L., Frederichs, T., Portilho-Ramos, R. C., Sousa, S. H. M. M., Crivellari, S., Cruz, F. W., Portilho-Ramos, R. C., Sousa, S. H. M. M., Crivellari, S., and Cruz, F. W.: Mid- to Late Holocene Contraction of the Intertropical Convergence Zone
- Over Northeastern South America, Paleoceanogr. Paleoclimatology, 36, https://doi.org/10.1029/2020PA003936, 2021.

- Cochrane, M. A., Alencar, A., Schulze, M. D., Souza, C. M., Nepstad, D. C., Lefebvre, P., and Davidson, E. A.: Positive Feedbacks in the Fire Dynamic of Closed Canopy Tropical Forests, Science, 284, 1832–1835, https://doi.org/10.1126/science.284.5421.1832, 1999.
- Colinvaux, P. A., De Oliveira, P. E., Moreno, J. E., Miller, M. C., and Bush, M. B.: A Long Pollen Record from Lowland Amazonia: Forest and Cooling in Glacial Times, Science, 274, 85–88, https://doi.org/10.1126/science.274.5284.85, 1996.
 - Contreras, D. A. and Meadows, J.: Summed radiocarbon calibrations as a population proxy: A critical evaluation using a realistic simulation approach, J. Archaeol. Sci., 52, 591–608, https://doi.org/10.1016/j.jas.2014.05.030, 2014.
- 1015 Cook, K. H. and Vizy, E. K.: Hydrodynamics of the Caribbean low-level jet and its relationship to precipitation, J. Clim., 23, 1477–1494, https://doi.org/10.1175/2009JCLI3210.1, 2010.

- Cordeiro, R. C., Turcq, B., Moreira, L. S., Rodrigues, R. de A. R., Lamego Simões Filho, F. F., Martins, G. S., Santos, A. B., Barbosa, M., Guilles da Conceição, M. C., Rodrigues, R. de C., Evangelista, H., Moreira-Turcq, P., Penido, Y. P., Sifeddine, A., and Seoane, J. C. S.: Palaeofires in Amazon: Interplay between land use change and palaeoclimatic events, Palaeogeogr. Palaeoclimatol. Palaeoecol., 415, 137–151, https://doi.org/10.1016/j.palaeo.2014.07.020, 2014.
- Coronato, A. M. J., Coronato, F., Mazzoni, E., Va, M., Ushuaia, S., Patago, C. N., Acade, U., and America, S.: The Physical Geography of Patagonia and Tierra del Fuego, 11, 2005.
- Correa-Metrio, A., Bush, M. B., Cabrera, K. R., Sully, S., Brenner, M., Hodell, D. A., Escobar, J., and Guilderson, T.: Rapid climate change and no-analog vegetation in lowland Central America during the last 86,000 years, Quat. Sci. Rev., 38, 63–75, https://doi.org/10.1016/j.quascirev.2012.01.025, 2012.
- Cracraft, J., Ribas, C. C., d'Horta, F. M., Bates, J., Almeida, R. P., Aleixo, A., Boubli, J. P., Campbell, K. E., Cruz, F. W., Ferreira, M., Fritz, S. C., Grohmann, C. H., Latrubesse, E. M., Lohmann, L. G., Musher, L. J., Nogueira, A., Sawakuchi, A. O., and Baker, P.: The Origin and Evolution of Amazonian Species Diversity, 225–244, https://doi.org/10.1007/978-3-030-31167-4 10, 2020.
- 1030 Crema, E. R. and Bevan, A.: Inference from Large Sets of Radiocarbon Dates: Software and Methods, Radiocarbon, 63, 23–39, https://doi.org/10.1017/RDC.2020.95, 2021.
 - Cruz, F. W., Burns, S. J., Karmann, I., Sharp, W. D., Vuille, M., Cardoso, A. O., Ferrari, J. A., Silva Dias, P. L., and Viana, O.: Insolation-driven changes in atmospheric circulation over the past 116,000 years in subtropical Brazil, Nature, 434, 63–66, https://doi.org/10.1038/nature03365, 2005.
- 1035 Cruz, F. W., Vuille, M., Burns, S. J., Wang, X., Cheng, H., Werner, M., Lawrence Edwards, R., Karmann, I., Auler, A. S., and Nguyen, H.: Orbitally driven east-west antiphasing of South American precipitation, Nat. Geosci., 2, 210–214, https://doi.org/10.1038/ngeo444, 2009.
 - Cuatrecasas, J.: Paramo vegetation and its lifeforms, in: Geo-ecology of the mountainous regions of the tropical Americas geo-ecologia de las regiones montanosas de las Americas tropicales, Ferd. Dümmlers, 163–186, 1968.
- Cuesta, F., Muriel, P., Llambí, L. D., Halloy, S., Aguirre, N., Beck, S., Carilla, J., Meneses, R. I., Cuello, S., Grau, A., Gámez, L. E., Irazábal, J., Jácome, J., Jaramillo, R., Ramírez, L., Samaniego, N., Suárez-Duque, D., Thompson, N., Tupayachi, A., Viñas, P., Yager, K., Becerra, M. T., Pauli, H., and Gosling, W. D.: Latitudinal and altitudinal patterns of plant community diversity on mountain summits across the tropical Andes, Ecography (Cop.)., 40, 1381–1394, https://doi.org/10.1111/ecog.02567, 2017.
- Daniau, A. L., Bartlein, P. J., Harrison, S. P., Prentice, I. C., Brewer, S., Friedlingstein, P., Harrison-Prentice, T. I., Inoue, J., Izumi, K., Marlon, J. R., Mooney, S., Power, M. J., Stevenson, J., Tinner, W., Andrič, M., Atanassova, J., Behling,

- H., Black, M., Blarquez, O., Brown, K. J., Carcaillet, C., Colhoun, E. A., Colombaroli, D., Davis, B. A. S., D'Costa, D., Dodson, J., Dupont, L., Eshetu, Z., Gavin, D. G., Genries, A., Haberle, S., Hallett, D. J., Hope, G., Horn, S. P., Kassa, T. G., Katamura, F., Kennedy, L. M., Kershaw, P., Krivonogov, S., Long, C., Magri, D., Marinova, E., McKenzie, G.
- M., Moreno, P. I., Moss, P., Neumann, F. H., Norstrm, E., Paitre, C., Rius, D., Roberts, N., Robinson, G. S., Sasaki, N., Scott, L., Takahara, H., Terwilliger, V., Thevenon, F., Turner, R., Valsecchi, V. G., Vannière, B., Walsh, M., Williams, N., and Zhang, Y.: Predictability of biomass burning in response to climate changes, Global Biogeochem. Cycles, 26, 1–12, https://doi.org/10.1029/2011GB004249, 2012.
- Dávila, S. L., Stinnesbeck, S. R., Gonzalez, S., Lindauer, S., Escamilla, J., and Stinnesbeck, W.: Guatemala's Late

 Pleistocene (Rancholabrean) fauna: Revision and interpretation, Quat. Sci. Rev., 219, 277–296,
 https://doi.org/10.1016/j.quascirev.2019.07.011, 2019.
 - Deplazes, G., Lückge, A., Peterson, L. C., Timmermann, A., Hamann, Y., Hughen, K. A., Röhl, U., Laj, C., Cane, M. A., Sigman, D. M., and Haug, G. H.: Links between tropical rainfall and North Atlantic climate during the last glacial period, Nat. Geosci., 6, 213–217, https://doi.org/10.1038/ngeo1712, 2013.
- Dillehay, T. D., Ocampo, C., Saavedra, J., Sawakuchi, A. O., Vega, R. M., Pino, M., Collins, M. B., Cummings, L. S., Arregui, I., Villagran, X. S., Hartmann, G. A., Mella, M., González, A., and Dix, G.: New archaeological evidence for an early human presence at Monte Verde, Chile, PLoS One, 10, 1–27, https://doi.org/10.1371/journal.pone.0141923, 2015.
 - Doughty, C. E., Wolf, A., and Malhi, Y.: The legacy of the Pleistocene megafauna extinctions on nutrient availability in Amazonia, Nat. Geosci., 6, 761–764, https://doi.org/10.1038/ngeo1895, 2013.
 - Doughty, C. E., Wolf, A., Morueta-Holme, N., Jørgensen, P. M., Sandel, B., Violle, C., Boyle, B., Kraft, N. J. B., Peet, R. K., Enquist, B. J., Svenning, J. C., Blake, S., and Galetti, M.: Megafauna extinction, tree species range reduction, and carbon storage in Amazonian forests, Ecography (Cop.)., 39, 194–203, https://doi.org/10.1111/ecog.01587, 2016a.
 - Doughty, C. E., Faurby, S., and Svenning, J. C.: The impact of the megafauna extinctions on savanna woody cover in South America, Ecography (Cop.)., 39, 213–222, https://doi.org/10.1111/ecog.01593, 2016b.
 - Dupont, L. M., Donner, B., Schneider, R., and Wefer, G.: Mid-Pleistocene environmental change in tropical Africa began as early as 1.05 Ma, Geology, 29, 195–198, https://doi.org/10.1130/0091-7613(2001)029<0195:MPECIT>2.0.CO;2, 2001.
 - Dupont, L. M., Schlütz, F., Ewah, C. T., Jennerjahn, T. C., Paul, A., and Behling, H.: Two-step vegetation response to enhanced precipitation in Northeast Brazil during Heinrich event 1, Glob. Chang. Biol., 16, 1647–1660, https://doi.org/10.1111/j.1365-2486.2009.02023.x, 2009.
 - Durigan, G. and Ratter, J. A.: The need for a consistent fire policy for Cerrado conservation, J. Appl. Ecol., 53, 11–15, https://doi.org/10.1111/1365-2664.12559, 2016.
 - Eiten, G.: The Cerrado vegetation of Brazil, Bot. Rev., 38, 201–341, 1972.

1070

- Endlicher, W. and Santana, A. Á.: The Climate of Southern Patagonia and its Ecological Aspects. A Century of Climatological Measurements in Punta Arenas., ANS. INST. PAT. Ser.Cs. Nts., 18, 1988.
 - Escobar-Torrez, K., Ledru, M., Cassino, R. F., Bianchini, P. R., and Yokoyama, E.: Long-and short-term vegetation change and inferred climate dynamics and anthropogenic activity in the central Cerrado during the Holocene, J. Quat. Sci., https://doi.org/10.1002/jqs.3567, 2023.
- Espinoza, J. C., Garreaud, R., Poveda, G., Arias, P. A., Molina-Carpio, J., Masiokas, M., Viale, M., and Scaff, L.: Hydroclimate of the Andes Part I: Main Climatic Features, Front. Earth Sci., 8, 1–20,

https://doi.org/10.3389/feart.2020.00064, 2020.

1090

1100

1105

1110

1115

- Felden, J., Möller, L., Schindler, U., Huber, R., Schumacher, S., Koppe, R., Diepenbroek, M., and Glöckner, F. O.: PANGAEA Data Publisher for Earth & Environmental Science, Sci. Data, 10, 1–9, https://doi.org/10.1038/s41597-023-02269-x, 2023.
- Fick, S. E. and Hijmans, R. J.: WorldClim 2: new 1-km spatial resolution climate surfaces for global land areas, Int. J. Climatol., 37, 4302–4315, https://doi.org/10.1002/joc.5086, 2017.
- Fine, P. V. A., Mesones, I., and Coley, P. D.: Herbivores promote habitat specialization by trees in Amazonian forests, Science, 305, 663–665, https://doi.org/10.1126/science.1098982, 2004.
- 1095 Fisch, G., Marengo, J. A., and Nobre, C. A.: Uma revisão geral sobre o clima da Amazônia, Acta Amaz., 28, 101–126, https://doi.org/10.1590/1809-43921998282126, 1998.
 - Flantua, S. G. A. and Hooghiemstra, H.: Anthropogenic pollen indicators: Global food plants and Latin American human indicators in the pollen record, Sci. Data, 10, 1–13, https://doi.org/10.1038/s41597-023-02613-1, 2023.
 - Flantua, S. G. A., Hooghiemstra, H., Vuille, M., Behling, H., Carson, J. F., Gosling, W. D., Hoyos, I., Ledru, M. P., Montoya, E., Mayle, F., Maldonado, A., Rull, V., Tonello, M. S., Whitney, B. S., and González-Arango, C.: Climate variability and human impact in South America during the last 2000 years: Synthesis and perspectives from pollen records, Clim. Past, 12, 483–523, https://doi.org/10.5194/cp-12-483-2016, 2016.
 - Fletcher, M. S. and Moreno, P. I.: Have the Southern Westerlies changed in a zonally symmetric manner over the last 14,000 years? A hemisphere-wide take on a controversial problem, Quat. Int., 253, 32–46, https://doi.org/10.1016/j.quaint.2011.04.042, 2012.
 - Foley, A.: CO2, climate, and vegetation feedbacks at the Last Glacial Maximum, 104, 1999.
 - Fontes, D., Cordeiro, R. C., Martins, G. S., Behling, H., Turcq, B., Sifeddine, A., Seoane, J. C. S., Moreira, L. S., and Rodrigues, R. A.: Paleoenvironmental dynamics in South Amazonia, Brazil, during the last 35,000 years inferred from pollen and geochemical records of Lago do Saci, Quat. Sci. Rev., 173, 161-180,https://doi.org/10.1016/j.quascirev.2017.08.021, 2017.
 - Fornace, K. L., Hughen, K. A., Shanahan, T. M., Fritz, S. C., Baker, P. A., and Sylva, S. P.: A 60,000-year record of hydrologic variability in the Central Andes from the hydrogen isotopic composition of leaf waxes in Lake Titicaca sediments, Earth Planet. Sci. Lett., 408, 263–271, https://doi.org/10.1016/j.epsl.2014.10.024, 2014.
 - Furquim, F. F., Scasta, J. D., and Overbeck, G. E.: Interactive effects of fire and grazing on vegetation structure and plant species composition in subtropical grasslands, Appl. Veg. Sci., 27, 1–13, https://doi.org/10.1111/avsc.12800, 2024.
 - Garreaud, R., Vuille, M., and Clement, A. C.: The climate of the Altiplano: Observed current conditions and mechanisms of past changes, Palaeogeogr. Palaeoclimatol. Palaeoecol., 194, 5–22, https://doi.org/10.1016/S0031-0182(03)00269-4, 2003.
 - Garreaud, R. D., Vuille, M., Compagnucci, R., and Marengo, J.: Present-day South American climate, Palaeogeogr. Palaeoclimatol. Palaeoecol., 281, 180–195, https://doi.org/10.1016/j.palaeo.2007.10.032, 2009.
 - Gill, J. L.: Ecological impacts of the late Quaternary megaherbivore extinctions, New Phytol., 201, 1163–1169, https://doi.org/10.1111/nph.12576, 2014.
 - Gill, R. B., Mayewski, P. A., Nyberg, J., Haug, G. H., and Peterson, L. C.: Drought and the maya collapse, Anc. Mesoamerica, 18, 283–302, https://doi.org/10.1017/S0956536107000193, 2007.
- Goebel, T., Waters, M. R., and O'Rourke, D. H.: The Late Pleistocene dispersal of modern humans in the Americas, Science, 319, 1497–1502, https://doi.org/10.1126/science.1153569, 2008.

- Goldberg, A., Mychajliw, A. M., and Hadly, E. A.: Post-invasion demography of prehistoric humans in South America, Nature, 532, 232–235, https://doi.org/10.1038/nature17176, 2016.
- Goodland, R.: A Physiognomic Analysis of the `Cerrado 'Vegetation of Central Brasil, 59, 411-419, 1971.

1140

1145

1150

1160

1165

- Gosling, W. D., Maezumi, S. Y., Heijink, B. M., Nascimento, M. N., Raczka, M. F., van der Sande, M. T., Bush, M. B., and McMichael, C. N. H.: Scarce fire activity in north and north-western Amazonian forests during the last 10,000 years, Plant Ecol. Divers., 14, 143–156, https://doi.org/10.1080/17550874.2021.2008040, 2021.
 - Gu, F., Chiessi, C. M., Zonneveld, K. A. F., and Behling, H.: Late Quaternary environmental dynamics inferred from marine sediment core GeoB6211-2 off southern Brazil, Palaeogeogr. Palaeoclimatol. Palaeoecol., 496, 48–61, https://doi.org/10.1016/j.palaeo.2018.01.015, 2018.
 - Gutierrez-Flores, I., Panca, M., and Oyague, E.: Fire as driver of plant communities and soil properties changes in Puna grasslands in Southern Peruvian Andes, Environ. Challenges, 17, 101044, https://doi.org/10.1016/j.envc.2024.101044, 2024.
 - Haas, O., Prentice, I. C., and Harrison, S. P.: The response of wildfire regimes to Last Glacial Maximum carbon dioxide and climate, Biogeosciences, 20, 3981–3995, https://doi.org/10.5194/bg-20-3981-2023, 2023.
 - Haberle, S. G. and Maslin, M. a: Late Quaternary Vegetation and Climate Change in the Amazon Basin Based on a 50,000 ODP Site 932, Year Pollen Record from the Amazon Fan, Quat. Res., 51, 27 - 38, https://doi.org/10.1006/qres.1998.2020, 1999.
 - Häggi, C., Chiessi, C. M., Merkel, U., Mulitza, S., Prange, M., Schulz, M., and Schefuß, E.: Response of the Amazon rainforest to late Pleistocene climate variability, Earth Planet. Sci. Lett., 479, 50–59, https://doi.org/10.1016/j.epsl.2017.09.013, 2017.
 - Hantson, S., Pueyo, S., and Chuvieco, E.: Global fire size distribution is driven by human impact and climate, Glob. Ecol. Biogeogr., 24, 77–86, https://doi.org/10.1111/geb.12246, 2015.
 - Harris, I., Osborn, T. J., Jones, P. D., and Lister, D. H.: Version 4 of the CRU TS monthly high-resolution gridded multivariate climate dataset, Sci. Data, 7, 2020.
 - Harrison, S. P., Villegas-Diaz, R., Cruz-Silva, E., Gallagher, D., Kesner, D., Lincoln, P., Shen, Y., Sweeney, L., Colombaroli, D., Ali, A., Barhoumi, C., Bergeron, Y., Blyakharchuk, T., Bobek, P., Bradshaw, R., Clear, J. L., Czerwiński, S., Daniau, A. L., Dodson, J., Edwards, K. J., Edwards, M. E., Feurdean, A., Foster, D., Gajewski, K., Gałka, M., Garneau, M., Giesecke, T., Gil Romera, G., Girardin, M. P., Hoefer, D., Huang, K., Inoue, J., Jamrichová,
- E., Jasiunas, N., Jiang, W., Jiménez-Moreno, G., Karpińska-Kołaczek, M., Kołaczek, P., Kuosmanen, N., Lamentowicz, M., Lavoie, M., Li, F., Li, J., Lisitsyna, O., López-Sáez, J. A., Luelmo-Lautenschlaeger, R., Magnan, G., Magyari, E. K., Maksims, A., Marcisz, K., Marinova, E., Marlon, J., Mensing, S., Miroslaw-Grabowska, J., Oswald, W., Pérez-Díaz, S., Pérez-Obiol, R., Piilo, S., Poska, A., Qin, X., Remy, C. C., Richard, P. J. H., Salonen, S., Sasaki, N., Schneider, H., Shotyk, W., Stancikaite, M., Šteinberga, D., Stivrins, N., Takahara, H., Tan, Z., Trasune, L.,
- Paillard, J.: The Reading Palaeofire Database: an expanded global resource to document changes in fire regimes from sedimentary charcoal records, Earth Syst. Sci. Data, 14, 1109–1124, https://doi.org/10.5194/essd-14-1109-2022, 2022.
 - Harvey, W. J., Nogué, S., Stansell, N., Petrokofsky, G., Steinman, B., and Willis, K. J.: The Legacy of Pre-Columbian Fire on the Pine-Oak Forests of Upland Guatemala, Front. For. Glob. Chang., 2, https://doi.org/10.3389/ffgc.2019.00034, 2019.

Umbanhowar, C. E., Väliranta, M., Vassiljev, J., Xiao, X., Xu, Q., Xu, X., Zawisza, E., Zhao, Y., Zhou, Z., and

Haug, G. H., Hughen, K. A., Sigman, D. M., Peterson, L. C., and Röhl, U.: Southward Migration of the Intertropical

- Convergence Zone Through the Holocene, Science., 293, 1304-1308, https://doi.org/10.1126/science.1059725, 2001.
- Haug, G. H., Günther, D., Peterson, L. C., Sigman, D. M., Hughen, K. A., and Aeschlimann, B.: Climate and the Collapse of Maya Civilization, Science, 299, 1731–1735, https://doi.org/10.1126/science.1080444, 2003.
- Hillyer, R., Valencia, B. G., Bush, M. B., Silman, M. R., and Steinitz-Kannan, M.: A 24,700-yr paleolimnological history from the Peruvian Andes, Quat. Res., 71, 71–82, https://doi.org/10.1016/j.yqres.2008.06.006, 2009.
 - Hodell, D. A., Anselmetti, F. S., Ariztegui, D., Brenner, M., Curtis, J. H., Gilli, A., Grzesik, D. A., Guilderson, T. J., Müller, A. D., Bush, M. B., Correa-Metrio, A., Escobar, J., and Kutterolf, S.: An 85-ka record of climate change in lowland Central America, Quat. Sci. Rev., 27, 1152–1165, https://doi.org/10.1016/j.quascirev.2008.02.008, 2008.
- Hogg, A. G., Heaton, T. J., Hua, Q., Palmer, J. G., Turney, C. S. M., Southon, J., Bayliss, A., Blackwell, P. G., Boswijk, G., Bronk Ramsey, C., Pearson, C., Petchey, F., Reimer, P., Reimer, R., and Wacker, L.: SHCal20 Southern Hemisphere Calibration, 0-55,000 Years cal BP, Radiocarbon, 62, 759–778, https://doi.org/10.1017/RDC.2020.59, 2020.

1190

- Holz, A., Kitzberger, T., Paritsis, J., and Veblen, T. T.: Ecological and climatic controls of modern wildfire activity patterns across southwestern South America, Ecosphere, 3, 1–25, https://doi.org/10.1890/ES12-00234.1, 2012.
- Hoorn, C., Wesselingh, F. P., Ter Steege, H., Bermudez, M. A., Mora, A., Sevink, J., Sanmartín, I., Sanchez-Meseguer, A., Anderson, C. L., Figueiredo, J. P., Jaramillo, C., Riff, D., Negri, F. R., Hooghiemstra, H., Lundberg, J., Stadler, T., Särkinen, T., and Antonelli, A.: Amazonia through time: Andean uplift, climate change, landscape evolution, and biodiversity, Science, 330, 927–931, https://doi.org/10.1126/science.1194585, 2010.
- Iriarte, J., Elliott, S., Maezumi, S. Y., Alves, D., Gonda, R., Robinson, M., Gregorio de Souza, J., Watling, J., and Handley, J.: The origins of Amazonian landscapes: Plant cultivation, domestication and the spread of food production in tropical South America, Quat. Sci. Rev., 248, 106582, https://doi.org/10.1016/j.quascirev.2020.106582, 2020.
 - Jaramillo, C., Rueda, M., and Mora, G.: Cenozoic Plant Diversity in the Neotropics, Science, 311, 1893–1896, https://doi.org/10.1126/science.1121380, 2006.
 - Jenny, B., Wilhelm, D., and Valero-Garcés, B. L.: The Southern Westerlies in Central Chile: Holocene precipitation estimates based on a water balance model for Laguna Aculeo (33°50′S), Clim. Dyn., 20, 269–280, https://doi.org/10.1007/s00382-002-0267-3, 2003.
 - Jesus, C. S. L. de, Delgado, R. C., Wanderley, H. S., Teodoro, P. E., Pereira, M. G., Lima, M., Rodrigues, R. de Á., and Silva Junior, C. A. da: Fire risk associated with landscape changes, climatic events and remote sensing in the Atlantic Forest using ARIMA model, Remote Sens. Appl. Soc. Environ., 26, https://doi.org/10.1016/j.rsase.2022.100761, 2022.
 - Jomelli, V., Favier, V., Vuille, M., Braucher, R., Martin, L., Blard, P. H., Colose, C., Brunstein, D., He, F., Khodri, M., Bourlès, D. L., Leanni, L., Rinterknecht, V., Grancher, D., Francou, B., Ceballos, J. L., Fonseca, H., Liu, Z., and Otto-Bliesner, B. L.: A major advance of tropical Andean glaciers during the Antarctic cold reversal, Nature, 513, 224–228, https://doi.org/10.1038/nature13546, 2014.
- Jouzel, J., Masson-Delmotte, V., Cattani, O., Dreyfus, G., Falourd, S., Hoffmann, G., Minster, B., Nouet, J., Barnola, J. M., Chappellaz, J., Fischer, H., Gallet, J. C., Johnsen, S., Leuenberger, M., Loulergue, L., Luethi, D., Oerter, H., Parrenin, F., Raisbeck, G., Raynaud, D., Schilt, A., Schwander, J., Selmo, E., Souchez, R., Spahni, R., Stauffer, B., Steffensen, J. P., Stenni, B., Stocker, T. F., Tison, J. L., Werner, M., and Wolff, E. W.: Orbital and millennial antarctic climate variability over the past 800,000 years, Science, 317, 793–796, https://doi.org/10.1126/science.1141038, 2007.
- 1205 Kaiser, J., Lamy, F., and Hebbeln, D.: A 70-kyr sea surface temperature record off southern Chile (Ocean Drilling Program Site 1233), Paleoceanography, 20, 1–15, https://doi.org/10.1029/2005PA001146, 2005.

- Kamino, L. H. Y., Rezende, É. A., Santos, L. J. C., Felippe, M. F., and Assis, W. L.: Atlantic Tropical Brazil, Springer International Publishing, 41–73 pp., https://doi.org/10.1007/978-3-030-04333-9 4, 2019.
- Kanner, L. C., Burns, S. J., Cheng, H., Edwards, R. L., and Vuille, M.: High-resolution variability of the South American summer monsoon over the last seven millennia: Insights from a speleothem record from the central Peruvian Andes, Quat. Sci. Rev., 75, 1–10, https://doi.org/10.1016/j.quascirev.2013.05.008, 2013.
 - Kitzberger, T. and Veblen, T. T.: Influences of humans and ENSO on fire history of Austrocedrus chilensis woodlands in northern Patagonia, Argentina, Ecoscience, 4, 508–520, https://doi.org/10.1080/11956860.1997.11682430, 1997.
 - Kitzberger, T., Tiribelli, F., Barberá, I., Gowda, J. H., Morales, J. M., Zalazar, L., and Paritsis, J.: Projections of fire probability and ecosystem vulnerability under 21st century climate across a trans-Andean productivity gradient in Patagonia, Sci. Total Environ., 839, https://doi.org/10.1016/j.scitotenv.2022.156303, 2022.

1220

1235

- Koch, A., Brierley, C., Maslin, M. M., and Lewis, S. L.: Earth system impacts of the European arrival and Great Dying in the Americas after 1492, Quat. Sci. Rev., 207, 13–36, https://doi.org/10.1016/j.quascirev.2018.12.004, 2019.
- Koutavas, A. and Joanides, S.: El Niño-Southern Oscillation extrema in the Holocene and Last Glacial Maximum, Paleoceanography, 27, 1–15, https://doi.org/10.1029/2012PA002378, 2012.
- Kukla, T., Winnick, M. J., Laguë, M. M., and Xia, Z.: The Zonal Patterns in Late Quaternary Tropical South American Precipitation, Paleoceanogr. Paleoclimatology, 38, 1–21, https://doi.org/10.1029/2022PA004498, 2023.
- Lamy, F., Kilian, R., Arz, H. W., Francois, J. P., Kaiser, J., Prange, M., and Steinke, T.: Holocene changes in the position and intensity of the southern westerly wind belt, Nat. Geosci., 3, 695–699, https://doi.org/10.1038/ngeo959, 2010.
- Laurent, P., Mouillot, F., Yue, C., Ciais, P., Moreno, M. V., and Nogueira, J. M. P.: Data Descriptor: FRY, a global database of fire patch functional traits derived from space-borne burned area products, 1–12, 2018.
 - Lea, D. W., Pak, D. K., Belanger, C. L., Spero, H. J., Hall, M. A., and Shackleton, N. J.: Paleoclimate history of Galápagos surface waters over the last 135,000 yr, Quat. Sci. Rev., 25, 1152–1167, https://doi.org/10.1016/j.quascirev.2005.11.010, 2006.
- Ledru, M.-P.: 3. Late Quaternary History and Evolution of the Cerrados as Revealed by Palynological Records, The Cerrados of Brazil, 33–50, https://doi.org/10.7312/oliv12042-004, 2002.
 - Ledru, M. P. and de Araújo, F. S.: The Cerrado and restinga pathways: two ancient biotic corridors in the neotropics, Front. Biogeogr., 15, 1–20, https://doi.org/10.21425/F5FBG59398, 2023.
 - Ledru, M. P., Ceccantini, G., Gouveia, S. E. M., López-Sáez, J. A., Pessenda, L. C. R., and Ribeiro, A. S.: Millenial-scale climatic and vegetation changes in a northern Cerrado (Northeast, Brazil) since the Last Glacial Maximum, Quat. Sci. Rev., 25, 1110–1126, https://doi.org/10.1016/j.quascirev.2005.10.005, 2006.
 - Ledru, M. P., Jomelli, V., Bremond, L., Ortuño, T., Cruz, P., Bentaleb, I., Sylvestre, F., Kuentz, A., Beck, S., Martin, C., Paillès, C., and Subitani, S.: Evidence of moist niches in the Bolivian Andes during the mid-Holocene arid period, Holocene, 23, 1547–1559, https://doi.org/10.1177/0959683613496288, 2013.
- Lenters, J. D. and Cook, K. H.: On the origin of the Bolivian high and related circulation features of the South American climate, J. Atmos. Sci., 54, 656–677, https://doi.org/10.1175/1520-0469(1997)054<0656:otootb>2.0.co;2, 1997.
 - Leyden, B. W.: Pollen evidence for climatic variability and cultural disturbance in the Maya Lowlands, Anc. Mesoamerica, 13, 85–101, https://doi.org/10.1017/S0956536102131099, 2002.
 - Lombardo, U., Iriarte, J., Hilbert, L., Ruiz-Pérez, J., Capriles, J. M., and Veit, H.: Early Holocene crop cultivation and landscape modification in Amazonia, Nature, 581, 190–193, https://doi.org/10.1038/s41586-020-2162-7, 2020.
 - Macias, D., Mazía, N., and Jacobo, E.: Grazing and neighborhood interactions limit woody encroachment in wet

- subtropical savannas, Basic Appl. Ecol., 15, 661-668, https://doi.org/10.1016/j.baae.2014.09.008, 2014.
- Maezumi, S. Y., Alves, D., Robinson, M., de Souza, J. G., Levis, C., Barnett, R. L., Almeida de Oliveira, E., Urrego, D., Schaan, D., and Iriarte, J.: The legacy of 4,500 years of polyculture agroforestry in the eastern Amazon, Nat. Plants, 4, 540–547, https://doi.org/10.1038/s41477-018-0205-y, 2018.
 - Maksic, J., Venancio, I. M., Shimizu, M. H., Chiessi, C. M., Piacsek, P., Sampaio, G., Cruz, F. W., and Alexandre, F. F.: Brazilian biomes distribution: Past and future, Palaeogeogr. Palaeoclimatol. Palaeoecol., 585, 110717, https://doi.org/10.1016/j.palaeo.2021.110717, 2022.
 - Marengo, J. A.: Interannual variability of surface climate in the Amazon basin, Int. J. Climatol., 12, 853–863, https://doi.org/10.1002/joc.3370120808, 1992.

1270

1275

1280

- Mark, S. Z., Abbott, M. B., Rodbell, D. T., and Moy, C. M.: XRF analysis of Laguna Pallcacocha sediments yields new insights into Holocene El Niño development, Earth Planet. Sci. Lett., 593, 117657, https://doi.org/10.1016/j.epsl.2022.117657, 2022.
- Marlon, J. R., Bartlein, P. J., Carcaillet, C., Gavin, D. G., Harrison, S. P., Higuera, P. E., Joos, F., Power, M. J., and Prentice, I. C.: Climate and human influences on global biomass burning over the past two millennia, Nat. Geosci., 1, 697–702, https://doi.org/10.1038/ngeo313, 2008.
 - Marlon, J. R., Bartlein, P. J., Daniau, A. L., Harrison, S. P., Maezumi, S. Y., Power, M. J., Tinner, W., and Vanniére, B.: Global biomass burning: A synthesis and review of Holocene paleofire records and their controls, Quat. Sci. Rev., 65, 5–25, https://doi.org/10.1016/j.quascirev.2012.11.029, 2013.
- Marlon, J. R., Kelly, R., Daniau, A. L., Vannière, B., Power, M. J., Bartlein, P., Higuera, P., Blarquez, O., Brewer, S., Brücher, T., Feurdean, A., Romera, G. G., Iglesias, V., Yoshi Maezumi, S., Magi, B., Mustaphi, C. J. C., and Zhihai, T.: Reconstructions of biomass burning from sediment-charcoal records to improve data-model comparisons, Biogeosciences, 13, 3225–3244, https://doi.org/10.5194/bg-13-3225-2016, 2016.
 - Martin, L. C. P., Blard, P. H., Lavé, J., Condom, T., Prémaillon, M., Jomelli, V., Brunstein, D., Lupker, M., Charreau, J., Mariotti, V., Tibari, B., Team, A., and Davy, E.: Lake tauca highstand (heinrich stadial 1a) driven by a southward shift of the bolivian high, Sci. Adv., 4, https://doi.org/10.1126/sciadv.aar2514, 2018.
 - Martins, A. K., Kochhann, K. G. D., Chiessi, C. M., Bauersachs, T., Zardin, T. N., Campos, M. C., Krahl, G., de Souza, L. V., Crivellari, S., Bahr, A., Kuhnert, H., Schwark, L., and Fauth, G.: Links between precipitation patterns over eastern tropical South America and productivity in the western tropical South Atlantic Ocean during the last deglacial, Quat. Int., 667, 29–40, https://doi.org/10.1016/j.quaint.2023.05.012, 2023.
 - Massaferro, J. I., Moreno, P. I., Denton, G. H., Vandergoes, M., and Dieffenbacher-Krall, A.: Chironomid and pollen evidence for climate fluctuations during the Last Glacial Termination in NW Patagonia, Quat. Sci. Rev., 28, 517–525, https://doi.org/10.1016/j.quascirev.2008.11.004, 2009.
 - Mayle, F. E., Burbridge, R., and Killeen, T. J.: Millennial-Scale Dynamics of Southern Amazonian Rain Forests, Science, 290, 2291–2294, https://doi.org/10.1126/science.290.5500.2291, 2000.
 - McMichael, C. N. H., Heijink, B. M., Bush, M. B., and Gosling, W. D.: On the scaling and standardization of charcoal data in paleofire reconstructions, Front. Biogeogr., 13, 1–9, https://doi.org/10.21425/F5FBG49431, 2021.
 - Meier, K. J. F., Jaeschke, A., Rethemeyer, J., Chiessi, C. M., Albuquerque, A. L. S., Wall, V., Friedrich, O., and Bahr, A.: Coupled Oceanic and Atmospheric Controls of Deglacial Southeastern South America Precipitation and Western South Atlantic Productivity, Front. Mar. Sci., 9, 1–20, https://doi.org/10.3389/fmars.2022.878116, 2022.
 - Mendes, V. R., Sawakuchi, A. O., M. Chiessi, C., Paulo, P. C., Rehfeld, K., and Mulitza, S.: Thermoluminescence and

- Optically Stimulated Luminescence Measured in Marine Sediments Indicate Precipitation Changes Over Northeastern Brazil, Paleoceanogr. Paleoclimatology, 34, 1476–1486, https://doi.org/10.1029/2019PA003691, 2019.
- MesoRad: Mesoamerican Radiocarbon Database (MesoRad). (tDAR id: 455305), https://doi.org/10.6067/XCV8455305, 2020.

1305

1320

- Miotti, L. and Salemme, M. C.: When Patagonia was colonized: People mobility at high latitudes during Pleistocene/Holocene transition, Quat. Int., 109–110, 95–111, https://doi.org/10.1016/S1040-6182(02)00206-9, 2003.
- Mistry, J.: Fire in the cerrado (savannas) of Brazil: An ecological review, Prog. Phys. Geogr., 22, 425–448, https://doi.org/10.1191/030913398668494359, 1998.
- Montade, V., Combourieu Nebout, N., Kissel, C., Haberle, S. G., Siani, G., and Michel, E.: Vegetation and climate changes during the last 22,000yr from a marine core near Taitao Peninsula, southern Chile, Palaeogeogr. Palaeoclimatol. Palaeoecol., 369, 335–348, https://doi.org/10.1016/j.palaeo.2012.11.001, 2013.
 - Montade, V., Peyron, O., Favier, C., Francois, J. P., and Haberle, S. G.: A pollen-climate calibration from western Patagonia for palaeoclimatic reconstructions, J. Quat. Sci., 34, 76–86, https://doi.org/10.1002/jqs.3082, 2019.
- 1300 Moreira, A. G.: Effects of fire protection on savanna structure in central Brazil, J. Biogeogr., 27, 1021–1029, https://doi.org/10.1046/j.1365-2699.2000.00422.x, 2000.
 - Moreno, P. I.: Timing and structure of vegetation, fire, and climate changes on the Pacific slope of northwestern Patagonia since the last glacial termination, Quat. Sci. Rev., 238, 106328, https://doi.org/10.1016/j.quascirev.2020.106328, 2020.
 - Moreno, P. I., Denton, G. H., Moreno, H., Lowell, T. V., Putnam, A. E., and Kaplan, M. R.: Radiocarbon chronology of the last glacial maximum and its termination in northwestern Patagonia, Quat. Sci. Rev., 122, 233–249, https://doi.org/10.1016/j.quascirev.2015.05.027, 2015.
 - Moreno, P. I., Videla, J., Valero-Garcés, B., Alloway, B. V., and Heusser, L. E.: A continuous record of vegetation, fire-regime and climatic changes in northwestern Patagonia spanning the last 25,000 years, Quat. Sci. Rev., 198, 15–36, https://doi.org/10.1016/j.quascirev.2018.08.013, 2018.
- Moreno, P. I., Henríquez, W. I., Pesce, O. H., Henríquez, C. A., Fletcher, M. S., Garreaud, R. D., and Villa-Martínez, R. P.:

 An early Holocene westerly minimum in the southern mid-latitudes, Quat. Sci. Rev., 251, 106730, https://doi.org/10.1016/j.quascirev.2020.106730, 2021.
 - Morley, R. J.: Cretaceous and Tertiary climate change and the past distribution of megathermal rainforests, Trop. Rainfor. Responses to Clim. Chang., 1–34, https://doi.org/10.1007/978-3-642-05383-2 1, 2011.
- Mosblech, N. A. S., Bush, M. B., Gosling, W. D., Hodell, D., Thomas, L., Van Calsteren, P., Correa-Metrio, A., Valencia, B. G., Curtis, J., and Van Woesik, R.: North Atlantic forcing of Amazonian precipitation during the last ice age, Nat. Geosci., 5, 817–820, https://doi.org/10.1038/ngeo1588, 2012.
 - Mulitza, S., Chiessi, C. M., Schefuß, E., Lippold, J., Wichmann, D., Antz, B., Mackensen, A., Paul, A., Prange, M., Rehfeld, K., Werner, M., Bickert, T., Frank, N., Kuhnert, H., Lynch-Stieglitz, J., Portilho-Ramos, R. C., Sawakuchi, A. O., Schulz, M., Schwenk, T., Tiedemann, R., Vahlenkamp, M., and Zhang, Y.: Synchronous and proportional deglacial changes in Atlantic meridional overturning and northeast Brazilian precipitation, Paleoceanography, 32, 622–633, https://doi.org/10.1002/2017PA003084, 2017.
 - Nanavati, W. P., Whitlock, C., Iglesias, V., and de Porras, M. E.: Postglacial vegetation, fire, and climate history along the eastern Andes, Argentina and Chile (lat. 41–55°S), Quat. Sci. Rev., 207, 145–160, https://doi.org/10.1016/j.quascirev.2019.01.014, 2019.
 - Nascimento, M. de N., Laurenzi, A. G., Valencia, B. G., Van, R., and Bush, M.: A 12,700-year history of

- paleolimnological change from an Andean microrefugium, Holocene, 29, 231–243, https://doi.org/10.1177/0959683618810400, 2019.
- Nascimento, M. N., Mosblech, N. A. S., Raczka, M. F., Baskin, S., Manrique, K. E., Wilger, J., Giosan, L., Benito, X., and Bush, M. B.: The adoption of agropastoralism and increased ENSO frequency in the Andes, Quat. Sci. Rev., 243, 106471, https://doi.org/10.1016/j.quascirev.2020.106471, 2020.

1340

1350

1355

1360

- Nehme, C., Todisco, D., Breitenbach, S. F. M., Couchoud, I., Marchegiano, M., Peral, M., Vonhof, H., Hellstrom, J., Tjallingi, R., Claeys, P., Borrero, L., and Martin, F.: Holocene hydroclimate variability along the Southern Patagonian margin (Chile) reconstructed from Cueva Chica speleothems, Glob. Planet. Change, 222, 104050, https://doi.org/10.1016/j.gloplacha.2023.104050, 2023.
- Nepstad, D. C., Veríssimo, A., Alencar, A., Nobre, C., Lima, E., Lefebvre, P., Schlesinger, P., Potter, C., Moutinho, P., Mendoza, E., Cochrane, M., and Brooks, V.: Large-scale impoverishment of amazonian forests by logging and fire, Nature, 398, 505–508, https://doi.org/10.1038/19066, 1999.
- Neves, E. G., Furquim, L. P., Levis, C., Rocha, B. C., Waitling, J. G., Ozorio de Almeida, F., Jaimes Betancourt, C., Junqueira, A. B., Moraes, C. P., Morcote-Rios, G., Shock, M. P., and Tamanaha, E. K.: Chapter 8: Peoples of the Amazon before European Colonization, https://doi.org/10.55161/lxit5573, 2021.
 - Novello, V. F., Cruz, F. W., Vuille, M., Stríkis, N. M., Edwards, R. L., Cheng, H., Emerick, S., De Paula, M. S., Li, X., Barreto, E. D. S., Karmann, I., and Santos, R. V: A high-resolution history of the South American Monsoon from Last Glacial Maximum to the Holocene, Sci. Rep., 7, 1–8, https://doi.org/10.1038/srep44267, 2017.
- Oliveira, C. A.: Os grupos pré-históricos ceramistas do Nordeste, in: Índios do Nordeste: temas e problemas 3, 2002.
 - De Oliveira, P. E., Barreto, A. M. F., and Suguio, K.: Late Pleistocene/Holocene climatic and vegetational history of the Brazilian caatinga: The fossil dunes of the middle Sao Francisco River, Palaeogeogr. Palaeoclimatol. Palaeoecol., 152, 319–337, https://doi.org/10.1016/S0031-0182(99)00061-9, 1999.
 - Olson, D. M., Dinerstein, E., Wikramanayake, E. D., Burgess, N. D., Powell, G. V. N., Underwood, E. C., D'amico, J. A., Itoua, I., Strand, H. E., Morrison, J. C., Loucks, C. J., Allnutt, T. F., Ricketts, T. H., Kura, Y., Lamoreux, J. F., Wettengel, W. W., Hedao, P., and Kassem, K. R.: Terrestrial Ecoregions of the World: A New Map of Life on Earth, Bioscience, 51, 933–938, https://doi.org/10.1641/0006-3568(2001)051[0933:TEOTWA]2.0.CO;2, 2001.
 - Paduano, G. M., Bush, M. B., Baker, P. A., Fritz, S. C., and Seltzer, G. O.: A vegetation and fire history of Lake Titicaca since the last glacial maximum, Palaeogeogr. Palaeoclimatol. Palaeoecol., 194, 259–279, https://doi.org/10.1016/S0031-0182(03)00281-5, 2003.
 - Pagán-Jiménez, J. R., Guachamín-Tello, A. M., Romero-Bastidas, M. E., and Constantine-Castro, A. R.: Late ninth millennium B.P. use of Zea mays L. at Cubilán area, highland Ecuador, revealed by ancient starches, Quat. Int., 404, 137–155, https://doi.org/10.1016/j.quaint.2015.08.025, 2016.
 - Palacios, D., Stokes, C. R., Phillips, F. M., Clague, J. J., Alcalá-Reygosa, J., Andrés, N., Angel, I., Blard, P. H., Briner, J.
 P., Hall, B. L., Dahms, D., Hein, A. S., Jomelli, V., Mark, B. G., Martini, M. A., Moreno, P., Riedel, J., Sagredo, E.,
 Stansell, N. D., Vázquez-Selem, L., Vuille, M., and Ward, D. J.: The deglaciation of the Americas during the Last
 Glacial Termination, Earth-Science Rev., 203, 103113, https://doi.org/10.1016/j.earscirev.2020.103113, 2020.
 - Perez, S. I., Postillone, M. B., Rindel, D., Gobbo, D., Gonzalez, P. N., and Bernal, V.: Peopling time, spatial occupation and demography of Late Pleistocene–Holocene human population from Patagonia, Quat. Int., 425, 214–223, https://doi.org/10.1016/j.quaint.2016.05.004, 2016.
 - Petit, J. R., Jouzel, J., Raynaud, D., Barkov, N. I., Barnola, J.-M., Basile, I., Bender, M., Chappellaz, J., Davis, M.,

- Delaygue, G., Delmotte, M., Kotlyakov, V. M., Legrand, M., Lipenkov, V. Y., Lorius, C., PÉpin, L., Ritz, C., Saltzman, E., and Stievenard, M.: Climate and atmospheric history of the past 420,000 years from the Vostok ice core, Antarctica, Nature, 399, 429–436, https://doi.org/10.1038/20859, 1999.
- Pinaya, J. L. D., Cruz, F. W., Ceccantini, G. C. T., Corrêa, P. L. P., Pitman, N., Vemado, F., Lopez, M. del C. S., Pereira-Filho, A. J., Grohmann, C. H., Chiessi, C. M., Strikis, N. M., Horák-Terra, I., Pinaya, W. H. L., Medeiros, V. B. de, Santos, R. de A., Akabane, T. K., Silva, M. A., Cheddadi, R., Bush, M., Henrot, A.-J., Louis, F., and Hamburckers, A., Boyer, F., Carré, M., Coissac, E., Ficetola, F., Huang, K., Lézine, A.-M., Nourelbait, M., Rhoujjati, A., Taberlet, P., Sarmiento, F., Abel-Schaad, D., Alba-Sánchez, F., Zheng, Z., and Oliveira, P. E. de: Brazilian montane rainforests expansion induced by Heinrich Stadial 1 event, Sci. Rep., 9, 17912, https://doi.org/10.1038/s41598-019-53036-1, 2019.
 - Pinaya, J. L. D., Pitman, N. C. A., Cruz, F. W., Akabane, T. K., Lopez, M. del C. S., Pereira-Filho, A. J., Grohman, C. H., Reis, L. S., Rodrigues, E. S. F., Ceccantini, G. C. T., and De Oliveira, P. E.: Humid and cold forest connections in South America between the eastern Andes and the southern Atlantic coast during the LGM, Sci. Rep., 14, 1–20, https://doi.org/10.1038/s41598-024-51763-8, 2024.
- Pinheiro, E. A. R., Metselaar, K., de Jong van Lier, Q., and de Araújo, J. C.: Importance of soil-water to the Caatinga biome, Brazil, Ecohydrology, 9, 1313–1327, https://doi.org/10.1002/eco.1728, 2016.
 - Piperno, D. R.: The origins of plant cultivation and domestication in the New World Tropics patterns, process, and new developments, Curr. Anthropol., 52, https://doi.org/10.1086/659998, 2011.
 - Piperno, D. R., Ranere, A. J., Holst, I., Iriarte, J., and Dickau, R.: Starch grain and phytolith evidence for early ninth millennium B.P. maize from the Central Balsas River Valley, Mexico, Proc. Natl. Acad. Sci. U. S. A., 106, 5019–5024, https://doi.org/10.1073/pnas.0812525106, 2009.

1390

- Pivello, V. R.: The use of fire in the cerrado and Amazonian rainforests of Brazil: Past and present, Fire Ecol., 7, 24–39, https://doi.org/10.4996/fireecology.0701024, 2011.
- Polissar, P. J., Abbott, M. B., Wolfe, A. P., Vuille, M., and Bezada, M.: Synchronous interhemispheric Holocene climate S. trends in the tropical Andes, Proc. Natl. Acad. Sci. U. A., 110, 14551-14556, https://doi.org/10.1073/pnas.1219681110, 2013.
- Ponce-Calderón, L. P., Rodríguez-Trejo, D. A., Villanueva-Díaz, J., Bilbao, B. A., Álvarez-Gordillo, G. D. C., and Vera-Cortés, G.: Historical fire ecology and its effect on vegetation dynamics of the lagunas de montebello national park, chiapas, méxico, IForest, 14, 548–559, https://doi.org/10.3832/ifor3682-014, 2021.
- Poveda, G., Espinoza, J. C., Zuluaga, M. D., Solman, S. A., Garreaud, R., and van Oevelen, P. J.: High Impact Weather Events in the Andes, Front. Earth Sci., 8, 1–32, https://doi.org/10.3389/feart.2020.00162, 2020.
 - Power, M. J., Marlon, J., Ortiz, N., Bartlein, P. J., Harrison, S. P., Mayle, F. E., Ballouche, A., Bradshaw, R. H. W., Carcaillet, C., Cordova, C., Mooney, S., Moreno, P. I., Prentice, I. C., Thonicke, K., Tinner, W., Whitlock, C., Zhang, Y., Zhao, Y., Ali, A. A., Anderson, R. S., Beer, R., Behling, H., Briles, C., Brown, K. J., Brunelle, A., Bush, M., Camill, P., Chu, G. Q., Clark, J., Colombaroli, D., Connor, S., Daniau, A. L., Daniels, M., Dodson, J., Doughty, E., Edwards, M. E., Finsinger, W., Foster, D., Frechette, J., Gaillard, M. J., Gavin, D. G., Gobet, E., Haberle, S., Hallett, D.
 - J., Higuera, P., Hope, G., Horn, S., Inoue, J., Kaltenrieder, P., Kennedy, L., Kong, Z. C., Larsen, C., Long, C. J., Lynch, J., Lynch, E. A., McGlone, M., Meeks, S., Mensing, S., Meyer, G., Minckley, T., Mohr, J., Nelson, D. M., New, J.,
 - Newnham, R., Noti, R., Oswald, W., Pierce, J., Richard, P. J. H., Rowe, C., Sanchez Goñi, M. F., Shuman, B. N.,
- Takahara, H., Toney, J., Turney, C., Urrego-Sanchez, D. H., Umbanhowar, C., Vandergoes, M., Vanniere, B., Vescovi, E., Walsh, M., Wang, X., Williams, N., Wilmshurst, J., and Zhang, J. H.: Changes in fire regimes since the last glacial

- maximum: An assessment based on a global synthesis and analysis of charcoal data, Clim. Dyn., 30, 887–907, https://doi.org/10.1007/s00382-007-0334-x, 2008.
- Power, M. J., Marlon, J. R., Bartlein, P. J., and Harrison, S. P.: Fire history and the global charcoal database: A new tool for hypothesis testing and data exploration, Palaeogeogr. Palaeoclimatol. Palaeoecol., 291, 52–59, https://doi.org/10.1016/j.palaeo.2009.09.014, 2010a.
 - Power, M. J., Bush, M., Behling, H., Horn, S., Mayle, F., and Urrego, D.: Paleofire activity in tropical America during the last 21 ka: A regional synthesis based on sedimentary charcoal, PAGES news, 18, 73–75, https://doi.org/10.22498/pages.18.2.73, 2010b.
- Prado, L. F., Wainer, I., Chiessi, C. M., Ledru, M. P., and Turcq, B.: A mid-Holocene climate reconstruction for eastern South America, Clim. Past, 9, 2117–2133, https://doi.org/10.5194/cp-9-2117-2013, 2013a.
 - Prado, L. F., Wainer, I., and Chiessi, C. M.: Mid-Holocene PMIP3/CMIP5 model results: Intercomparison for the South American Monsoon System, Holocene, 23, 1915–1920, https://doi.org/10.1177/0959683613505336, 2013b.
 - Prates, L. and Perez, S. I.: Late Pleistocene South American megafaunal extinctions associated with rise of Fishtail points and human population, Nat. Commun., 12, 1–11, https://doi.org/10.1038/s41467-021-22506-4, 2021.

1425

- Pym, F.C., Franco-Gaviria, F., Espinoza, I.G., Urrego, D.H., 2023. The timing and ecological consequences of Pleistocene megafaunal decline in the eastern Andes of Colombia. Quat. Res. (United States) 114, 1–17. https://doi.org/10.1017/qua.2022.66
- Raczka, M. F., Bush, M. B., and De Oliveira, P. E.: The collapse of megafaunal populations in southeastern Brazil, Quat. Res. (United States), 89, 103–118, https://doi.org/10.1017/qua.2017.60, 2018.
- Ramos-Neto, M. B. and Pivello, V. R.: Lightning fires in a Brazilian Savanna National Park: Rethinking management strategies, Environ. Manage., 26, 675–684, https://doi.org/10.1007/s002670010124, 2000.
- Raven, P. H., Gereau, R. E., Phillipson, P. B., Chatelain, C., Jenkins, C. N., and Ulloa, C. U.: The distribution of biodiversity richness in the tropics, Sci. Adv., 6, 5–10, https://doi.org/10.1126/sciadv.abc6228, 2020.
- Razik, S., Chiessi, C. M., Romero, O. E., and von Dobeneck, T.: Interaction of the South American Monsoon System and the Southern Westerly Wind Belt during the last 14kyr, Palaeogeogr. Palaeoclimatol. Palaeoecol., 374, 28–40, https://doi.org/10.1016/j.palaeo.2012.12.022, 2013.
 - Rehm, E. M. and Feeley, K. J.: The inability of tropical cloud forest species to invade grasslands above treeline during climate change: Potential explanations and consequences, Ecography (Cop.)., 38, 1167–1175, https://doi.org/10.1111/ecog.01050, 2015.
 - Reimer, P. J., Austin, W. E. N., Bard, E., Bayliss, A., Blackwell, P. G., Bronk Ramsey, C., Butzin, M., Cheng, H., Edwards, R. L., Friedrich, M., Grootes, P. M., Guilderson, T. P., Hajdas, I., Heaton, T. J., Hogg, A. G., Hughen, K. A., Kromer, B., Manning, S. W., Muscheler, R., Palmer, J. G., Pearson, C., van der Plicht, J., Reimer, R. W., Richards, D. A., Scott, E. M., Southon, J. R., Turney, C. S. M., Wacker, L., Adolphi, F., Büntgen, U., Capano, M., Fahrni, S. M.,
- Fogtmann-Schulz, A., Friedrich, R., Köhler, P., Kudsk, S., Miyake, F., Olsen, J., Reinig, F., Sakamoto, M., Sookdeo, A., and Talamo, S.: The IntCal20 Northern Hemisphere Radiocarbon Age Calibration Curve (0–55 cal kBP), Radiocarbon, 62, 725–757, https://doi.org/10.1017/rdc.2020.41, 2020.
 - Rein, B., Lückge, A., Reinhardt, L., Sirocko, F., Wolf, A., and Dullo, W. C.: El Niño variability off Peru during the last 20,000 years, Paleoceanography, 20, 1–18, https://doi.org/10.1029/2004PA001099, 2005.
- Ribeiro, M. C., Martensen, A. C., Metzger, J. P., Tabarelli, M., Scarano, F., and Fortin, M.-J.: The Brazilian Atlantic Forest: A Shrinking Biodiversity Hotspot, in: Biodiversity Hotspots, Springer Berlin Heidelberg, Berlin, Heidelberg,

- 405-434, https://doi.org/10.1007/978-3-642-20992-5 21, 2011.
- Richardson, J. E., Pennington, R. T., Pennington, T. D., and Hollingsworth, P. M.: Rapid diversification of a species-rich genus of neotropical rain forest trees, Science, 293, 2242–2245, https://doi.org/10.1126/science.1061421, 2001.
- Riris, P. and Arroyo-Kalin, M.: Widespread population decline in South America correlates with mid-Holocene climate change, Sci. Rep., 9, 1–10, https://doi.org/10.1038/s41598-019-43086-w, 2019.
 - WebPlotDigitizer version 5.2:

1470

- da Rosa, Á. A. S., Kerber, L., Pinheiro, F. L., and Manfroi, J.: A Look into the Past: Fossils from the Campos Sulinos Region, in: South Brazilian Grasslands, Springer International Publishing, Cham, 45–81, https://doi.org/10.1007/978-3-031-42580-6 3, 2023.
- Rozas-Davila, A., Correa-Metrio, A., McMichael, C. N. H., and Bush, M. B.: When the grass wasn't greener: Megafaunal ecology and paleodroughts, Quat. Sci. Rev., 266, 107073, https://doi.org/10.1016/j.quascirev.2021.107073, 2021.
- Rull, V.: Neotropical biodiversity: Timing and potential drivers, Trends Ecol. Evol., 26, 508–513 https://doi.org/10.1016/j.tree.2011.05.011, 2011.
- Sage, R.F., Coleman, J.R., 2001. Effects of low atmospheric CO2 on plants: More than a thing of the past. Trends Plant Sci. https://doi.org/10.1016/S1360-1385(00)01813-6
 - Salemme, M. C. and Miotti, L. L.: Archeological Hunter-Gatherer Landscapes Since the Latest Pleistocene in Fuego-Patagonia, in: Developments in Quaternary Sciences, vol. 11, 437–483, https://doi.org/10.1016/S1571-0866(07)10022-1, 2008.
- Salgado-Labouriau, M. L. L., Casseti, V., Ferraz-Vicentini, K. R. R., Martin, L., Soubiès, F., Suguio, K., and Turcq, B.: Late quaternary vegetational and climatic changes in cerrado and palm swamp from Central Brazil, Palaeogeogr. Palaeoclimatol. Palaeoecol., 128, 215–226, https://doi.org/10.1016/S0031-0182(96)00018-1, 1997.
 - Sawakuchi, A. O., Schultz, E. D., Pupim, F. N., Bertassoli, D. J., Souza, D. F., Cunha, D. F., Mazoca, C. E., Ferreira, M. P., Grohmann, C. H., Wahnfried, I. D., Chiessi, C. M., Cruz, F. W., Almeida, R. P., and Ribas, C. C.: Rainfall and sea level drove the expansion of seasonally flooded habitats and associated bird populations across Amazonia, Nat. Commun., 13, 4945, https://doi.org/10.1038/s41467-022-32561-0, 2022.
 - Schiferl, J., Kingston, M., Åkesson, C. M., Valencia, B. G., Rozas-Davila, A., McGee, D., Woods, A., Chen, C. Y., Hatfield, R. G., Rodbell, D. T., Abbott, M. B., and Bush, M. B.: A neotropical perspective on the uniqueness of the Holocene among interglacials, Nat. Commun., 14, 1–10, https://doi.org/10.1038/s41467-023-43231-0, 2023.
- Segura, H., Junquas, C., Espinoza, J. C., Vuille, M., Jauregui, Y. R., Rabatel, A., Condom, T., and Lebel, T.: New insights into the rainfall variability in the tropical Andes on seasonal and interannual time scales, Clim. Dyn., 53, 405–426, https://doi.org/10.1007/s00382-018-4590-8, 2019.
 - Shakun, J. D., Clark, P. U., He, F., Marcott, S. A., Mix, A. C., Liu, Z., Otto-Bliesner, B., Schmittner, A., and Bard, E.: Global warming preceded by increasing carbon dioxide concentrations during the last deglaciation, Nature, 484, 49–54, https://doi.org/10.1038/nature10915, 2012.
 - da Silva Junior, C. A., Teodoro, P. E., Delgado, R. C., Teodoro, L. P. R., Lima, M., de Andréa Pantaleão, A., Baio, F. H. R., de Azevedo, G. B., de Oliveira Sousa Azevedo, G. T., Capristo-Silva, G. F., Arvor, D., and Facco, C. U.: Persistent fire foci in all biomes undermine the Paris Agreement in Brazil, Sci. Rep., 10, 1–14, https://doi.org/10.1038/s41598-020-72571-w, 2020.
- Simon, M. F., Grether, R., De Queiroz, L. P., Skemae, C., Pennington, R. T., and Hughes, C. E.: Recent assembly of the Cerrado, a neotropical plant diversity hotspot, by in situ evolution of adaptations to fire, Proc. Natl. Acad. Sci. U. S. A.,

106, 20359-20364, https://doi.org/10.1073/pnas.0903410106, 2009.

1495

1500

1505

1510

- Strauss, A., Mariano Rodrigues, I. M., Baeta, A., Villagran, X. S., Alves, M., Pugliese, F., Bissaro, M., de Oliveira, R. E., de Souza, G. N., Bueno, L., de Sousa, J. C. M., Morrow, J. J., Reinhard, K. J., Hermenegildo, T., Perez, G. C., Chim, E.
 N., de Oliveira dos Santos, R., de Paiva, M., Kipnis, R., and Neves, W.: The Archaeological Record of Lagoa Santa (East-Central Brazil): From the Late Pleistocene to Historical Times, 227–281, https://doi.org/10.1007/978-3-030-35940-9 12, 2020.
 - Stríkis, N. M., Cruz, F. W., Cheng, H., Karmann, I., Edwards, R. L., Vuille, M., Wang, X., de Paula, M. S., Novello, V. F., and Auler, A. S.: Abrupt variations in South American monsoon rainfall during the Holocene based on a speleothem record from central-eastern Brazil, Geology, 39, 1075–1078, https://doi.org/10.1130/G32098.1, 2011.
 - Stríkis, N. M., Chiessi, C. M., Cruz, F. W., Vuille, M., Cheng, H., De Souza Barreto, E. A., Mollenhauer, G., Kasten, S., Karmann, I., Edwards, R. L., Bernal, J. P., and Sales, H. D. R.: Timing and structure of Mega-SACZ events during Heinrich Stadial 1, Geophys. Res. Lett., 42, 5477–5484, https://doi.org/10.1002/2015GL064048, 2015.
 - Stríkis, N. M., Cruz, F. W., Barreto, E. A. S., Naughton, F., Vuille, M., Cheng, H., Voelker, A. H. L., Zhang, H., Karmann, I., Lawrence Edwards, R., Auler, A. S., Santos, R. V., and Sales, H. R.: South American monsoon response to iceberg the North Proc. Natl. Acad. Sci. U. S. 115, 3788-3793, discharge in Atlantic, A., https://doi.org/10.1073/pnas.1717784115, 2018.
 - Stute, M., Forster, M., Frischkorn, H., Serejo, A., Clark, J. F., Schlosser, P., Broecker, W. S., and Bonani, G.: Cooling of Tropical Brazil (5°C) During the Last Glacial Maximum, Science, 269, 379–383, https://doi.org/10.1126/science.269.5222.379, 1995.
 - Suárez, R.: The human colonization of the Southeast Plains of South America: Climatic conditions, technological innovations and the peopling of Uruguay and south of Brazil, Quat. Int., 431, 181–193, https://doi.org/10.1016/j.quaint.2016.02.018, 2017.
 - Theissen, K. M., Dunbar, R. B., Rowe, H. D., and Mucciarone, D. A.: Multidecadal- to century-scale arid episodes on the northern Altiplano during the middle Holocene, Palaeogeogr. Palaeoclimatol. Palaeoecol., 257, 361–376, https://doi.org/10.1016/j.palaeo.2007.09.011, 2008.
 - Thompson, L. G., Davis, M. E., Mosley-Thompson, E., Sowers, T. A., Henderson, K. A., Zagorodnov, V. S., Lin, P. N., Mikhalenko, V. N., Campen, R. K., Bolzan, J. F., Cole-Dai, J., and Francou, B.: A 25,000-year tropical climate history from Bolivian ice cores, Science, 282, 1858–1864, https://doi.org/10.1126/science.282.5395.1858, 1998.
- Troll, C.: The Cordilleras of the Tropical Americas: Aspects of Climatic, Phytogeographical and Agrarian Ecology, in: Geo-ecologia de Las Regiones Montañosas de Las Américas Tropicales, Ferd. Dümmlers, 1968.
 - Urrego, D. H., Silman, M. R., and Bush, M. B.: The Last Glacial Maximum: Stability and change in a western Amazonian cloud forest, J. Quat. Sci., 20, 693–701, https://doi.org/10.1002/jqs.976, 2005.
 - Utida, G., Cruz, F. W., Santos, R. V, Wang, H., Pessenda, L. C. R., Novello, V. F., Vuille, M., Stríkis, M., Guedes, C. C. F., and Borella, A. C.: Climate changes in Northeastern Brazil from deglacial to Meghalayan periods and related environmental impacts, 250, 2020.
 - Valencia, B. G., Urrego, D. H., Silman, M. R., and Bush, M. B.: From ice age to modern: A record of landscape change in an Andean cloud forest, J. Biogeogr., 37, 1637–1647, https://doi.org/10.1111/j.1365-2699.2010.02318.x, 2010.
- Venancio, I. M., Shimizu, M. H., Santos, T. P., Lessa, D. O., Portilho-Ramos, R. C., Chiessi, C. M., Crivellari, S., Mulitza, S., Kuhnert, H., Tiedemann, R., Vahlenkamp, M., Bickert, T., Sampaio, G., Albuquerque, A. L. S., Veiga, S., Nobre, P., and Nobre, C.: Changes in surface hydrography at the western tropical Atlantic during the Younger Dryas, Glob. Planet.

Change, 184, 103047, https://doi.org/10.1016/j.gloplacha.2019.103047, 2020.

1530

1535

1540

1545

1555

- Vera, C., Higgins, W., Amador, J., Ambrizzi, T., Garreaud, R., Gochis, D., Gutzler, D., Lettenmaier, D., Marengo, J., Mechoso, C. R., Nogues-Paegle, J., Dias, P. L. S., and Zhang, C.: Toward a Unified View of the American Monsoon Systems, J. Clim., 19, 4977–5000, https://doi.org/10.1175/JCLI3896.1, 2006.
 - Villa-Martínez, R., Villagrán, C., and Jenny, B.: The last 7500 cal yr B.P. of westerly rainfall in Central Chile inferred from a high-resolution pollen record from Laguna Aculeo (34°S), Quat. Res., 60, 284–293, https://doi.org/10.1016/j.yqres.2003.07.007, 2003.
 - Villavicencio, N. A., Lindsey, E. L., Martin, F. M., Borrero, L. A., Moreno, P. I., Marshall, C. R., and Barnosky, A. D.: Combination of humans, climate, and vegetation change triggered Late Quaternary megafauna extinction in the Última Esperanza region, southern Patagonia, Chile, Ecography (Cop.)., 39, 125–140, https://doi.org/10.1111/ecog.01606, 2016.
 - Vuille, M.: Atmospheric circulation over the Bolivian Altiplano during dry and wet periods and extreme phases of the southern oscillation, Int. J. Climatol., 19, 1579–1600, https://doi.org/10.1002/(SICI)1097-0088(19991130)19:14<1579::AID-JOC441>3.0.CO;2-N, 1999.
 - Vuille, M. and Keimig, F.: Interannual variability of summertime convective cloudiness and precipitation in the central Andes derived from ISCCP-B3 data, J. Clim., 17, 3334–3348, https://doi.org/10.1175/1520-0442(2004)017<3334:IVOSCC>2.0.CO;2, 2004.
 - Vuille, M., Bradley, R. S., Healy, R., Werner, M., Hardy, D. R., Thompson, L. G., and Keimig, F.: Modeling δ18O in precipitation over the tropical Americas: 2. Simulation of the stable isotope signal in Andean ice cores, J. Geophys. Res. Atmos., 108, https://doi.org/10.1029/2001jd002039, 2003.
 - Wang, X., Auler, A. S., Edwards, R. L., Cheng, H., Ito, E., Wang, Y., Kong, X., and Solheid, M.: Millennial-scale precipitation changes in southern Brazil over the past 90,000 years, Geophys. Res. Lett., 34, n/a-n/a, https://doi.org/10.1029/2007GL031149, 2007.
- Wang, X., Edwards, R. L., Auler, A. S., Cheng, H., Kong, X., Wang, Y., Cruz, F. W., Dorale, J. A., and Chiang, H.-W.: Hydroclimate changes across the Amazon lowlands over the past 45,000 years, Nature, 541, 204–207, https://doi.org/10.1038/nature20787, 2017.
 - Westerhold, T., Marwan, N., Drury, A. J., Liebrand, D., Agnini, C., Anagnostou, E., Barnet, J. S. K., Bohaty, S. M., De Vleeschouwer, D., Florindo, F., Frederichs, T., Hodell, D. A., Holbourn, A. E., Kroon, D., Lauretano, V., Littler, K., Lourens, L. J., Lyle, M., Pälike, H., Röhl, U., Tian, J., Wilkens, R. H., Wilson, P. A., and Zachos, J. C.: An astronomically dated record of Earth's climate and its predictability over the last 66 million years, Science, 369, 1383–1388, https://doi.org/10.1126/SCIENCE.ABA6853, 2020.
 - Whitlock, C., Bianchi, M. M., Bartlein, P. J., Markgraf, V., Marlon, J., Walsh, M., and McCoy, N.: Postglacial vegetation, climate, and fire history along the east side of the Andes (lat 41-42.5°S), Argentina, Quat. Res., 66, 187–201, https://doi.org/10.1016/j.yqres.2006.04.004, 2006.
 - Wille, M., Hooghiemstra, H., Behling, H., Van Der Borg, K., and Negret, A. J.: Environmental change in the Colombian subandean forest belt from 8 pollen records: The last 50 kyr, https://doi.org/10.1007/PL00006921, 2001.
 - Williams, A. N.: The use of summed radiocarbon probability distributions in archaeology: a review of methods, J. Archaeol. Sci., 39, 578–589, https://doi.org/10.1016/j.jas.2011.07.014, 2012.
- Williams, J. W., Grimm, E. C., Blois, J. L., Charles, D. F., Davis, E. B., Goring, S. J., Graham, R. W., Smith, A. J., Anderson, M., Arroyo-Cabrales, J., Ashworth, A. C., Betancourt, J. L., Bills, B. W., Booth, R. K., Buckland, P. I.,

- Curry, B. B., Giesecke, T., Jackson, S. T., Latorre, C., Nichols, J., Purdum, T., Roth, R. E., Stryker, M., and Takahara, H.: The Neotoma Paleoecology Database, a multiproxy, international, community-curated data resource, Quat. Res. (United States), 89, 156–177, https://doi.org/10.1017/qua.2017.105, 2018.
- Wong, M. L., Battisti, D. S., Liu, X., Ding, Q., and Wang, X.: A North–South Dipole Response of the South Atlantic Convergence Zone During the Mid-Holocene, Geophys. Res. Lett., 50, 1–14, https://doi.org/10.1029/2023GL105130, 2023.

- Wunderling, N., von der Heydt, A. S., Aksenov, Y., Barker, S., Bastiaansen, R., Brovkin, V., Brunetti, M., Couplet, V., Kleinen, T., Lear, C. H., Lohmann, J., Roman-Cuesta, R. M., Sinet, S., Swingedouw, D., Winkelmann, R., Anand, P., Barichivich, J., Bathiany, S., Baudena, M., Bruun, J. T., Chiessi, C. M., Coxall, H. K., Docquier, D., Donges, J. F., Falkena, S. K. J., Klose, A. K., Obura, D., Rocha, J., Rynders, S., Steinert, N. J., and Willeit, M.: Climate tipping point interactions and cascades: a review, Earth Syst. Dyn., 15, 41–74, https://doi.org/10.5194/esd-15-41-2024, 2024.
- Zular, A., Sawakuchi, A. O., Chiessi, C. M., D'Horta, F. M., Cruz, F. W., Demattê, J. A. M., Ribas, C. C., Hartmann, G. A., Giannini, P. C. F., and Soares, E. A. A.: The role of abrupt climate change in the formation of an open vegetation enclave in northern Amazonia during the late Quaternary, Glob. Planet. Change, 172, 140–149, https://doi.org/10.1016/j.gloplacha.2018.09.006, 2019.